Acute Embryotoxicity of Mono-2-Ethylhexyl Phthalate (MEHP) in Mice: Nutrition, Epigenomics, and Environment

by

Karilyn E. Sant

A dissertation submitted in partial fulfillment
of the requirements for the degree of
Doctor of Philosophy
(Toxicology)
in the University of Michigan
2014

Doctoral Committee:

Professor Craig Harris, Co-Chair
Associate Professor Dana C. Dolinoy, Co-Chair
Professor Rita Loch-Caruso
Assistant Professor Maureen A. Sartor

Acknowledgements

First, I'd like to thank Dr. Craig Harris for putting up with me over the 2 years during my MPH degree and these 4.5 years. You encouraged me to think independently, and constantly inspired the scientific "dreamer" in me. You heard every one of my good, and sometimes very dumb, ideas and really helped to shape the way that I look at research. You have given me the ultimate doctoral experience, enabling me to participate in the various processes that I will encounter in my future career. Your door was literally always open, whether I wanted to talk about work, the crazy things we've seen around Ann Arbor, or our outside lives and hobbies. You have been the ultimate mentor, and I know that we will be in touch for many years to come.

Thank you to Dr. Dana Dolinoy. You were always willing to make time for all of your students, and gave me a bit of a lab "home" over the years. I learned so much from you professionally, but you also served as an amazing personal mentor. As a young, successful female faculty member with a family, you have shown myself and others that you really can do it all with hard work, perseverance, and most of all balance.

Thank you to Dr. Rita Loch-Caruso, for igniting my interest in toxicology. I had always been interested in environmental health, but interactions with Rita during undergrad were the true reason that I'm here today. Rita has been a great professional mentor for me, and has always had an open door.

Thanks to Dr. Maureen Sartor for her great deal of patience. I came into her bioinformatics course 4 years ago, barely able to function, and learned a great deal by the end of the semester. These are skills that I will be able to utilize throughout my career.

Thank you to the numerous student researchers that have rotated in the Harris Lab over the years, especially Erin Scarlett, Lindsey Jacobs, and Grace Kuan for their assistance with this

project. A big thank you to Joe Jilek for being a great friend, co-researcher, and co-teacher over the years. Our friendship began when we met while “dumpster diving” during undergrad, and honestly, I don’t know any other friends who can say something like that.

A constant thank you to the members of other labs that have been both friends and great resources, especially to Chris Faulk, Tamara Jones, Julie Kim, Lisa Marchlewicz, Muna Nahar, Olivia Tretter, and Caren Weinhouse of the Dolinoy lab, and to Faith Bjork, Iman Hassan, and Cassandra Korte of the Loch-Caruso lab. I have learned so much from all of you, and you all often brought a good laugh or smile to my day.

Thank you to Dr. Sushama Pavgi, Dr. Lynn Carpenter, and Dr. Laura Eidietis for serving as excellent teaching mentors over the years. I feel like my time as a GSI or giving lectures in your courses really helped to shape my presentation abilities and realize my passion for teaching.

Thank you to Sue Crawford, for putting up with my annoying shenanigans over the years. Whenever I had any question, and I mean ANY, Sue always had an answer. Thank you to Nancy Polderdyke for always being a great resource for me. I felt like a nag for always needing something, but Nancy always was so sweet and generous regardless.

Special thanks to Brian Shay at the University of Michigan Biomedical Mass Spec facility for teaching me the “art” of MS work and being patient with me during our methods development, and Nancy Cangelose at Texas A&M University for coordinating the use of facilities for analysis of our samples.

Finally, I am very grateful for the support of my family and closest friends over the years. Without their support, I don’t know what I would have done. My parents have always encouraged creativity, individualistic thought, the power of intelligence, and also “not sweating the small

stuff". They have sacrificed so much for me throughout my life, and it often was a thankless job. Thanks to Derrick, for being my stubborn brother, who is so different yet all too similar to myself. To Shari, for taking me in during the tough times, literally, and being a great friend in addition to my aunt. And, of course, a special thanks to Tyler. I'm sure I was an absolute joy to deal with all of these stressful times, and yet you were always my biggest supporter.

Table of Contents

List of Figures

CHAPTER I

CHAPTER II

CHAPTER III

CHAPTER IV

CHAPTER V

CHAPTER VI

List of Tables

CHAPTER II

CHAPTER III

CHAPTER IV

CHAPTER V

CHAPTER VI

List of Abbreviations

C_1	one-carbon (metabolism)
CNS	central nervous system
cys	cysteine
cySS	cystine
DEHP	di-2-ethylhexyl phthalate
DMG	dimethyl glycine
DMSO	dimethyl sulfoxide
DNMT	DNA methyltransferase
EEF	extra-embryonic fluid
EMB	embryo
GAAC	general amino acid control
GD	gestational day
GSH	glutathione
GSSG	glutathione disulfide
HBSS	Hanks' balanced salt solution
Hcy	homocysteine
HNP	histiotrophic nutrition pathway
LUMA	LUminometric Methylation Assay
mWEC	mouse whole embryo culture
Mat2a	methionine adenosyltransferase 2a
MEHP	mono-2-ethylhexyl phthalate
NSRCA	nutrient starvation and redox control of autophagy
NTD	neural tube defect
RME	receptor-mediated endocytosis
ROS	reactive oxygen species
SAM	S-adenosylmethionine
SLC	solute carrier
TBSS	Tyrode's balanced salt solution
VYS	visceral yolk sac
WEC	whole embryo culture

Abstract

Acute Embryotoxicity of Mono-2-Ethylhexyl Phthalate (MEHP) in Mice: Nutrition, Epigenomics, and Environment

Mono-2-ethylhexyl phthalate (MEHP) is the primary metabolite of di-2-ethylhexyl phthalate (DEHP), a ubiquitous toxicant used in the production of plastics. Studies have associated prenatal phthalate exposure with a spectrum of adverse health outcomes including neurodevelopmental disorders, although mechanisms are unknown. The importance of adequate fetal nutrition for neurodevelopment has been well-studied, but the role of histiotrophic nutrition pathways (HNPs) in embryonic development is not well characterized. This work aimed to 1) determine whether chemical inhibition of HNPs may result in epigenetic modifications during early organogenesis, 2) elucidate the mechanisms by which the toxicological compounds DEHP and MEHP may induce teratogenesis, 3) characterize whether environmental toxicants such as MEHP may alter HNP function, C_1 metabolism, and epigenetic programming in the conceptus, and 4) examine the transcriptomic and epigenomic profiles of conceptal tissues following MEHP treatment to identify modes of action and potential contributing factors to teratogenesis. Whole embryo culture was used to investigate rodent conceptuses during early organogenesis. Treatment with leupeptin, a protease inhibitor known to decrease HNPs, altered one-carbon (C_1) metabolism and decreased global DNA methylation in the embryo (EMB) and visceral yolk sac (VYS). MEHP treatment reduced embryonic growth, increased the prevalence of open neural tubes (NTD) in EMB, and increased susceptibility to oxidation. After 6-h MEHP treatment, decreased EMB and VYS expression of genes in pathways involved in the metabolism of amino acids, energy

metabolism, and oxidative phosphorylation occurred. Total HNP function, defined as the clearance of extra-conceptal proteins into the conceptal tissues and fluids, was reduced in a dose-dependent manner after 3-h MEHP treatment. C_1 metabolism was increased by 24-h MEHP treatment, suggesting time-dependent response in nutrient uptake and metabolism due to exposures. Global embryonic DNA methylation was decreased after 24 h exposure to MEHP and in EMB with NTDs. Global histone methylation at the H3K4 and H3K27 loci was increased in EMBs with NTDs and treated VYSs. Parallel transcriptomic and epigenomic analysis examined the effects of MEHP treatment and also NTD status. Pathway analysis of expression and DNA methylation data revealed disrupted nutrient metabolism, increased xenobiotic metabolism, and induction of pathways governing cellular fate such as increased autophagy. This research demonstrates that MEHP may induce nutrient starvation and redox control of autophagy (NSRCA), and these findings suggest that NSRCA may play a crucial role in teratogenesis.

Chapter I

Introduction

I. Overview

Prenatal exposures to environmental chemicals have been linked to agent-initiated susceptibility to diseases and adverse health outcomes observed later in life. This has prompted investigations to identify the precise developmental windows of susceptibility and the mechanisms by which these agent-initiated changes may act. The overwhelming majority of these studies have focused on chemical insults and dietary manipulations initiated during the fetal stages of development. However, the body of research has failed to acknowledge the influence of environmental, chemical, and nutritional factors on abnormal programming originating during the earlier organogenesis stages where embryonic form and function are first being established. For this reason, very little is known about the specific molecular targets, regulatory pathways, or modes of action that may be impacted by chemical agents during this critical phase of development, nor their consequences on disease later in life. This work seeks to identify the consequences of common environmental toxicant exposures, elucidate mechanisms of acute toxicity during early organogenesis, and identify mechanisms by which these acute influences may increase susceptibility to altered epigenetic gene regulation and developmental defects.

II. Phthalates and Development

Phthalates are a class of endocrine-disrupting compounds found ubiquitously in the environment. They are a common component in plastics, supplying flexibility to the product structure, and are often included in cosmetic formulas. Exposures to one of the most common phthalates, di-2-ethylhexyl phthalate (DEHP), has been associated with a myriad of adverse health outcomes, including increased risk for cancers, reproductive dysfunction, and increased risk for obesity [1-3]. DEHP is rapidly hydrolyzed to mono-2-ethylhexyl phthalate (MEHP), its primary metabolite (Fig. 1.1). MEHP has been demonstrated in humans and animals to cross the placenta and gestational membranes [4,5]. Because developmental plasticity is easily influenced by environment, DEHP and MEHP exposures *in utero* are a major concern. Human and animal studies have demonstrated numerous biochemical and cell cycle changes and nervous tissues due to phthalate exposures, such as DEHP and MEHP, including impaired neuronal activation, proliferation, differentiation, axon guidance, apoptosis, neurotrophin concentrations, and increased brain lipid content [6-12]. Likewise, early phthalate exposures have been associated with numerous behavioral and cognitive abnormalities, including aggression, attention problems, autism spectrum disorders, depression, and various social impairments [13-15]. Structural defects have also been observed due to prenatal phthalate exposure, including anterior neural tube defects, such as anencephaly and exencephaly [16,17]. Though associations between phthalate exposures during development and adverse neurodevelopment have been established, mechanisms surrounding phthalate specificity for the developing nervous system have yet to be elucidated.

III. Neurulation and Neural Tube Defects

Mammalian development is a tightly-regulated process during which spatial and temporal coordination of signaling, metabolism, proliferation, differentiation, and cell death are crucial for tissue patterning, organogenesis, and overall growth. Numerous signal transduction pathways are known to coordinate these processes, establishing the blueprints for cellular growth and replication. A few of these pathways are particularly critical during early embryogenesis, including the Wnt pathways (β-catenin and planar cell polarity), bone morphogenic protein (BMP)/TGF-β receptor pathway, sonic hedgehog (Shh) pathway, and Notch-Delta pathway [18]. These pathways all involve the presence of activating extracellular ligands, and all result in the binding of transcription factors to direct gene expression. These signaling ligands are responsible for the establishment of cell polarity, and patterning along the dorsal-ventral and anterior-posterior axes. Specifically, Shh is secreted from the mesodermal notochord following gastrulation, establishing a ventral signal for the neural plate [19]. BMPs, on the other hand, are secreted from the ectoderm, establishing the dorsal signal [19]. The coordination of these two signals establishes a dorsal-ventral axis for the neural plate, providing guidance for the induction of neurulation. Disruption to any one of these processes may result in altered structure, function, or potentially spontaneous abortion.

During early chordate development, the neural plate folds and fuses to form the neural tube, called neurulation [20]. This tube is formed by ectodermal cells directly dorsal to the notochord, and will give rise to the central nervous system (CNS) [21]. The neural plate is folded, and the neural folds fuse using coordinated signaling of cadherin molecules and integrated movement of the actin cytoskeleton [22-24]. Because this migration is guided through signaling pathways, disruption of pathways involved in dorsal-ventral patterning and folding during early

organogenesis have been correlated with detrimental effects of the CNS, including neural tube defects (NTDs) [25-30].

Despite intervention efforts, NTDs remain one of the most prevalent birth defects worldwide. The most prevalent and well-known NTD is spina bifida, a debilitating disease that significantly reduces quality of life or even longevity. The global prevalence of NTDs is 1 per every 1000 live births, though rates range from 0.2-2 per 1000 live births based upon geography, race, and ethnicity [31,32]. Spontaneous abortion is believed to occur in between 15-31% of pregnancies, and it is suggested that NTDs incidence is greater in spontaneous abortions [33-37]. Several nations have employed folate fortification of foods and prenatal vitamins, as folate supplementation of maternal diet has been associated with nearly a 30% decreased risk for NTDs [38-41]. However, the mechanism by which folate is beneficial is unknown [42,43].

IV. Redox Control of Teratogenesis

DEHP and MEHP have been repeatedly demonstrated to induce oxidative stress in various tissues [44-48]. Oxidative stress is classically defined as the imbalance of cellular environment towards a more oxidized, rather than reduced, state, though more recent definitions have included disrupted redox signaling and control [49]. Under normal conditions, the cell is in a balanced state, where the reducing power of the cell is able to eradicate the damage that would be done by oxidizing species. The endogenous antioxidant response, provided by reduced glutathione (GSH) and other active compounds, is involved in the metabolism of potentially harmful agents and restoring the reducing power of the cell. The biosynthesis of many of these innate antioxidants is governed by the nuclear translocation of the transcription factor Nrf2. Nrf2 can bind to a specific sequence of DNA, known as the antioxidant response element (ARE), which is found in many chemoprotective gene promoters, including those involved in the antioxidant response of Nrf2 [50,51]. The generation of

damaging reactive oxygen species (ROS) may be able to overwhelm the innate antioxidant defenses, leading to oxidizing cellular conditions. This oxidizing environment may cause lipid peroxidation, DNA damage, irregular gene expression, or altered degradation of proteins.

Teratogenesis is the production of congential malformations by developmental toxicant exposures. A "proposed" mechanism for many teratogens involved cellular dysregulation via oxidative stress and altered redox signaling [52]. During development, shifts in embryonic cell redox potentials may guide cell fate towards proliferation in a reduced state, or towards differentiation, apoptosis or necrosis in increasingly oxidized states [52]. In more severe cases, this may decrease growth of tissues, decrease overall size, or induce spontaneous abortion. Differential regulation of redox potentials may influence the mode of teratogenesis, as the susceptibility to thiol oxidation of redox couples is variable [52]. In this way, developmental exposures to chemicals may oxidize different redox couples and their corresponding cellular response pathways, producing chemical-specific structural defects. Likewise, exposures to the same chemicals at ranging developmental time points may also produce differing structural defects, as susceptibility to oxidative damage and ability to activate the endogenous antioxidant response pathways vary throughout development [52]. Thus, the timing of exposures and specificity of thiol targets are important factors in teratogenesis. During this window of development, environmental agents and conditions that result in increased ROS and oxidative stress have been shown to increase the incidence of NTDs [27,40,53-55], and supplementation of antioxidants has been shown to reduce risk for NTDs [40,41,55,56].

V. Histiotrophic Nutrition Pathways (HNPs)

During the first trimester of gestation, the placenta is not yet formed and the conceptus is isolated from direct maternal nutritional input. It has been previously suggested that this

environmental isolation was an evolutionary adaptation to provide protection to the developing conceptus from ROS [57]. During this time, the conceptus relies primarily on the receptor-mediated endocytosis (RME) of nutrients via the visceral yolk sac (VYS) brush border and subsequent proteolysis and degradation of these proteins, in a process known as HNPs (Fig. 1.2) [58-61]. Maternal nutrients and proteins are secreted by the uterine glands into the exocoelomic fluids surrounding the implanted embryo [57,62]. HNPs are then responsible for the RME and subsequent proteolysis of the nutrient-containing vesicles in order to provide substrates necessary for cellular functions [63-66]. The protein clatherin lines pitted regions of the plasma membranes of the brush border, which are abundant in receptor proteins, giving rise to a targeted region for RME [67-69]. Two cellular membrane proteins, megalin and cubilin, are responsible for the RME of numerous ligands, nutrients, and miscellaneous cellular substrates across cellular membranes throughout the conceptus, including the initial uptake via the VYS brush border [70]. These transporters, collectively known as the multiligand endocytotic receptor complex (MERC), thus serve as a biochemical gateway into the conceptus.

Following the RME of exogenous proteins and their respective cargoes, these vesicle-bound nutrients must be further processed before they become available for cellular use. Endocytotic vesicles in the VYS fuse with lysosomes initiating removal of vitamin, peptide and mineral cargoes and proteolysis of the bulk proteins. Proteins are degraded into the amino acid building blocks required for protein and DNA synthesis while other bound nutrients and cargoes are used for metabolic processes in the VYS, which may then diffuse into the extraembryonic fluid (EEF) or into the vitelline vasculature for transport to the embryo [71]. Studies suggest that the developing embryo undergoes several rounds of this process at various epithelial interfaces,

including the neuroepithelium where the RME protein, megalin, is more abundantly expressed [72,73].

VI. One-Carbon Metabolism and Epigenetic Gene Regulation

Though folate is the best-known protective compound against NTDs, the entire class of methyl donor dietary nutrients have been implicated as nutri-preventative for the CNS during development [74]. Common dietary methyl donors, including folate, choline, and betaine, are metabolized by numerous vitamins and enzymes, including B-vitamins and methyltransferases. The MERC is crucial for the uptake of several methyl donors and co-factors in their metabolism, including methionine, folate and vitamin B_{12} [70,75,76]. The process by which these dietary methyl donors are metabolized is called one-carbon (C_1) metabolism, and it is crucial for maintenance of a myriad of cellular functions. C_1 metabolism is the process by which S-adenosylmethionine (SAM), the primary cellular methyl donor, is generated (Fig. 1.3) [77]. In C_1 metabolism, dietary methyl donors are enzymatically metabolized to the amino acid methionine. Though methionine is required for protein synthesis, maintenance of a pool of methionine for C_1 metabolism is essential. The enzyme methionine adenosyltransferase 2a (*Mat2a*) is responsible for the conversion of methionine to SAM, which is then utilized in various cellular processes including post-translational modifications as well as epigenetic regulation.

Cell growth, differentiation, and tissue patterning during organogenesis are controlled in part by epigenetic mechanisms, which set the patterns of gene expression responsible for determination of cell fate, form, and function. These epigenetic modifications include DNA methylation, histone modifications, and non-coding RNA interactions, which may induce or

silence gene expression. Thus, epigenetic gene regulation provides environmental, temporal, and nutritional variations that DNA sequence, alone, cannot explain.

DNA methylation is a widely studied epigenetic mechanism. DNA methylation occurs most often in CG dinucleotides (CpGs) throughout the genome in mammals, though epigenetic marks are also prevalent across biological classifications [78]. Methylation of CpG sites is initiated by the DNA methyltransferase (DNMT) class of enzymes, taking SAM and converting it to S-adenosylhomocysteine while placing methyl marks on cytosine DNA residues. Canonically, DNA methylation in key regulatory regions of gene promoters may disrupt transcription factor binding, causing gene silencing.

Methylation of histone residues is another common epigenetic regulatory mechanism, which has variable effects on gene expression depending upon the locus. Histone 3, a key protein in chromatin structure, can become methylated by SAM as well. This methylation may occur at numerous loci, but is most common at the lysine-4 (H3K4) and lysine-27 (H3K27) residues. H3K4 and H3K27 methylation are typically considered activating and repressive marks, respectively [79,80]. Methylation at these loci may occur as mono-, di-, or tri-methylation, and the degree of methylation may correspond with the function of the epigenetic mark.

During development, epigenetic regulation is crucial for differentiation and normal development. After fertilization, DNA undergoes widespread demethylation of parental marks [81,82]. Several loci retain their methylation marks, known as imprinted genes. At implantation, methylation marks are strategically placed and replaced to regulate gene expression and differentiation. By the end of embryogenesis and early organogenesis, DNA methylation marks are fully programmed throughout the genome. Histone methylation is more dynamic, and marks can be applied and removed to influence chromatin structure and function throughout the cell

cycle. Again, the placement of these marks is crucial for normal differentiation and development, and have been found to correspond with the pluripotent status of embryonic cells [80]. H3K27 methylation is highest immediately post-fertilization, and then marks are progressively lost throughout embryogenesis; H3K4 methylation is low at the time of fertilization and becomes progressively more methylated as development progresses [83].

In all, HNPs have numerous downstream consequences, affecting processes involved in fundamental gene regulation and differentiation. If disruption of HNPs were to occur, it is possible that C_1 metabolism and thus SAM would become depleted, and this may decrease the methyl groups available for epigenetic gene regulation. In this case, it is likely that dysregulation and dysfunction would occur in embryonic tissues, and abnormal development may follow.

VII. Developmental Origins of Health and Disease

The developmental origins of health and disease (DOHaD) hypothesis proposes that *in utero* environmental conditions, such as nutrition and toxicant exposures, may predispose individuals to disease later in life. During this sensitive period of development, the EMB exhibits a great deal of developmental plasticity. Modulation to the embryonic environment may manifest as altered epigenetic programming or metabolic dysfunction that alters the gene expression profile and overall growth trajectory of the EMB. Because of the dynamic changes to the epigenetic landscape during embryogenesis and early organogenesis, exposures or decreased nutrition may result in aberrant placement of epigenetic marks. Because these marks are semi-permanent, the resultant gene expression changes may present throughout the lifetime [84]. Likewise, decreased nutrient availability during this susceptible period may result in a "thrifty phenotype" in the offspring, altering the metabolism throughout the lifecourse [85]. In this way, it is possible for

malnutrition during development and low birth weight to result in conditions such as obesity or diabetes due to embryonic metabolic programming.

Though we are primarily concerned with the etiology of NTDs and teratogenesis in this study, the outcomes measured in this work may also help to shape health and disease throughout the lifecourse. EMB that present with NTDs at this stage in the development may not survive to term, or the neural tube may fully close by the end of gestation. However, the delay in neural tube closure may still represent physiological, metabolic, and molecular changes to the CNS or even the whole organism.

VIII. DEHP and MEHP: Potential Mechanisms of Teratogenesis

DEHP and MEHP have been demonstrated to induce oxidative stress in various tissues and cell lines, as measured by several antioxidant and inflammatory response pathways [46,48,86-90]. Therefore, it is possible that DEHP and MEHP cause developmental toxicity via induction of oxidative stress. However, stress in developmental tissues has yet to be characterized, especially in the fetal brain and gestational membranes. Previous published and unpublished studies have demonstrated the capacity for compounds which induce oxidative stress to limit HNPs, and thus there is the potential for DEHP and MEHP to act through a related mechanism [91].

Numerous studies have investigated the epigenetic consequences of phthalate exposures. Phthalate exposures have been demonstrated to alter histone and DNA methylation in many different tissues, though the embryo and fetal brain have not been well-studied [92-95]. Likewise, the effects of phthalates on C_1 metabolism in the developing conceptus, namely the embryo and fetal brain, have not been well-studied. No studies have investigated the ability of phthalates or

other endocrine disruptors to inhibit or hinder HNPs, so the upstream consequences for epigenetic potential have yet to be characterized during embryogenesis.

Teratogenesis may be measured by many different outcomes, including limb growth, congenital heart defects, and NTDs. NTDs were selected as the teratogenic outcome of interest for this study for several reasons: 1) There is a growing body of literature surrounding prenatal exposures to phthalates and neurodevelopmental, cognitive, and neurodegenerative effects, and 2) Our preliminary studies demonstrated that NTDs were the most prevalent anatomical defect observed, and 3) The mechanisms by which NTDs are produced remain relatively uncharacterized.

IX. Study Overview and Objectives

This dissertation seeks to 1) determine whether chemical inhibition of HNPs may result in epigenetic modifications during early organogenesis, 2) elucidate the mechanisms by which the toxicological compounds DEHP and MEHP may induce teratogenesis, 3) characterize whether environmental toxicants such as MEHP may alter HNP function, C_1 metabolism, and epigenetic programming in the conceptus, and 4) examine the transcriptomic and epigenomic profiles of conceptal tissues following MEHP treatment to identify modes of action and potential contributing factors to teratogenesis.

It is hypothesized that MEHP-induced oxidative stress will disrupt HNPs, C_1 metabolism, epigenetic programming, and gene expression and induce morphological defects (Figure 1.4).

X. Funding and Institutional Approval

The experimental animal protocols utilized in this study were approved by the University of Michigan Committee on Use and Care of Animals, and in accordance with the Institute of

Animal Laboratory Resources guidelines for humane animal use. This work was supported by the Bill and Melinda Gates Foundation (Grand Challenges Exploratons – Rd. 7) and the University of Michigan National Institute of Environmental Health Sciences (NIEHS) Core Center "Lifestage Exposures and Adult Disease" (P30 ES017885). Support was also provided to K.S. by an NRSA institutional training grant (T32 ES007062).

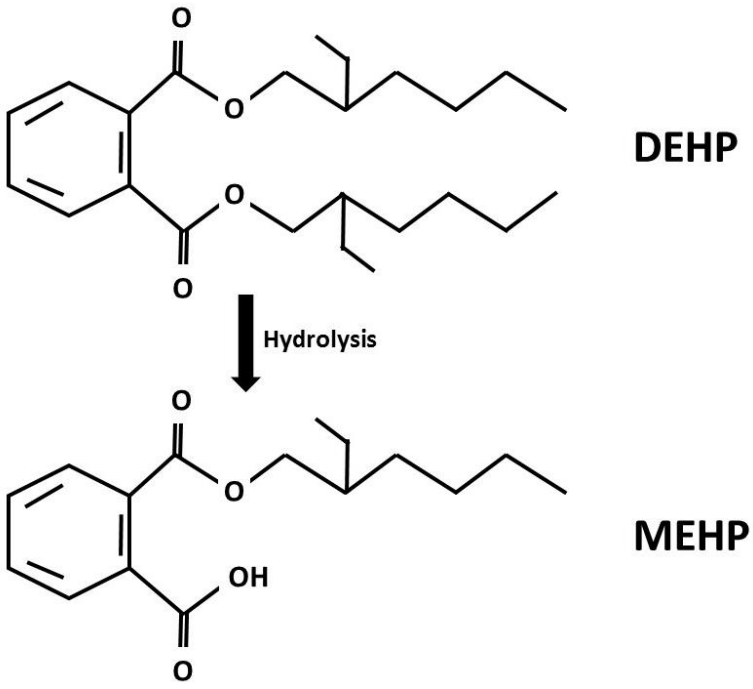

Figure 1.1. Chemical structures of DEHP and MEHP. DEHP is rapidly hydrolyzed to MEHP.

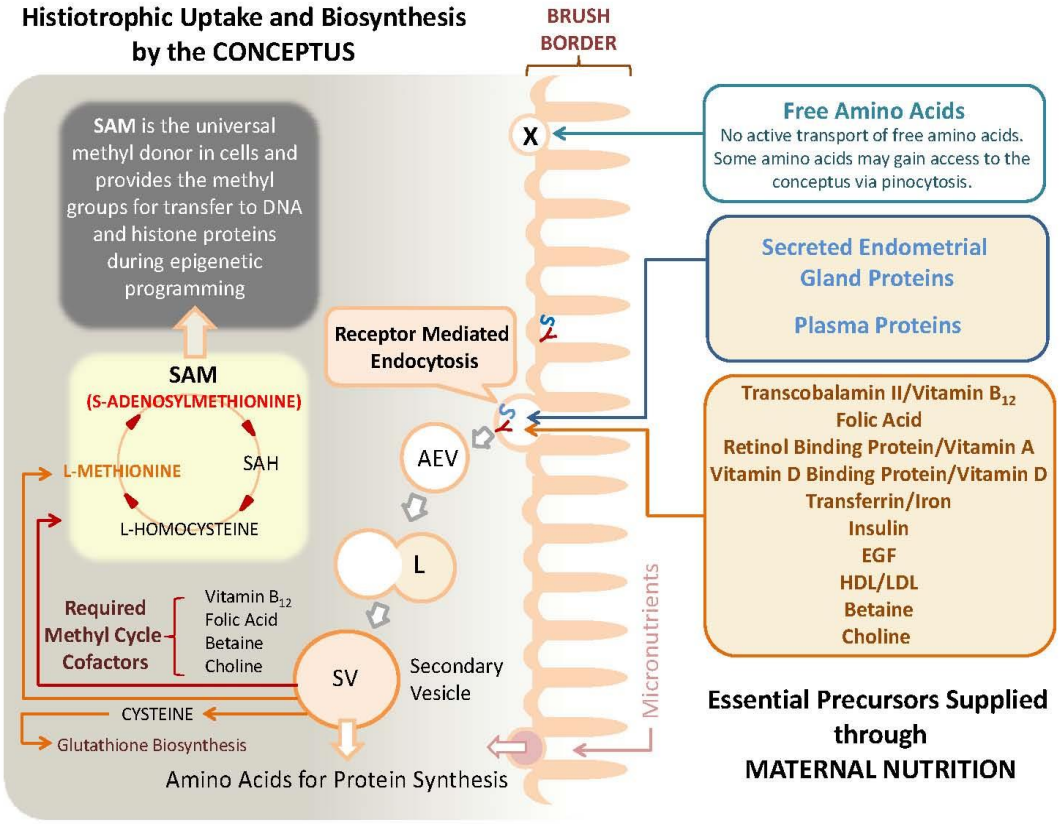

Figure 1.2. The role of histiotrophic nutrition pathways (HNPs) in the uptake and metabolism of nutrients by the conceptus. HNPs are a multi-step nutritional process, involving the receptor-mediated endocytosis of proteins and bound cargoes, followed by lysosomal proteolysis of captured proteins within the secondary vesicles.

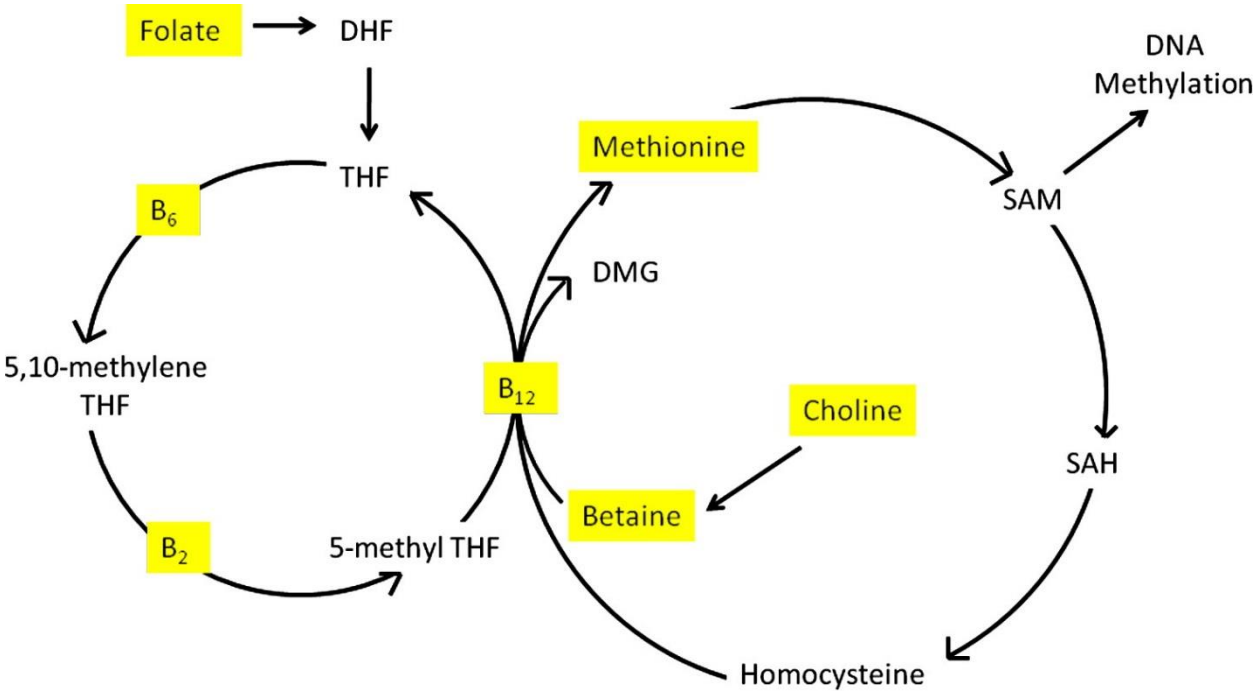

Figure 1.3. Involvement of dietary micronutrients in one-carbon metabolism. Substrates obtained via diet are highlighted in yellow. (1) Vitamin B6 is a cofactor to serine hydroxymethyltransferase in the conversion of tetrahydrofolate (THF) to 5,10-methylene THF. (2) Vitamin B2 is a precursor to FAD, which is a cofactor to methylenetetrahydrofolate reductase (MTHFR) in the conversion of 5,10-methylene THF to 5-methyl THF. (3) Vitamin B12 is a precursor to methionine synthase, involved in the production of methionine from homocysteine and betaine. DHF, Dihydrofolate; FAD, flavin adenine dinucleotide; DMG, dimethyl glycine; MTHFR, methylenetetrahydrofolate reductase; SAH, S-adenosylhomocysteine; THF, tetrahydrofolate.

Figure 1.3 reused and modified from Anderson, O.S., K.E. Sant, and D.C. Dolinoy, *Nutrition and epigenetics: an interplay of dietary methyl donors, one-carbon metabolism and DNA methylation.* The Journal of Nutritional Biochemistry, 2012. **23**(8): p. 853-859. Permission for reuse approved by Rightslink and Copyright Clearance Center, Inc on October 2, 2014.

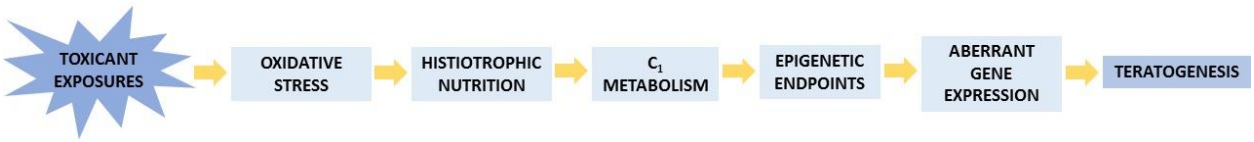

Figure 1.4. Model representing the hypothesized mode of action for teratogenesis due to toxicant exposures during early organogenesis. Two modes of action are believed to intersect at dysregulation of gene expression, and these mechanistically disrupt crucial developmental processes in the conceptus.

References

1. Kim, S.H. and M.J. Park, *Phthalate exposure and childhood obesity.* Ann Pediatr Endocrinol Metab, 2014. **19**(2): p. 69-75.
2. Caldwell, J.C., *DEHP: genotoxicity and potential carcinogenic mechanisms-a review.* Mutat Res, 2012. **751**(2): p. 82-157.
3. Kavlock, R., et al., *NTP Center for the Evaluation of Risks to Human Reproduction: phthalates expert panel report on the reproductive and developmental toxicity of di(2-ethylhexyl) phthalate.* Reproductive Toxicology, 2002. **16**(5): p. 529-653.
4. Jensen, M.S., et al., *Phthalates and Perfluorooctanesulfonic Acid in Human Amniotic Fluid: Temporal Trends and Timing of Amniocentesis in Pregnancy.* Environmental Health Perspectives, 2012. **120**(6): p. 897-903.
5. Mose, T., et al., *Phthalate monoesters in perfusate from a dual placenta perfusion system, the placenta tissue and umbilical cord blood.* Reproductive Toxicology, 2007. **23**(1): p. 83-91.
6. Tanida, T., et al., *Fetal and neonatal exposure to three typical environmental chemicals with different mechanisms of action: mixed exposure to phenol, phthalate, and dioxin cancels the effects of sole exposure on mouse midbrain dopaminergic nuclei.* Toxicol Lett, 2009. **189**(1): p. 40-7.
7. Xu, Y., et al., *Di-(2-ethylhexyl)-phthalate affects lipid profiling in fetal rat brain upon maternal exposure.* Arch Toxicol, 2007. **81**(1): p. 57-62.
8. Chen, T., et al., *Mono-(2-ethylhexyl) phthalate impairs neurodevelopment: inhibition of proliferation and promotion of differentiation in PC12 cells.* Toxicol Lett, 2011. **201**(1): p. 34-41.
9. Lin, C.H., et al., *Activation of Trim17 by PPARgamma is involved in di(2-ethylhexyl) phthalate (DEHP)-induced apoptosis on Neuro-2a cells.* Toxicol Lett, 2011. **206**(3): p. 245-51.
10. Smith, C.A., A. Macdonald, and M.R. Holahan, *Acute postnatal exposure to di(2-ethylhexyl) phthalate adversely impacts hippocampal development in the male rat.* Neuroscience, 2011. **193**: p. 100-8.
11. Sun, W., et al., *Perinatal exposure to Di-(2-ethylhexyl)-Phthalate leads to cognitive dysfunction and phospho-tau level increase in aged rats.* Environ Toxicol, 2014. **29**(5): p. 596-603.
12. Hokanson, R., et al., *DEHP, bis(2)-ethylhexyl phthalate, alters gene expression in human cells: possible correlation with initiation of fetal developmental abnormalities.* Hum Exp Toxicol, 2006. **25**(12): p. 687-95.
13. Engel, S.M., et al., *Prenatal phthalate exposure is associated with childhood behavior and executive functioning.* Environ Health Perspect, 2010. **118**(4): p. 565-71.
14. Testa, C., et al., *Di-(2-ethylhexyl) phthalate and autism spectrum disorders.* ASN Neuro, 2012. **4**(4): p. 223-9.
15. Miodovnik, A., et al., *Endocrine disruptors and childhood social impairment.* Neurotoxicology, 2011. **32**(2): p. 261-7.
16. Shiota, K. and S. Mima, *Assessment of the teratogenicity of di(2-ethylhexyl)phthalate and mono(2-ethylhexyl)phthalate in mice.* Arch Toxicol, 1985. **56**(4): p. 263-6.
17. Shiota, K. and H. Nishimura, *Teratogenicity of di(2-ethylhexyl) phthalate (DEHP) and di-n-butyl phthalate (DBP) in mice.* Environ Health Perspect, 1982. **45**: p. 65-70.
18. National Academy Press and National Research Council, *Scientific frontiers in developmental toxicology and risk assessment* 2000, Washington, D.C.: National Academy Press.
19. Liem, K.F., T.M. Jessell, and J. Briscoe, *Regulation of the neural patterning activity of sonic hedgehog by secreted BMP inhibitors expressed by notochord and somites.* Development, 2000. **127**(22): p. 4855-4866.
20. Gammill, L.S. and M. Bronner-Fraser, *Neural crest specification: migrating into genomics.* Nat Rev Neurosci, 2003. **4**(10): p. 795-805.
21. Greene, N.D. and A.J. Copp, *Development of the vertebrate central nervous system: formation of the neural tube.* Prenat Diagn, 2009. **29**(4): p. 303-11.

22. Gilbert, S.F., *The central nervous system and the epidermis*, in *Developmental Biology, 6th edition*2000, Sinauer Associates.
23. Ferreira, M.C. and S.R. Hilfer, *Calcium regulation of neural fold formation: visualization of the actin cytoskeleton in living chick embryos.* Dev Biol, 1993. **159**(2): p. 427-40.
24. Taneyhill, L.A., *To adhere or not to adhere: the role of Cadherins in neural crest development.* Cell Adh Migr, 2008. **2**(4): p. 223-30.
25. Copp, A. and N. Greene, *Genetics and development of neural tube defects.* The Journal of Pathology, 2010. **220**(2): p. 217-230.
26. Copp, A.J. and N.D. Greene, *Neural tube defects--disorders of neurulation and related embryonic processes.* Wiley Interdiscip Rev Dev Biol, 2013. **2**(2): p. 213-27.
27. Dheen, S., et al., *Recent studies on neural tube defects in embryos of diabetic pregnancy: an overview.* Current medicinal chemistry, 2009. **16**(18): p. 2345-54.
28. Fournier-Thibault, C., et al., *Sonic hedgehog regulates integrin activity, cadherin contacts, and cell polarity to orchestrate neural tube morphogenesis.* The Journal of neuroscience, 2009. **29**(40): p. 12506-20.
29. Klingensmith, J., et al., *Roles of bone morphogenetic protein signaling and its antagonism in holoprosencephaly.* American Journal of Medical Genetics Part C: Seminars in Medical Genetics, 2010. **154C**(1): p. 43-51.
30. Murdoch, J.N. and A.J. Copp, *The relationship between sonic Hedgehog signaling, cilia, and neural tube defects.* Birth Defects Research Part A: Clinical and Molecular Teratology, 2010. **88**(8): p. 633-652.
31. Mitchell, L.E., *Epidemiology of neural tube defects.* American Journal of Medical Genetics Part C: Seminars in Medical Genetics, 2005. **135C**(1): p. 88-94.
32. Feuchtbaum, L.B., et al., *Neural tube defect prevalence in California (1990-1994): eliciting patterns by type of defect and maternal race/ethnicity.* Genet Test, 1999. **3**(3): p. 265-72.
33. Creasy, M.R. and E.D. Alberman, *Congenital malformations of the central nervous system in spontaneous abortions.* J Med Genet, 1976. **13**(1): p. 9-16.
34. Gaskins, A.J., et al., *Maternal prepregnancy folate intake and risk of spontaneous abortion and stillbirth.* Obstet Gynecol, 2014. **124**(1): p. 23-31.
35. Alijotas-Reig, J. and C. Garrido-Gimenez, *Current concepts and new trends in the diagnosis and management of recurrent miscarriage.* Obstet Gynecol Surv, 2013. **68**(6): p. 445-66.
36. Rai, R. and L. Regan, *Recurrent miscarriage.* The Lancet. **368**(9535): p. 601-611.
37. Wilcox, A.J., et al., *Incidence of Early Loss of Pregnancy.* New England Journal of Medicine, 1988. **319**(4): p. 189-194.
38. Pitkin, R.M., *Folate and neural tube defects.* The American journal of clinical nutrition, 2007. **85**(1): p. 285S-288S.
39. Centers for Disease Control and Prevention, *Folic Acid Helps Prevent Neural Tube Defects*, National Center on Birth Defects and Developmental Disabilities, Editor 2014.
40. Carmichael, S.L., W. Yang, and G.M. Shaw, *Periconceptional nutrient intakes and risks of neural tube defects in California.* Birth Defects Research Part A: Clinical and Molecular Teratology, 2010. **88**(8): p. 670-678.
41. Zhang, B.-Y., et al., *Correlation Between Birth Defects and Dietary Nutrition Status in a High Incidence Area of China.* Biomedical and Environmental Sciences, 2008. **21**(1): p. 37-44.
42. Pitkin, R.M., *Folate and neural tube defects.* Am J Clin Nutr, 2007. **85**(1): p. 285S-288S.
43. Denny, K.J., et al., *Neural tube defects, folate, and immune modulation.* Birth Defects Res A Clin Mol Teratol, 2013. **97**(9): p. 602-9.
44. Tetz, L.M., et al., *Mono-2-ethylhexyl phthalate induces oxidative stress responses in human placental cells in vitro.* Toxicology and Applied Pharmacology, 2013. **268**(1): p. 47-54.
45. Tseng, I.L., et al., *Phthalates induce neurotoxicity affecting locomotor and thermotactic behaviors and AFD neurons through oxidative stress in Caenorhabditis elegans.* PLoS ONE, 2013. **8**(12): p. e82657.

46. Wang, W., et al., *Mono-(2-ethylhexyl) phthalate induces oxidative stress and inhibits growth of mouse ovarian antral follicles.* Biol Reprod, 2012. **87**(6): p. 152.
47. Wang, W., et al., *Di (2-ethylhexyl) phthalate inhibits growth of mouse ovarian antral follicles through an oxidative stress pathway.* Toxicol Appl Pharmacol, 2012. **258**(2): p. 288-95.
48. Ambruosi, B., et al., *In vitro acute exposure to DEHP affects oocyte meiotic maturation, energy and oxidative stress parameters in a large animal model.* PLoS ONE, 2011. **6**(11): p. e27452.
49. Jones, D.P., *Redefining oxidative stress.* Antioxid Redox Signal, 2006. **8**(9-10): p. 1865-79.
50. Wasserman, W.W. and W.E. Fahl, *Functional antioxidant responsive elements.* Proceedings of the National Academy of Sciences, 1997. **94**(10): p. 5361-5366.
51. Nguyen, T., P. Nioi, and C.B. Pickett, *The Nrf2-Antioxidant Response Element Signaling Pathway and Its Activation by Oxidative Stress.* Journal of biological chemistry, 2009. **284**(20): p. 13291-13295.
52. Hansen, J.M. and C. Harris, *Redox control of teratogenesis.* Reproductive Toxicology, 2013. **35**(0): p. 165-179.
53. Graf, W., et al., *Comparison of erythrocyte antioxidant enzyme activities and embryologic level of neural tube defects.* European journal of pediatric surgery, 1995. **5**(Supplement 1): p. 8-11.
54. Morgan, S., et al., *Oxidative stress during diabetic pregnancy disrupts cardiac neural crest migration and causes outflow tract defects.* Birth defects research. A Clinical and molecular teratology, 2008. **82**(6): p. 453-63.
55. Zhao, W., et al., *Neural tube defects and maternal biomarkers of folate, homocysteine, and glutathione metabolism.* Birth Defects Research Part A: Clinical and Molecular Teratology, 2006. **76**(4): p. 230-236.
56. Simán, C.M. and U.J. Eriksson, *Vitamin C supplementation of the maternal diet reduces the rate of malformation in the offspring of diabetic rats.* Diabetologia, 1997. **40**(12): p. 1416-1424.
57. Burton, G.J., J. Hempstock, and E. Jauniaux, *Nutrition of the human fetus during the first trimester--a review.* Placenta, 2001. **22 Suppl A**: p. S70-7.
58. Ambroso, J.L., et al., *Fluorometric analysis of endocytosis and lysosomal proteolysis in the rat visceral yolk sac during whole embryo culture.* Teratology, 1997. **56**(3): p. 201-209.
59. Fisher, C.E. and S.E.M. Howie, *The role of megalin (LRP-2/Gp330) during development.* Developmental Biology, 2006. **296**(2): p. 279-297.
60. Hammad, S.M., et al., *Megalin Acts in Concert with Cubilin to Mediate Endocytosis of High Density Lipoproteins.* Journal of biological chemistry, 2000. **275**(16): p. 12003-12008.
61. Moestrup, S.K. and P.J. Verroust, *Megalin- and Cubilin-Mediated Endocytosis of Protein-Bound Vitamins, Lipids, and Hormones in Polarized Epithelia.* Annual Review of Nutrition, 2001. **21**(1): p. 407-428.
62. Burton, G.J., et al., *Uterine glands provide histiotrophic nutrition for the human fetus during the first trimester of pregnancy.* J Clin Endocrinol Metab, 2002. **87**(6): p. 2954-9.
63. Beckman, D.A., et al., *Sources of amino acids for protein synthesis during early organogenesis in the rat. 1. Relative contributions of free amino acids and of proteins.* Placenta, 1990. **11**(2): p. 109-121.
64. Beckman, D.A., et al., *Sources of amino acids for protein synthesis during early organogenesis in the rat. 2. Exchange with amino acid and protein pools in embryo and yolk sac.* Placenta, 1991. **12**(1): p. 37-46.
65. Freeman, S.J. and J.B. Lloyd, *Evidence that protein ingested by the rat visceral yolk sac yields amino acids for synthesis of embryonic protein.* Journal of embryology and experimental morphology, 1983. **73**: p. 307-15.
66. Lloyd, J.B., R.L. Brent, and D.A. Beckman, *Sources of amino acids for protein synthesis during earlyorganogenesis in the rat. 3. Methionine incorporation.* Placenta, 1996. **17**(8): p. 629-634.
67. Huxham, M. and F. Beck, *Receptor mediated coated vesicle transport of rat IgG across the 11.5 day in vitro rat yolk sac endoderm.* Cell Biol Int Rep, 1981. **5**(12): p. 1073-81.

68. Sahali, D., et al., *Characterization of a 280-kD protein restricted to the coated pits of the renal brush border and the epithelial cells of the yolk sac. Teratogenic effect of the specific monoclonal antibodies.* J Exp Med, 1988. **167**(1): p. 213-8.
69. Le Panse, S., P. Verroust, and E.I. Christensen, *Internalization and recycling of glycoprotein 280 in BN/MSV yolk sac epithelial cells: a model system of relevance to receptor-mediated endocytosis in the renal proximal tubule.* Exp Nephrol, 1997. **5**(5): p. 375-83.
70. Birn, H., *The kidney in vitamin B12 and folate homeostasis: characterization of receptors for tubular uptake of vitamins and carrier proteins.* American Journal of Physiology - Renal Physiology, 2006. **291**(1): p. F22-F36.
71. Ambroso, J. and C. Harris, *Assessment of Histiotrophic Nutrition Using Fluorescent Probes*, in *Developmental Toxicology*, C. Harris and J.M. Hansen, Editors. 2012, Humana Press. p. 407-423.
72. Drake, C.J., et al., *Differential distribution of cubilin and megalin expression in the mouse embryo.* Anat Rec A Discov Mol Cell Evol Biol, 2004. **277**(1): p. 163-70.
73. Muller, D., A. Nykjaer, and T.E. Willnow, *From holoprosencephaly to osteopathology: role of multifunctional endocytic receptors in absorptive epithelia.* Ann Med, 2003. **35**(5): p. 290-9.
74. Zeisel, S.H., *Importance of methyl donors during reproduction.* Am J Clin Nutr, 2009. **89**(2): p. 673S-7S.
75. Christensen, E. and P. Verroust, *Megalin and cubilin, role in proximal tubule function and during development.* Pediatric Nephrology, 2002. **17**(12): p. 993-999.
76. Gelineau-van Waes, J., et al., *Microarray analysis of E9.5 reduced folate carrier (RFC1; Slc19a1) knockout embryos reveals altered expression of genes in the cubilin-megalin multiligand endocytic receptor complex.* BMC Genomics, 2008. **9**(1): p. 156.
77. Anderson, O.S., K.E. Sant, and D.C. Dolinoy, *Nutrition and epigenetics: an interplay of dietary methyl donors, one-carbon metabolism and DNA methylation.* The Journal of Nutritional Biochemistry, 2012. **23**(8): p. 853-859.
78. Dodge, J., et al., *De novo methylation of MMLV provirus in embryonic stem cells: CpG versus non-CpG methylation.* Gene, 2002. **289**(1-2): p. 41-48.
79. Shilatifard, A., *Molecular implementation and physiological roles for histone H3 lysine 4 (H3K4) methylation.* Curr Opin Cell Biol, 2008. **20**(3): p. 341-8.
80. Pan, G., et al., *Whole-genome analysis of histone H3 lysine 4 and lysine 27 methylation in human embryonic stem cells.* Cell Stem Cell, 2007. **1**(3): p. 299-312.
81. Hajkova, P., et al., *Epigenetic reprogramming in mouse primordial germ cells.* Mechanisms of development, 2002. **117**(1-2): p. 15-23.
82. Reik, W., W. Dean, and J. Walter, *Epigenetic reprogramming in mammalian development.* Science, 2001. **293**(5532): p. 1089-1093.
83. Reik, W., *Stability and flexibility of epigenetic gene regulation in mammalian development.* Nature, 2007. **447**(7143): p. 425-432.
84. Feil, R. and M.F. Fraga, *Epigenetics and the environment: emerging patterns and implications.* Nat Rev Genet, 2012. **13**(2): p. 97-109.
85. Hales, C.N. and D.J. Barker, *The thrifty phenotype hypothesis.* Br Med Bull, 2001. **60**: p. 5-20.
86. Baek, I.J., et al., *Effects of endocrine disrupting chemicals on expression of phospholipid hydroperoxide glutathione peroxidase mRNA in rat testes.* J Vet Sci, 2007. **8**(3): p. 213-8.
87. Law, M.Y. and D.E. Moody, *In vitro inhibition of mouse and rat glutathione S-transferases by di(2-ethylhexyl) phthalate, mono(2-ethylhexyl) phthalate, 2-ethylhexanol, 2-ethylhexanoic acid and clofibric acid.* Toxicol In Vitro, 1991. **5**(3): p. 207-10.
88. Fan, J., et al., *Molecular mechanisms mediating the effect of mono-(2-ethylhexyl) phthalate on hormone-stimulated steroidogenesis in MA-10 mouse tumor Leydig cells.* Endocrinology, 2010. **151**(7): p. 3348-62.
89. Erkekoglu, P., et al., *Induction of ROS, p53, p21 in DEHP- and MEHP-exposed LNCaP cells-protection by selenium compounds.* Food Chem Toxicol, 2011. **49**(7): p. 1565-71.

90. Erkekoglu, P., et al., *Evaluation of cytotoxicity and oxidative DNA damaging effects of di(2-ethylhexyl)-phthalate (DEHP) and mono(2-ethylhexyl)-phthalate (MEHP) on MA-10 Leydig cells and protection by selenium.* Toxicol Appl Pharmacol, 2010. **248**(1): p. 52-62.
91. Ambroso, J. and C. Harris, *In vitro embryotoxicity of the cysteine proteinase inhibitors benzyloxycarbonyl-phenylalanine-alanine-diazomethane (Z-Phe-Ala-CHN2) and benzyloxycarbonyl-phenylalanine-phenylalanine-diazomethane (Z-Phe-Phe-CHN2).* Teratology, 1994. **50**(3): p. 214-228.
92. Singh, S. and S.S. Li, *Epigenetic effects of environmental chemicals bisphenol a and phthalates.* Int J Mol Sci, 2012. **13**(8): p. 10143-53.
93. Wu, S., et al., *Dynamic epigenetic changes involved in testicular toxicity induced by di-2-(ethylhexyl) phthalate in mice.* Basic Clin Pharmacol Toxicol, 2010. **106**(2): p. 118-23.
94. Wu, S., et al., *Dynamic effect of di-2-(ethylhexyl) phthalate on testicular toxicity: epigenetic changes and their impact on gene expression.* Int J Toxicol, 2010. **29**(2): p. 193-200.
95. LaRocca, J., et al., *The impact of first trimester phthalate and phenol exposure on IGF2/H19 genomic imprinting and birth outcomes.* Environ Res, 2014. **133**: p. 396-406.

Chapter II

Inhibition of proteolysis in histiotrophic nutrition pathways alters DNA methylation and one-carbon metabolism in the organogenesis-stage rat conceptus

Text has been previously published in Sant, K. E., Dolinoy D.C., et al. (2013). "Inhibition of proteolysis in histiotrophic nutrition pathways alters DNA methylation and one-carbon metabolism in the organogenesis-stage rat conceptus." The Journal of Nutritional Biochemistry 24(8): 1479-1487. Permission for reuse approved by Rightslink and Copyright Clearance Center, Inc on October 2, 2014.

Introduction

Cell differentiation that gives rise to form and function during embryogenesis is achieved through a highly coordinated and integrated program of cell signaling and gene expression. Both embryonic and extraembryonic cells within the conceptus contain identical genetic codes from which variable gene expression is programmed epigenetically in spatial and temporal patterns. DNA methylation is an important process involved in the epigenetic regulation of gene expression along with chromatin modification and noncoding RNAs. DNA hypermethylation is generally associated with gene silencing, while hypomethylation is associated with transcriptional activation [1,2]. Cells within the very early preimplantation embryo (EMB) exist in a globally demethylated state and then undergo remethylation in a cell- and gene-selective manner to establish specific

differentiation characteristics as embryogenesis progresses [3,4]. In mature cells, a large proportion of the genome becomes methylated and is, therefore, not expressed [1].

Regulatory regions in promoter sequences of actively expressed genes remain hypomethylated and enriched in open-chromatin marks to remain transcriptionally poised to respond to a wide variety of signals and stimuli [5]. While the roles of several chemicals and dietary components have been characterized in the disruption of these processes [6,7], very little is known about the mechanisms through which specific nutrients and other environmental or developmental stress factors interact to modify the epigenome during differentiation and embryonic development.

Alterations in maternal diet during the preimplantation and fetal phases of development have been shown to reduce the conceptual availability of whole protein, amino acids (methionine), folate, choline and cobalamin (vitamin B_{12}) and are also known to elicit changes in the epigenome through reprogramming of DNA methylation patterns [8]. These dietary nutrients are the source of precursors, vitamins and cofactors required for one-carbon (C_1) metabolism, the process that culminates in S-adenosylmethionine (SAM) biosynthesis. SAM is the universal methyl donor for DNA methylation and is generated in its final form from L-methionine and adenosine triphosphate (ATP) by the enzymatic activity of methionine adenosyltransferase 2a (Mat2a). C_1 precursors must be constantly supplied to the conceptus, suggesting that maternal diet and micronutrient bioavailability are crucial for proper epigenetic regulation of developmental processes.

Embryonic and fetal nutrition plays a critical role in growth, differentiation and developmental plasticity [9]. During organogenesis, the early postimplantation-stage mammalian conceptus is physically isolated from direct access to maternal micronutrients, as the placenta is not yet fully functional. Thus, the organogenesis-stage conceptus obtains very few nutrients

through transcellular transport and must rely on the receptor-mediated endocytosis (RME) or pinocytosis of proteins and nutrients via the visceral yolk sac (VYS) endothelium [10-13]. Proteolytic degradation of bulk maternal protein in lysosomes of trophoblast-derived tissues provides the conceptus with the majority of amino acids necessary for de novo protein biosynthesis [14-17]. In addition to the bulk proteins, RME provides access for other substrates, vitamins and cofactors, which enter cells by the same pathways bound to specific carrier proteins. The RME, proteolysis and processing of nutrients, termed histiotrophic nutrition pathways (HNPs), comprise the primary route of nutrition during organogenesis. HNPs are, therefore, also responsible for the maintenance of C_1 metabolism during organogenesis (Fig. 2.1).

Leupeptin, a naturally occurring inhibitor of proteolytic degradation, reduces amino acid and micronutrient availability for cellular processes such as protein synthesis, glutathione (GSH) biosynthesis and C_1 metabolism [18] (Fig. 2.1). Treatment with leupeptin mimics nutritional deficiency in the conceptus and has been shown to decrease the activity of HNPs [10]. Because substrates obtained via HNPs such as methionine, folate, choline, and vitamin B_{12} are required for SAM biosynthesis, leupeptin treatment during organogenesis may be used as a model to study developmental outcomes associated with nutritional deficiencies. While several studies have begun to investigate the epigenetic and morphological consequences of these nutritional deficiencies during embryonic development, the role of HNPs in these outcomes has yet to be characterized [8]. This study examines a unique window of developmental susceptibility where alterations in HNP lead to compromised C_1 metabolism and a reduction of global DNA methylation during organogenesis. Within this context, we propose to test the hypothesis that leupeptin, a protease inhibitor, disrupts HNP functions in the organogenesis-stage conceptus,

reducing the availability of methionine required for biosynthesis of SAM by the C_1 pathway and, thereby, altering patterns of DNA methylation.

Materials & Methods

Chemicals and reagents

Leupeptin hemisulfate salt and deuterated isotopic standards (Homocysteine-d_8 and N,N-dimethyl-d_6-glycine HCl) for mass spectrometry quantification of C_1 components were purchased from Sigma (St. Louis, MO, USA). L-Methionine (methyl-d3) and D,L-cysteine (3,3-d_2) were purchased from Cambridge Isotope Laboratories (Andover, MA, USA). S-Adenosyl-L-methionine-d_3 (S-methyl-d_3) tetra (p-toluenesulfonate) salt was from C/D/N Isotopes (Pointe-Claire, Quebec, Canada). All other reagents and chemicals were purchased from standard vendors and were of the appropriate purity for culture and analytical applications. Antibodies for immunoblots were purchased from Abcam (Cambridge, MA, USA) [Anti-Mat2a antibody (Rabbit polyclonal) — ab77471] and Santa Cruz Biotechnology (Santa Cruz, CA) [Actin antibody (Goat polyclonal) — sc-1615; Alkaline phosphatase secondary antibody (donkey anti-goat) — sc-2022; Alkaline phosphatase secondary antibody (chicken-anti-rabbit) — sc-2959].

Whole embryo culture (WEC)

Female Sprague–Dawley rats were time-mated and obtained from Charles River (Portage, MI, USA). Females were checked for positive pregnancy by vaginal smear on the morning following copulation. The morning of a sperm-positive result was designated as gestational day

(GD) 0. Animals were kept on a 12-h–12-h light/dark cycle and were given food and water ad libitum. On the day of each experiment, dams were anesthetized, exsanguinated and sacrificed as previously described [19]. Conceptuses were explanted on GD10, prepared for culture and placed into 60-ml culture bottles containing 10 ml of control medium. Two different leupeptin exposure protocols were used, both starting with conceptuses explanted into culture on GD10. The first group, designated as "26 h," was exposed to 50 μM leupeptin by direct addition to the culture medium on the morning of explant and was assessed on GD11 after a total of 26 h in culture. In the second group, designated as "6 h," conceptuses were cultured for 20 h in control medium from GD10 and then treated with 100 μM leupeptin on GD11, beginning after the 95% O_2/5% CO_2 gas change, for a total treatment duration of 6 h. Conceptuses from four to six different litters were age-matched based on extent of neural tube closure and degree of axial rotation at the time of tissue collection and randomized across treatment groups to remove age and litter bias. Control medium contained 5 ml heat-inactivated rat serum and 5 ml 1× Hank's balanced salt solution (HBSS), supplemented with 43 μl of penicillin–streptomycin (10,000 U/ml). No more than 10 conceptuses were cultured in each bottle. To optimize growth, bottles were gassed on GD10 after explantation with 20% O_2/5% CO_2 and on the morning of GD11 with 95% O_2/5% CO_2. Culture bottles were incubated at 37°C in a roller apparatus throughout the culture period as described previously [10,19,20].

Exposure and sample collection

Leupeptin was suspended in double-distilled water and added to each culture bottle at the time of exposure to yield a 50-μM final concentration in the culture medium for 26-h exposures or a 100-μM final concentration for 6-h exposures. These concentrations were optimized for stage of

embryonic development and duration of culture based upon morphology, growth parameters, viability and the ability to inhibit proteolysis in WEC [10,21]. WEC of rat conceptuses for 26 h in concentrations of leupeptin up to 100 μM, beginning on GD10, maintains complete viability but reduces total EMB and VYS protein content. The 26-h exposures of 50 μM leupeptin result in viable, but much smaller, embryos with few gross anatomical defects but with a high incidence of avascular VYS, anophthalmia and some other defects of the optic field. No defects or growth restrictions were seen in the 6-h exposures under any condition. At the conclusion of the exposure, conceptuses were removed from the culture bottles and washed 2× in HBSS. The VYS and EMB were manually separated for each conceptus using watchmaker's forceps.

VYS and EMB samples for DNA isolation were pooled in duplicate, snap frozen and stored at−74°C. Samples to be assayed for Mat2a activity were pooled in triplicate and placed in 250 μl of reaction mixture composed of 50mMTris ethanesulfonic acid (TES), 50 mM KCl, 15 mM $MgCl_2$ and 0.3 mM EDTA prior to beginning the Mat2a activity protocol [22]. Samples for analysis of C_1 components were collected in 100 μl of reducing agent, consisting of 200 mM dithiothreitol and 100 mM NaOH in water. EMB and VYS tissues collected for immunoblotting were placed into 50 μl of radioimmunoprecipitation assay (RIPA) buffer, briefly sonicated and stored at −80°C until their use in the immunoblot protocol.

Mat2a specific activity

Mat2a activity was quantified in EMB and VYS crude homogenates based on the measured rates of new SAM biosynthesis from methionine and ATP. EMBs and VYSs were manually separated, placed into 250 μl of TES reaction buffer and snap frozen until incubation and

processing. Samples were thawed, gently sonicated and allowed to equilibrate by incubation at 37°C for 10 min. After that time, 20 μML-methionine and 5 mM ATP were added to the incubation mixture and allowed to react for 1 h at 37°C. Sodium acetate buffer (0.1 M) and 10% perchloric acid were added to the incubation mixture to terminate the reaction. The samples were then centrifuged at 10,500g for 2 min, the supernatant was removed to a new tube, and samples were processed for SAM determination as described above. Protein pellets were solubilized in 0.25 M sodium hydroxide, and total protein was determined using the bicinchoninic acid (BCA) procedure (Pierce, Rockford, IL, USA). Activities are expressed as μmol SAM synthesized/min, and data were normalized to protein values (mg) for determination of specific activities.

RNA isolation and quantitative polymerase chain reaction (qPCR)

RNA was isolated from EMB and VYS using the RNeasy Mini Kit (Qiagen, Valencia, CA, USA) as performed on a QIAcube (Qiagen). RNA was converted into cDNA using the RT2 First Strand Kit (SABiosciences, Valencia, CA, USA). Commercially available qPCR primers for Mat2a, Dnmt1, Dnmt3a, Dnmt3b and housekeeping gene ActB (SABiosciences) were used to detect changes in gene expression. cDNA, primers, and SYBR Green master mix (Qiagen) were added onto a 384-well plate, with each gene being run in triplicate for each sample. PCR was performed at the University of Michigan Microarray Core Facility using the 7900HT Fast Real-Time PCR System (Applied Biosystems, Carlsbad, CA, USA). Controls without template and controls without reverse transcriptase were performed for each sample to ensure run quality. Results were normalized to actin expression for each respective tissue and treatment.

Western/immunoblotting

Samples were thawed and sonicated in RIPA buffer. Protein concentrations were determined by BCA assay. Thirty micrograms of protein per sample was loaded and separated on a 12% sodium dodecyl sulfate polyacrylamide gel electrophoresis gel and transferred to a polyvinylidene fluoride membrane. The membrane was blocked overnight with tris-buffered saline with Tween (TBST)-milk at 4°C prior to a 2-h incubation with anti-Mat2a rabbit polyclonal antibody (Abcam, Cambridge, MA, USA) at a concentration of 1 μg/ml. The membrane was then washed with TBST prior to 2-h incubation with alkaline phosphatase (AP)-conjugated chicken anti-rabbit IgG (Santa Cruz, Santa Cruz, CA, USA) at a concentration of 1 μg/ml. Secondary antibody fluorescence was developed following reaction with ECF Substrate (GE Healthcare Life Sciences, Piscataway, NJ, USA) and visualized with a Fujifilm FLA-5000 Imager (Valhalla, NY, USA). Because Mat2a and actin have similar molecular weights, the membrane was cleared using Restore Western Blot Stripping Buffer (Pierce), washed twice with phosphate-buffered saline and washed twice with TBST. The membrane was then incubated for 2 h with anti-actin goat polyclonal antibody (Santa Cruz) at a concentration of 1 μg/ml. The membrane was washed with TBST and incubated for 2 h with AP-conjugated donkey anti-goat IgG (Santa Cruz) at a concentration of 1 μg/ml. Signals were visualized as above, and densitometric measurements were taken for both the Mat2a and actin images using Image Reader software (Fujifilm). Mat2a/actin ratios were calculated from densitometry data for all control and leupeptin-treated samples. Relative ratios from the normalized control and treated values were calculated to determine percent change between treatment groups.

C_1 component quantitation

Quantitation of SAM, total cysteine, methionine, homocysteine (Hcy) and dimethylglycine (DMG) was performed using a liquid chromatography–tandem mass spectrometry method for a TSQ Quantum (Thermo Scientific, Rockford, IL, USA) coupled with a Waters 2695 Separations Module outfitted with a Luna C18(2) 5-μm 250× 4.6-mm column and 4-mm C18 guard column (Phenomenex, Torrance, CA, USA) and recorded using Xcalibur software (Thermo Scientific). Sample preparation was done using a modified version of the protocol outlined by Weaving [23]. Briefly, samples were sonicated and incubated in the reducing agent at room temperature for 15 min. At this time, isotopic standards for each analyte were added at concentrations of 500 ng/ml SAM, 200 ng/ml DMG, 500 ng/ml cysteine, 10 ng/ml Hcy and 1000 ng/ml methionine. To suspend the C_1 components, 500 μl of a mixture containing 0.1% formic acid and 0.05% trifluoroacetic acid in water was added to each vial. Vials were centrifuged at 9000g for 2 min, and the supernatant was transferred to a high-performance liquid chromatographic vial for analysis.

Mobile phases were prepared, with buffer A being comprised of water with 0.1% formic acid and buffer B comprised of acetonitrile with 0.1% formic acid. An instrument method was programmed to start at 100% A, linearly transition to 90% A and 10% B over 10 min, return to 100% A after 15 s and hold there to equilibrate for a total of 30 min. Flow rate was set to 0.5 ml/min, and the injection volume was set at 10 μl. *m/z* transitions were optimized for detection of analytes and isotopic standards as follows: 399.1-249.9 (SAM), 402.1-249.9 (S-adenosylmethionine-d_3), 122.0-76.0 (cysteine), 124.0-78.0 (cysteine-d_2), 150.0-104.0 (methionine), 153.0-107.0 (methionine-d_3), 136.0-90.0 (Hcy), 140.0-94.0 (homocysteine-d_8), 104.0-58.0 (DMG) and 110.0-64.0 (N, N-dimethyl-d_6-glycine HCl). All parameters were optimized by direct infusion into the MS and tuning. Analyte concentrations were calculated by determining the ratio of analyte peaks to the known isotopic peak concentrations. Because

leupeptin may alter cellular protein pools, data were normalized using the control protein concentrations.

DNA isolation

Genomic DNA was isolated from EMB and VYS tissue using a phenol–chloroform extraction procedure. Briefly, thawed samples were homogenized in 540 µl of buffer ATL (Qiagen) and digested overnight at 50°C after addition of 60 µl proteinase K (Qiagen). Approximately 12 µl of 100 mg/µl RNase A (Qiagen) was added to the mixture before repeated extractions from phenol–chloroform isoamyl alcohol in phase-lock gel tubes (5 PRIME), followed by a chloroform-only wash. Finally, samples were precipitated in ethanol and dried prior to storage in Tris-EDTA buffer until use.

LUminometric Methylation Assay (LUMA) assay

LUMA was used to measure global methylation of EMB and VYS DNA [24-26]. Methylation-sensitive and -insensitive enzymatic digestion of 300 ng genomic DNA at CCGG sites was completed using HpaII and MspI enzymes (Invitrogen), respectively. Cleavage with EcoRI (Invitrogen) was also completed as an internal control. Annealing buffer (Qiagen) was added after digestion, and the products were analyzed using the PyroMark Q96 MD system (Qiagen). GTGTCACATGTGTG was used as the dispensation order to eliminate background. The MspI/HpaII ratios were calculated relative to the EcoRI control, and the percent methylation of each sample was calculated using the equation: $1-[(\text{HpaII/EcoRI})/(\text{MspI/EcoRI})]\times 100$. Samples were run in triplicate to account for within-sample variation.

Mat2a promoter methylation

Sodium bisulfite conversion of EMB and VYS DNA was completed utilizing the EpiTect Bisulfite Kit (Qiagen), and subsequent cleanup was accomplished using the QIAcube platform (Qiagen). PCR and pyrosequencing primers were designed using the PyroMark Assay Design 2.0 Software (Qiagen). The assay was designed against the reverse bisulfite-converted strand, and primer sequences and sequence for analysis are listed in Table 1. Within the sequence to analyze, the letter 'R' represents a site where a purine (either A or G) is interrogated, giving complementation to either cytosine or thymine. The primer amplicon falls within a CpG island on the Mat2a promoter upstream of the transcriptional start site. Of the eight sites investigated for CG methylation using this pyrosequencing assay, site 7 interrogates methylation at the GC box required for binding of the transcriptional factor Sp1 (Fig. 2.2). The region of interest was amplified using the bisulfite-converted DNA (2 µl), HotStarTaq master mix (Qiagen), reverse primer (0.5 pmol) and a biotinylated forward primer (0.5 pmol) in a PCR with an annealing temperature of 54°C. Amplified products were verified using gel electrophoresis and analyzed in duplicate using the PyroMark Q96 MD System (Qiagen) and a predetermined sequence-to-analyze run (Table 2.1). Two samples were excluded from the VYS leupeptin 26-h exposure group due to SNPs in the Mat2a locus.

Statistical analyses

Values presented are means±S.D. Statistical significance was determined using unpaired two-tailed Student's t tests and a confidence level of 95%. Statistical outliers were removed using a threshold of 1.5 times the interquartile range outside of the first and third quartile values.

Results

Mat2a specific activity

Mat2a enzyme specific activities (μmol SAM/min/mg protein) were determined in EMB and VYS based on SAM biosynthesis from methionine and ATP and were normalized to total protein concentrations (Fig. 2.3). Mat2a specific activities were almost identical (P=.991) in control EMB (3.06±0.42) and VYS (3.07±1.32). Following leupeptin treatment, Mat2a specific activities decreased significantly after 6 h in EMB (2.17±0.48) by 29% (P=.022). Similarly, leupeptin treatment in the VYS (0.08±0.02) reduced Mat2a specific activity by 97% (P=.007).

Mat2a and DNA methyltransferase (Dnmt) expression

Mat2a expression in EMB (1.34±0.05) was significantly higher than Mat2a expression in VYS (1.20±0.10; P=.020) (Fig. 2.4). No significant changes in Mat2a expression due to leupeptin treatment were produced in EMB (1.30±0.11; P=.429) or in VYS (1.24±0.13; P=.580). No changes were observed in Dnmt1, Dnmt3a or Dnmt3b expression due to leupeptin treatment, nor did expression differ by tissue for any gene (P>.1).

Mat2a and total protein quantification

Leupeptin treatment during the 6-h incubation on GD11 produced a 15.7%±0.1% decrease in Mat2a protein concentration in the EMB and a 59.2%±0.1% decrease in the VYS based on densitometry from the immunoblots (Fig. 2.5A,B). Mat2a densitometry results were normalized to the actin values from the same column of the gel. Total protein values, as determined by the BCA assay, were increased by 79.3% in the VYS and 18.4% in the EMB following 6-h leupeptin treatment (Fig. 2.5C). The total protein effects of leupeptin treatment significantly differed by tissue (P=.001), and the increase in the VYS was statistically significant (P<.001).

C_1 component concentrations

C_1 component concentrations (μg) were quantified for each sample to determine whether leupeptin inhibition of protease activities in the VYS results in depletion of cellular substrates for C1 metabolism in the EMB and VYS after a 6-h exposure (Table 2.2). Control EMB SAM concentrations (1.22±0.30; n=6) were significantly greater than control VYS concentrations (0.21±0.06; n=6; P<.001). Although SAM concentrations were decreased in EMB due to leupeptin treatment, variability was high in the leupeptin-treated samples. For this reason, no statistically significant difference was observed between control EMB and leupeptin-treated EMB (0.75± 0.81; n=6; P=.237). In the VYS, leupeptin-treatment significantly reduced SAM concentrations compared to control concentrations (0.10±0.07; P=.012).

Methionine concentrations in control EMB (1.74±0.58; n=6) were significantly higher than control VYS methionine concentrations (0.67±0.34; n=6; P=.003) (Table 2.2). Leupeptin treatment significantly reduced methionine concentrations in EMB (0.24±0.10; n=6; P=.001) as well as in VYS (0.17±0.01; n=4; P=.015). Cysteine concentrations in control EMB (6.37±2.18;

n=6) and control VYS did not significantly differ (4.81±1.55; n=5; P=.211). Leupeptin treatment significantly reduced cysteine concentrations in EMB (2.67±0.81; n=6; P=.003). Leupeptin treatment yielded a 56% increase in cysteine concentrations in VYS, though this change was not statistically significant (7.52±2.59; n=6; P=.071).

Control EMB Hcy concentrations (0.46±0.04; n=5) and control VYS concentrations did not significantly differ (0.57±0.20; n=6; P=.258). Leupeptin treatment yielded no significant effect on Hcy in EMB (0.47±0.90; n=5; P=.998) or in VYS (0.54±0.12; n=6; P=.738). DMG concentrations were below the limit of detection in VYS for this method, so no results can be reported on this trend. In EMB, leupeptin-treated EMB (0.11±0.03; n=6) had higher DMG concentrations than controls, though this change was not statistically significant (0.09±0.03; n=6; P=.196).

Global methylation levels

Global DNA methylation status was quantified in the conceptus using the LUMA assay. Embryos and VYSs were assayed separately on GD11 with and without leupeptin treatment as described for each of the 26-h and 6-h exposure protocols. Control EMB DNA was found to be 75.63%±3.30% and 72.42%±3.29% methylated in the 6-h and 26-h protocols, respectively (Fig. 6). These differences were not significant. Untreated VYS controls were methylated at a significantly lower rate than their corresponding embryos at 57.94%±8.20% and 53.44%±6.64%, respectively, for the 6-h (P<.001) and 26-h (P<.001) protocols. Leupeptin treatment significantly reduced embryo methylation to 71.00%±3.71% after 6-h exposure (P=.009) in the EMB and to 50.58%±6.55% (P=.05) in the VYS compared to untreated controls (Fig. 2.6A). Leupeptin

treatment for 26 h in the VYS reduced the global methylation percentage to 66.00%±5.13% in the EMB (P=.007) and to 45.45%±9.45% in the VYS (P=.05) (Fig. 2.6B).

Mat2a promoter methylation

Because Mat2a contains several CpG sites flanking an Sp1 transcription factor binding site, it was important to identify whether changes in histiotrophic nutrition may indirectly affect genome-wide epigenetic regulation via hypermethylation of the Mat2a promoter and decreased Mat2a expression and activity. After disruption of endocytosis, no significant changes in methylation at CpG sites in the Mat2a promoter were observed (Fig. 2.7). Mat2a exhibited low methylation levels at this locus across all tissues, exposures and exposure durations (Fig. 2.7A,B). The individual CpG site 7 (Fig. 2.7C,D) showed increased methylation levels compared to other sites in the Mat2a locus, but did not reveal significant methylation effects by tissue type or exposure group.

Discussion

Genetics play a large role in instructing phenotypic outcomes during development, but these regulatory controls are complemented by nutrients, environmental factors, and physical insults that inform the epigenetic patterning required for differentiation and the establishment of terminal cell fates and functions. Because the placenta is not yet formed or fully functional during the early post-implantation phases of development, histiotrophic uptake of maternal proteins and their cargos, as facilitated by RME, represents the primary source of nutrient supply during organogenesis. While well established in rodent models, the relevant importance of histiotrophic

processes in human embryonic development has been debated. Even though significant anatomical differences exist between the maternal–conceptal interface and the duration of gestation of rodents and humans, recent evidence also strongly supports a significant role for HNP in mediating nutrient uptake in the human conceptus until the time when the placenta becomes fully functional at the end of the first trimester [27,28]. Nutrients, in the form of vitamins, precursors and cofactors that are important for C_1 metabolism and other cellular processes, are believed to be obtained exclusively through HNP by uptake across maternal–conceptual interfaces such as the syncytiotrophoblast and VYS during the organogenesis stage of embryonic development [14,15,28]. Bulk proteins are captured into vesicles, fused with lysosomes in these tissues and degraded by cysteine proteases to provide amino acids for embryonic biosynthesis. Leupeptin inhibition of lysosomal proteolysis in the VYS during early organogenesis prevents the degradation of maternal proteins, thus limiting the availability of methionine and other components required for biosynthesis of SAM in the embryonic C_1 pathways. Our hypothesis states that interruption of HNPs should decrease SAM biosynthesis and its cellular concentrations due to the reduced supply of substrates and precursors required for C_1 metabolism and, as a result, affect the overall extent of DNA methylation required to sustain normal epigenetic programming.

In the HNP model, leupeptin should cause a decrease in C_1 precursors available for methylation processes. Table 2.2 shows changes in methionine and total cysteine in both the EMB and the VYS, although the magnitude of these changes differs by tissue. Methionine is significantly decreased due to leupeptin treatment in both the EMB and VYS, as would be expected from disruption of HNPs. Total cysteine, on the other hand, decreased in the EMB and increased in the VYS. Decreases in total cysteine in the EMB can be explained by inhibition of source protein degradation in the VYS. Increases in total cysteine in the VYS may be related to changes in the

dynamic balance of cysteine transport and utilization that occur in biosynthesis pathways, such as incorporation into GSH. Hcy and DMG (C_1 metabolic products) remain unchanged following treatment and exhibit no tissue differences in cellular concentrations.

The disruption of HNPs and altered methionine and cysteine in the EMB and VYS are accompanied by an approximate 52% decrease in SAM in the VYS and a 39% decrease in SAM in the EMB. The significant decrease in SAM in the VYS is expected based on the reduction of methionine available for synthesis. A change in the EMB was noted, but was not significant, due to the high variability of SAM in the EMB after leupeptin treatment. This suggests that leupeptin treatment introduces a degree of instability in the EMB, likely resulting in disruption of multiple cellular processes. The difference in SAM concentrations between EMB and VYS is also notable. SAM concentrations in the EMB are nearly six times those found in the VYS.

In this study, we have identified several C_1 metabolism-related outcomes that are affected by the disruption of HNPs and the attenuated provision of nutrients to the developing conceptus. SAM is the critical final product of C_1 metabolism and is essential for its role in for epigenetic programming. Variations in several other C_1 substrates and cofactors that contribute to SAM biosynthesis (folate, choline, vitamin B_{12}) have also been associated with malformations and abnormal developmental outcomes. The conceptal bioavailability of these substrates and cofactors as a function of maternal diet and changes in their concentrations due to chemicals and environmental factors has yet to be characterized. In future studies, we hope to determine whether depletion of these substrates required by the C_1 pathway occurs due to exposure in utero and whether dietary supplementation of C_1 metabolic precursors may be a potential intervention against developmental growth deficiencies and embryotoxicity.

The enzyme Mat2a is responsible for the final catalytic step in SAM biosynthesis, combining adenosine from ATP with methionine. Lack of sufficient precursors could limit SAM biosynthesis as proposed, but other direct effects on the enzyme itself cannot be ruled out. Six-hour GD11 exposure to leupeptin in WEC produced a significant reduction in Mat2a specific activity in both the EMB and the VYS, which is consistent with observed decreases in SAM concentrations. Mat2a specific activities (Fig. 2.3) were normalized to total sample protein according to accepted protocols. Because of leupeptin's inhibition of proteolytic activity in the VYS and the continued endocytotic uptake of maternal proteins, total protein in the VYS was significantly increased over that normally found in the untreated VYS (Fig. 2.5C). This results in a decrease in Mat2a protein to total protein ratio. Because this affects the specific activity calculation, Mat2a specific activity was also calculated using control protein values for normalization (Fig. 2.8). The reductions in Mat2a specific activity in both the EMB and VYS remained statistically significant, again supporting the decreases in SAM concentrations.

Mat2a expression was unchanged in both the EMB and the VYS after treatment, and DNA methylation was extremely low in the CpG island flanking the Sp1 regulatory region of the *Mat2a* promoter. The *Mat2a* promoter region was found to be virtually unmethylated, indicating that any further decreases in methylation due to the leupeptin-induced reductions in SAM availability are, therefore, not expected. The lack of significant alterations in Mat2a expression and methylation can be expected, as the product of this gene plays a very important functional role in the cell in catalyzing the final step of SAM biosynthesis and would, therefore, be expected to be constitutively expressed. Regulation is likely to be mediated through cellular sensors that may not be easily induced or suppressed. As the universal methyl donor in cells, SAM availability is critical for methylation processes in epigenetic programming such as for DNA and histone methylation.

Because methylation is a semipermanent modification, methylation would not be a likely regulatory mechanism for Mat2a expression.

Immunoblot data suggest reduced Mat2a protein concentrations in both the EMB and VYS due to leupeptin treatment, with a more profound decrease in Mat2a in the VYS. However, these changes may not be entirely accurate due to the significant leupeptin-induced differences in relative total protein concentrations in the EMB and VYS. Decreased proteolysis due to leupeptin treatment increases the total cellular protein content, mostly contained in endocytotic vesicles, and reduces the relative proportion of intrinsic proteins and enzymes active in cellular processes. Thus, this decrease in Mat2a abundance in the EMB and VYS may be partly artifactual due to these altered protein proportions.

Because both Mat2a specific activity and protein concentration decrease with inhibition of HNPs, it is important to consider the regulation of the Mat2a protein. It is possible that redox signaling may play a role in Mat2a regulation. Oxidative modifications to the cysteine-150 residue of the Mat2a peptide has been shown to lead to a loss of activity and dissociation of the tetrameric complex, likely because the residue falls within the Mat2a ATP binding site [29]. Thus, it is possible that oxidative stress may be able to decrease the catalytic activity of Mat2a by a directed posttranslational modification. Preliminary evidence from our laboratory suggests that attenuation of HNP activity leads to decreases in GSH biosynthesis and a shift to more oxidizing conditions in the conceptus [30]. Direct regulation of Mat2a may also explain changes in specific activity and protein abundance. Degradation of the Mat2a protein by compensatory protease activity may be increased due to leupeptin treatment. It is also possible that the Mat2a protein has a high turnover rate. If the Mat2a protein has fast rates of both biosynthesis and degradation, disruption of HNPs would decrease the amount of amino acids needed for new protein synthesis and shift the balance

in favor of lower Mat2a concentrations. Ultimately, these regulatory changes may lead to altered Mat2a function and cellular abundance.

Epigenetic modifications, like DNA methylation, are crucial for normal development. The disruption of HNPs and resulting decrease in C_1 components such as SAM may lead to a decrease in the substrates available for methylation processes and/or changes in methylation and demethylation enzymes required for modifications. Expression of Dnmt1, Dnmt3a and Dnmt3b was unchanged in both the EMB and VYS. Because these are the enzymes directly involved in the placement of methyl groups on the DNA, it is suggested that regulation of DNA methylation in this case does not occur at the transcriptional level. It is likely that these enzymes are constitutively expressed during this period of development, as epigenetic patterning is being established in tissues.

Using the LUMA assay to measure global DNA methylation at CCGG sites, it was shown that EMB and VYS differ significantly with regards to their baseline percentage of global methylation. Average methylation values in the EMB approached 72%, while VYS values were found to be about 58%. The EMB and VYS tissues differ with respect to their relative states of terminal differentiation, cellular homogeneity, imprinting patterns and embryonic germ line of origin, all of which have been previously noted as being important factors for differential methylation status [31]. It is quite possible that differences of similar magnitude may also exist within the EMB proper based on the high degree of cell and tissue heterogeneity present during this stage of development, but the details of spatial methylation patterns are not known.

Along with significant differences in basal levels of global methylation, for each of the treatment protocols, leupeptin produced a significant additional reduction in DNA methylation in EMBs from 6% to 9% and in VYS from 11% to 15%. The ability of leupeptin to significantly

reduce global methylation levels in WEC after only 6 h of treatment is remarkable. Of interest is the observation that leupeptin exposure for periods of time much longer than 6 h did not produce any additional changes in the percentage decrease in global DNA methylation levels. This suggests that the full range of methylation-related events occurs rapidly in the conceptus and that a threshold of change exists, beyond which no additional demethylation will occur. Several different factors could be responsible for the decrease in global methylation levels, including (a) a reduction in the developmentally programmed and ongoing DNA remethylation events aided by insufficient SAM availability; (b) the inability of the conceptus to maintain established DNA methylation marks, including those that are replicated through successive cell generations via enzymatic DNMT1 maintenance activity; and (c) the demethylation of existing DNA methylation marks. Further investigations into the regulation of DNMT function by environmental and biochemical factors will be required to understand this potential mechanism of susceptibility. Because epigenetic programming during this stage of development is crucial for differentiation, normal tissue patterning and growth, significant modifications of the global epigenome would be expected to exert their effects on embryonic viability and the elicitation of morphological defects. Based on the significant decreases in global methylation observed, however, it is reasonable to expect that methylated regulatory sites throughout the epigenome may be subject to demethylation. Thus, epigenome-wide DNA methylation studies will be necessary to fully identify the subset of regulatory regions that are sensitive to epigenetic change during this phase of development.

To summarize, decreased amounts of C_1 precursors lead to decreased SAM and global DNA methylation. It is likely that Mat2a plays a large role in the regulation of these methylation processes, as SAM concentrations mimic Mat2a activity. It is unknown at this time how other changes in HNPs, such as disruption of RME, may also alter these processes. Because RME is

responsible for the uptake of C_1 substrates such as folate, choline, betaine and B vitamins at this stage of development, modifications to the endocytotic potential of the VYS may be able to produce detrimental epigenetic effects in the developing EMB. Future investigation into the relationships between toxicant-induced changes in these processes and the nutrient environment of the conceptus is necessary to understand the pathways by which developmental exposures may contribute to abnormal epigenetic programming.

In conclusion, this study identifies a window of susceptibility during which the developing epigenome may be affected by nutrients and environmental factors during organogenesis. Disruption of HNPs leads to decreased availability of C_1 components, reduced Mat2a activity and decreased global DNA methylation in the VYS and EMB. All of these changes indicate that histiotrophic nutrition is crucial for epigenomic programming in the early organogenesis-stage conceptus. Tissue-specific differences between EMB and VYS were evident throughout this study, corresponding with divergence in degrees of differentiation and homogeneity. Environmental hindrance of HNPs may epigenetically alter gene expression in the conceptus, and these changes may be detrimental throughout the life course. Further investigation into the specific pathways and products being altered by dietary factors and chemical exposures, namely, HNPs and C_1 metabolism, which lead to developmental abnormalities and predisposition to disease throughout the life course, is crucial to understanding the overlaying role of embryonic nutrition during development.

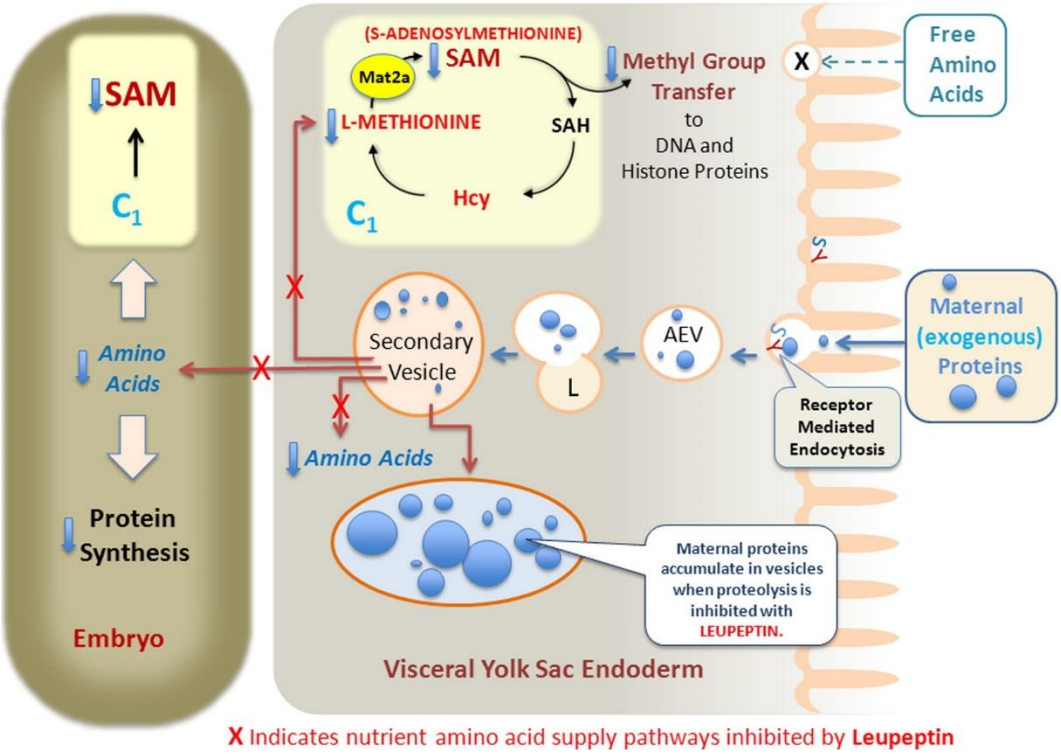

Figure 2.1. HNPs influence C_1 metabolism, SAM biosynthesis and DNA methylation. HNPs are the primary mechanism of nutrient supply during early organogenesis. Histiotrophic functions include RME and proteolysis of endogenous nutrient proteins taken up through the VYS brush border. After proteolysis, resulting amino acids are made available for cellular functions such as protein biosynthesis and C_1 metabolism. Leupeptin treatment inhibits proteolysis, limits the availability of critical substrates through pathways (marked with an X) and results in limited biosynthesis of biomolecules (down arrows). This figure summarizes our hypothesis, showing the reduction of precursors to pathways, through which SAM, the primary methyl donor for DNA (and other molecule) methylation, is generated. The lack of SAM will limit DNA methylation and result in the observed global DNA hypomethylation.

Figure 2.2. Sequence of the 5' flanking region of the rat Mat2a gene. The forward (biotinylated) and reverse primers bind to the bisulfite-converted sequence of the italicized region above, producing a 201-bp pyrosequencing amplicon highlighted in the box. A sequencing primer anneals to the TATA box region and extends in the opposite direction to interrogate eight individual CpG sites for methylation surrounding the Sp1 transcription factor binding GC box.

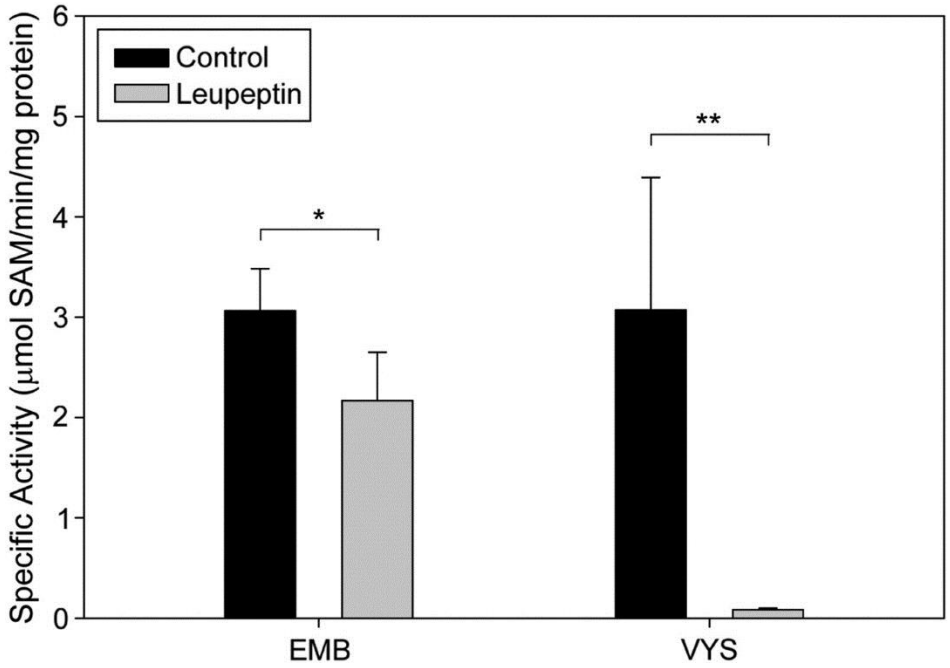

Figure 2.3. Mat2a specific activity after 6-h leupeptin exposure. Mat2a specific activities are decreased by leupeptin exposure in both EMB and VYS. Mat2a activity is similar in the EMB (n = 4) and VYS (n = 5) under control conditions. Specific activity is significantly reduced by leupeptin treatment in the EMB (n = 5; P = .022) and in the VYS (n = 5; P = .007). **P < .01; *P < .05.

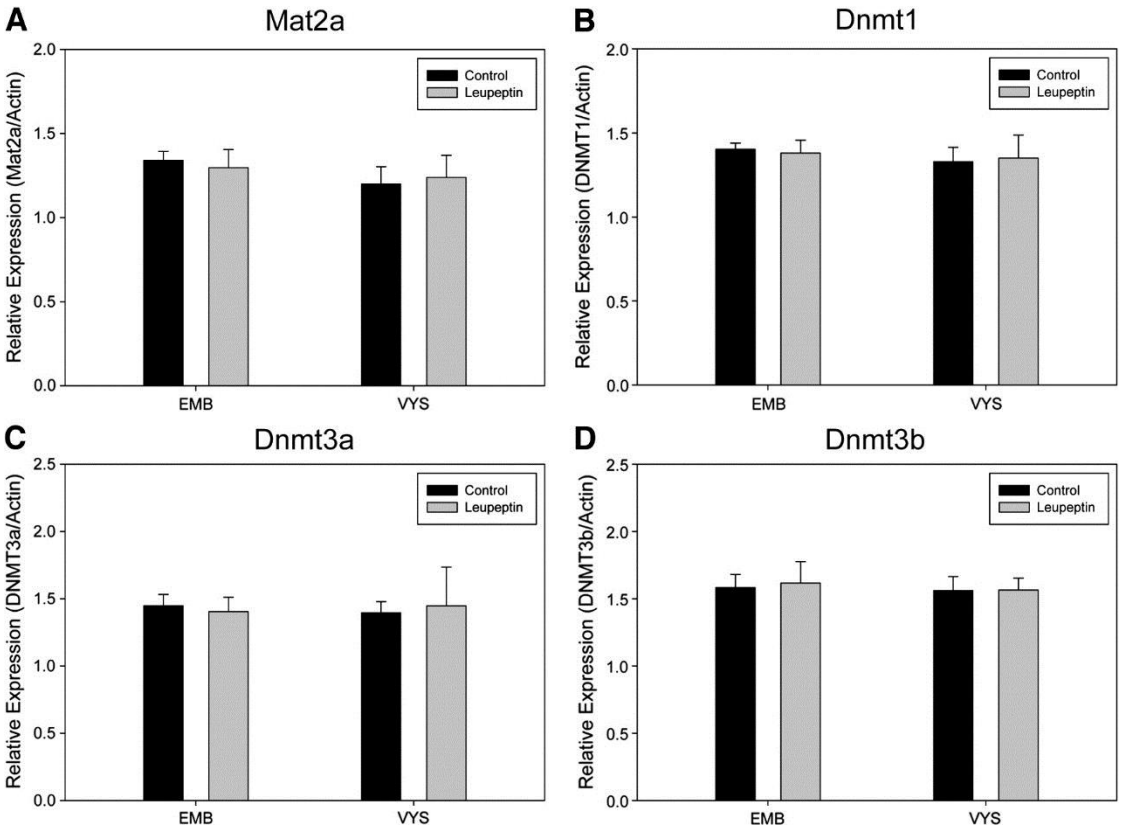

Figure 2.4. Mat2a, DNMT1, DNMT3a and DNMT3b gene expression after 6-h leupeptin treatment. Mat2a gene expression was significantly higher in the EMB (n = 5) than the VYS (n = 6; P = .02). No statistically significant changes were noted between control (n = 5) and leupeptin-treated (n = 6) EMB for any of the gene targets tested (P > .1). Likewise, no significant changes occurred in the control (n = 6) or leupeptin-treated (n = 6) VYS samples (P > .1) for all targets.

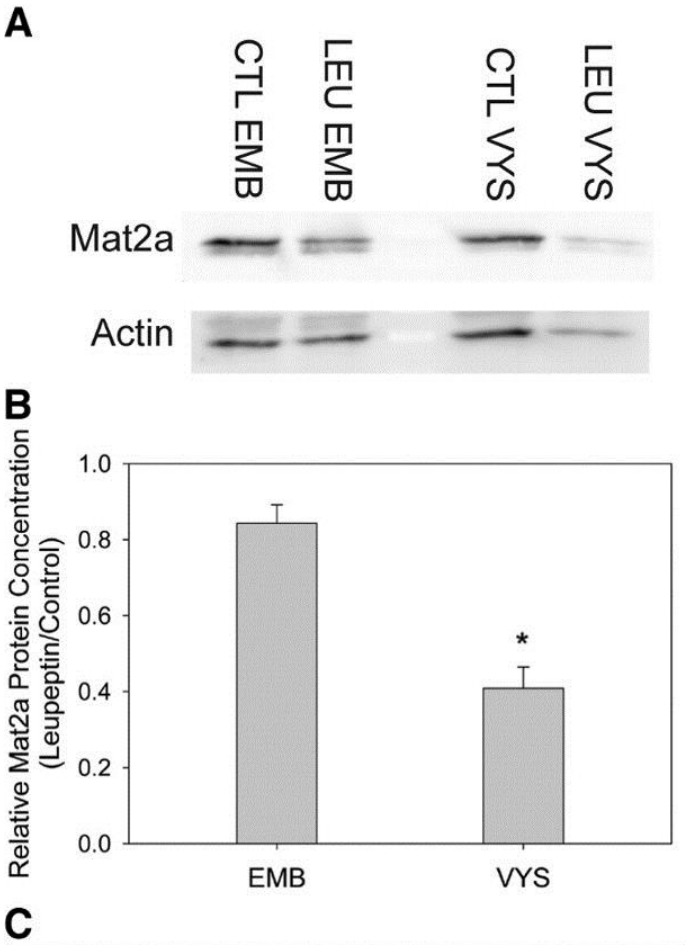

C

Total protein (ug) by tissue and treatment

Tissue	Control	Leupeptin-treated	% Change
EMB	736.8 ± 65.2	872.1 ± 219.4	+ 18.4%
VYS	594.3 ± 134.2	1065.3 ± 105.5**	+ 79.3%

Figure 2.5. Mat2a protein concentrations and total protein content after 6-h leupeptin treatment. Densitometric readings following Western blotting (A) revealed a significant effect difference between EMB (n = 3) and VYS (n = 3; P = .001), indicating that leupeptin treatment produced a more significant decrease in the Mat2a protein in the VYS (−59%) than the EMB (−16%) (B). However, the accumulation of extrinsic proteins due to leupeptin treatment also results in an 18% increase in total protein in the EMB and 79% in the VYS (C). *P = .001; **P < .001.

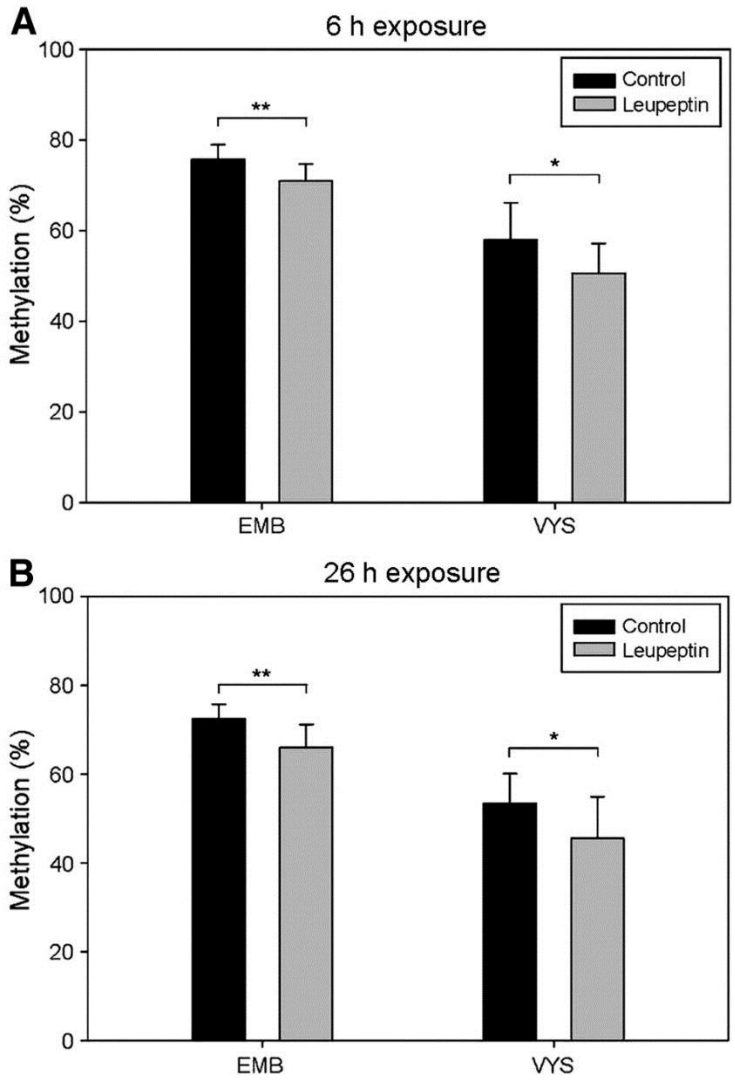

Figure 2.6. Global percent methylation for EMB and VYS tissues after 6-h or 26-h exposure determined by LUMA. EMB percent methylation is significantly higher than VYS methylation across all tissues ($P < .001$). (A) Control EMB (n = 10) was significantly higher than leupeptin EMB (n = 10) after 6-h exposure ($P = .009$). Control VYS (n = 11) methylation was significantly higher than leupeptin VYS (n = 8; $P = .05$). (B) Control EMB (n = 9) was significantly higher than leupeptin EMB (n = 8) after 26-h exposure ($P = .007$). Control VYS (n = 10) was higher than leupeptin VYS (n = 8; $P = .05$). (A and B) Control EMB and leupeptin EMB both showed significant decreases in percent methylation between 6- and 26-h exposure ($P = .05$ and .03, respectively). VYS showed no significant change over time. **$P < .01$; *$P < .05$.

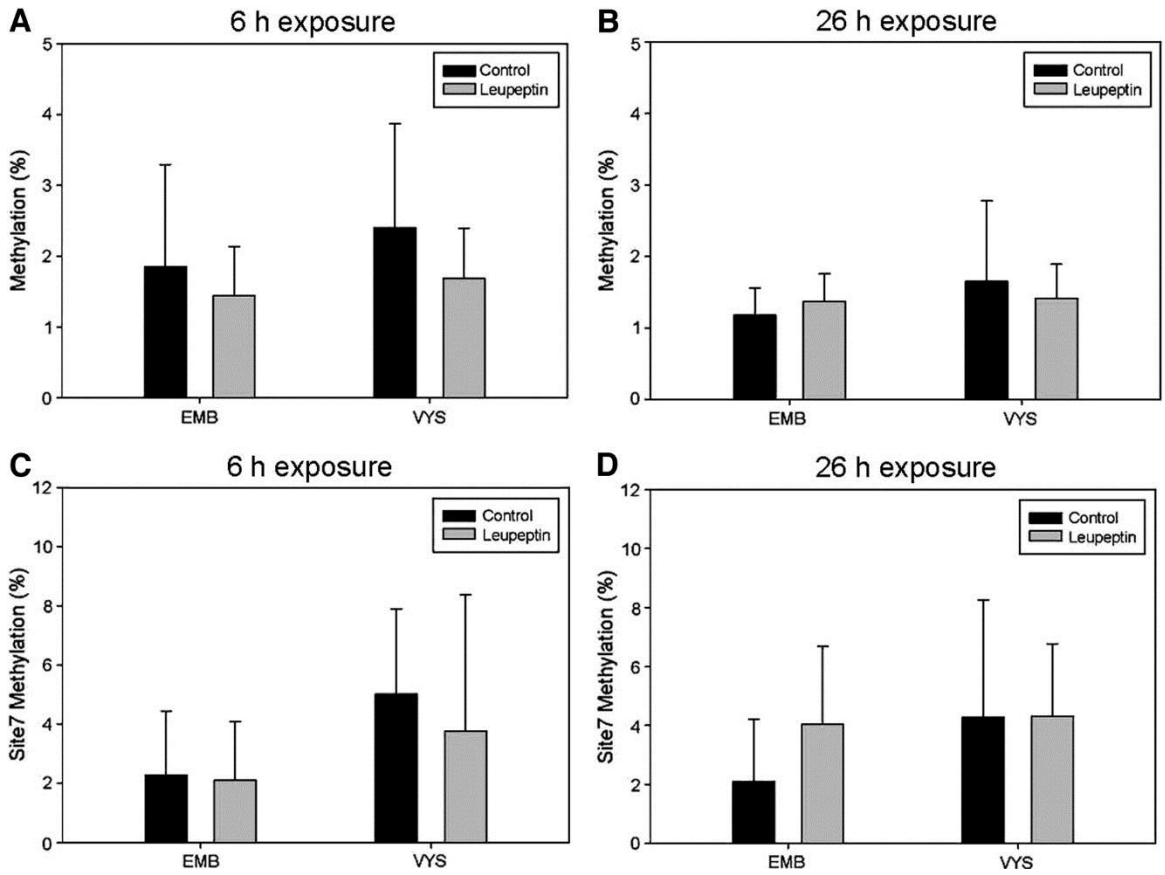

Figure 2.7. Mat2a promoter methylation levels determined by pyrosequencing. The Mat2a promoter exhibits low methylation levels surrounding the Sp1 binding site in both the EMB and VYS after 6-h or 26-h leupeptin exposure. (A) No significant difference was detected between control EMB (n = 10) and leupeptin EMB (n = 10) after 6-h exposure, or between control VYS (n = 10) and leupeptin VYS (n = 9). (B) Likewise, there was no significant difference between control EMB (n = 8) and leupeptin EMB (n = 8) after 26-h exposure, or between control VYS (n = 8) and leupeptin VYS (n = 6). (C) Although individual CpG site 7 methylation is above average for the Mat2a locus assayed, no significant changes in methylation were apparent for tissues after 6-h leupeptin exposure. (D) No statistically significant changes in CpG site 7 methylation were detected after 26-h leupeptin exposure.

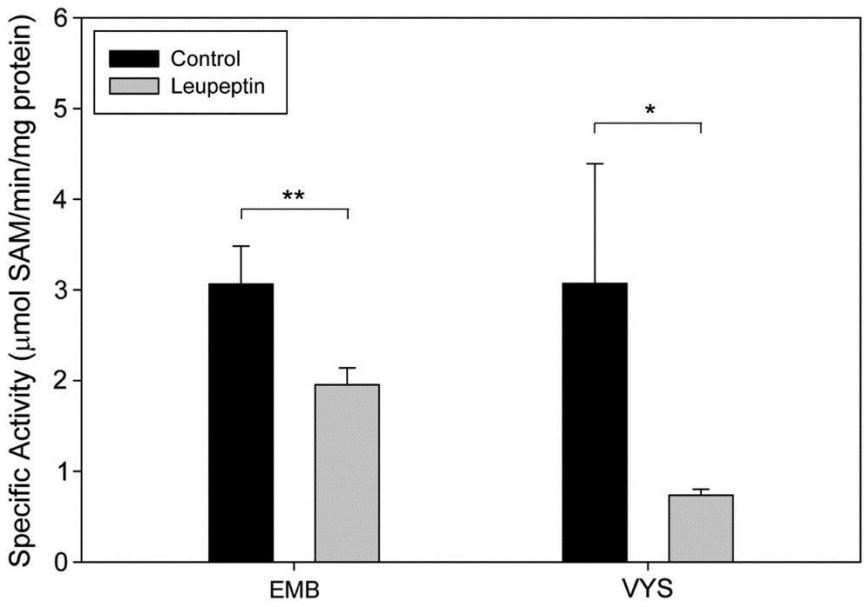

Figure 2.8. Control-normalized Mat2a specific activity after 6-h leupeptin exposure. Because leupeptin inhibits protein degradation in the VYS without diminishing the continuous uptake of extraconceptal proteins from the media via RME, treated VYSs accumulate more total protein than the corresponding controls. This results in the protein of interest representing a significantly lower proportion of the total measured protein content in the VYS. In order to account for the exogenously increased protein in the VYS, Mat2a specific activities were also calculated using the concurrent control protein concentrations to normalize the data. Using this approach, leupeptin treatment on GD11 produced a significant 36% decrease in Mat2a specific activity in the EMB (1.95 ± 0.19; P = .003). In the VYS, leupeptin treatment yielded a significant 76% decrease in Mat2a specific activity (0.74 ± 0.07; P = .017). These results corresponded with the specific activity data shown in Fig. 3, strengthening the relationship between leupeptin treatment and the reduction in Mat2a specific activity.

Table 2.1. PCR and pyrosequencing primers (5' to 3') and analyzed sequence for the Mat2a promoter.

Primer type	Primer sequence	Melting temp (°C)
Forward-biotinylated	GTTATTAGGATGATTAATTATTGTTAGG	54.5
Reverse	ACCCAATATTTATAAAACAACTCC	56.3
Sequencing	CAATATTTATAAAACAACTCC	40.8
Sequence to analyze	CRCRCRCRCCCRACTCRAACCCCRCCCCTCRACRTCRCRCRCCAATACRCCACRAACAAACRAAT	

Table 2.2. Leupeptin-induced effects on bioavailability (µg) of C1 metabolism components concentrations in EMB and VYS.

Component	Control	Leupeptin-treated
SAM		
EMB	1.22 ± 0.30	0.75 ± 0.81
VYS	0.21 ± 0.06[a]	0.10 ± 0.07[c]
Methionine		
EMB	1.74 ± 0.58	0.24 ± 0.10[b]
VYS	0.67 ± 0.34a	0.17 ± 0.01[c]
Cysteine (total)		
EMB	6.37 ± 2.18	2.67 ± 0.81b
VYS	4.81 ± 1.55	7.52 ± 2.59
Hcy		
EMB	0.46 ± 0.04	0.47 ± 0.90
VYS	0.57 ± 0.20	0.54 ± 0.12
DMG		
EMB	0.09 ± 0.03	0.11 ± 0.03
VYS	ND	ND

'ND' signifies that no data were collected due to results falling below the limit of detection.

[a] Indicates a significant difference between control EMB and control VYS (P<.05).

[b] indicates a significant difference between control EMB and leupeptin-treated EMB (P<.05).

[c] indicates a significant difference between control VYS and leupeptin-treated VYS (P<.05).

References

1. Bird, A.P., *Gene number, noise reduction and biological complexity.* Trends in Genetics, 1995. **11**(3): p. 94-100.
2. Dolinoy, D.C., J.R. Weidman, and R.L. Jirtle, *Epigenetic gene regulation: Linking early developmental environment to adult disease.* Reproductive Toxicology, 2007. **23**(3): p. 297-307.
3. Reik, W., W. Dean, and J. Walter, *Epigenetic Reprogramming in Mammalian Development.* Science, 2001. **293**(5532): p. 1089-1093.
4. Senner, C.E., *The role of DNA methylation in mammalian development.* Reproductive biomedicine online, 2011. **22**(6): p. 529-535.
5. Melcer, S. and E. Meshorer, *Chromatin plasticity in pluripotent cells.* Essays in Biochemistry, 2010. **48**(1): p. 245-62.
6. Bernal, A.J. and R.L. Jirtle, *Epigenomic disruption: The effects of early developmental exposures.* Birth Defects Research Part A: Clinical and Molecular Teratology, 2010. **88**(10): p. 938-944.
7. Faulk, C. and D.C. Dolinoy, *Timing is everything: The when and how of environmentally induced changes in the epigenome of animals.* Epigenetics, 2011. **6**(7): p. 791-797.
8. Burdge, G.C. and K.A. Lillycrop, *Nutrition, Epigenetics, and Developmental Plasticity: Implications for Understanding Human Disease.* Annual Review of Nutrition, 2010. **30**(1): p. 315-339.
9. Bateson, P., et al., *Developmental plasticity and human health.* Nature, 2004. **430**(6998): p. 419-421.
10. Ambroso, J.L., et al., *Fluorometric analysis of endocytosis and lysosomal proteolysis in the rat visceral yolk sac during whole embryo culture.* Teratology, 1997. **56**(3): p. 201-209.
11. Fisher, C.E. and S.E.M. Howie, *The role of megalin (LRP-2/Gp330) during development.* Developmental Biology, 2006. **296**(2): p. 279-297.
12. Hammad, S.M., et al., *Megalin Acts in Concert with Cubilin to Mediate Endocytosis of High Density Lipoproteins.* Journal of biological chemistry, 2000. **275**(16): p. 12003-12008.
13. Moestrup, S.K. and P.J. Verroust, *Megalin- and Cubilin-Mediated Endocytosis of Protein-Bound Vitamins, Lipids, and Hormones in Polarized Epithelia.* Annual Review of Nutrition, 2001. **21**(1): p. 407-428.
14. Beckman, D.A., et al., *Sources of amino acids for protein synthesis during early organogenesis in the rat. 1. Relative contributions of free amino acids and of proteins.* Placenta, 1990. **11**(2): p. 109-121.
15. Beckman, D.A., et al., *Sources of amino acids for protein synthesis during early organogenesis in the rat. 2. Exchange with amino acid and protein pools in embryo and yolk sac.* Placenta, 1991. **12**(1): p. 37-46.
16. Freeman, S.J. and J.B. Lloyd, *Evidence that protein ingested by the rat visceral yolk sac yields amino acids for synthesis of embryonic protein.* J Embryol Exp Morphol, 1983. **73**(1): p. 307-315.
17. Lloyd, J.B., R.L. Brent, and D.A. Beckman, *Sources of amino acids for protein synthesis during earlyorganogenesis in the rat. 3. Methionine incorporation.* Placenta, 1996. **17**(8): p. 629-634.
18. Freeman, S.J. and J.B. Lloyd, *Inhibition of proteolysis in rat yolk sac as a cause of teratogenesis. Effects of leupeptin in vitro and in vivo.* Journal of embryology and experimental morphology, 1983. **78**(1): p. 183-193.
19. Harris, C., M. Dixon, and J.M. Hansen, *Glutathione depletion modulates methanol, formaldehyde and formate toxicity in cultured rat conceptuses.* Cell Biology and Toxicology, 2004. **20**(3): p. 133-145.
20. Fantel, A.G., R. Bechter, and D. Beckman, *Rat Embryo Cultures for In Vitro Teratology*, in *Current Protocols in Toxicology*, L.G. Costa, et al., Editors. 2001, John Wiley & Sons, Inc. p. 13.2.1–13.2.12.

21. Ambroso, J. and C. Harris, *In vitro embryotoxicity of the cysteine proteinase inhibitors benzyloxycarbonyl-phenylalanine-alanine-diazomethane (Z-Phe-Ala-CHN2) and benzyloxycarbonyl-phenylalanine-phenylalanine-diazomethane (Z-Phe-Phe-CHN2).* Teratology, 1994. **50**(3): p. 214-228.
22. Jani, T.S., et al., *Inhibition of methionine adenosyltransferase II induces FasL expression, Fas-DISC formation and caspase-8-dependent apoptotic death in T leukemic cells.* Cell Res, 2009. **19**(3): p. 358-369.
23. Weaving, G., et al., *Simultaneous quantitation of homocysteine, cysteine and methionine in plasma and urine by liquid chromatography-tandem mass spectrometry.* Annals of Clinical Biochemistry, 2006. **43**(6): p. 474-480.
24. Karimi, M., S. Johansson, and T. Ekström, *Using LUMA: a Luminometric-Based Assay for Global DNA-Methylation.* Epigenetics, 2006. **1**(1): p. 45-48.
25. Karimi, M., et al., *LUMA (LUminometric Methylation Assay)—A high throughput method to the analysis of genomic DNA methylation.* Experimental Cell Research, 2006. **312**(11): p. 1989-1995.
26. Poage, G.M., et al., *Global Hypomethylation Identifies Loci Targeted for Hypermethylation in Head and Neck Cancer.* Clinical cancer research, 2011. **17**(11): p. 3579-3589.
27. Burton, G.J., J. Hempstock, and E. Jauniaux, *Nutrition of the human fetus during the first trimester--a review.* Placenta, 2001. **22 Suppl A**: p. S70-7.
28. Burton, G.J., et al., *Uterine glands provide histiotrophic nutrition for the human fetus during the first trimester of pregnancy.* J Clin Endocrinol Metab, 2002. **87**(6): p. 2954-9.
29. Pajares, M., et al., *The role of cysteine-150 in the structure and activity of rat liver S-adenosyl-L-methionine synthetase.* Biochem J., 1991. **274**: p. 225-229.
30. Harris, C., et al., *Inhibition of glutathione biosynthesis alters compartmental redox status and the thiol proteome in organogenesis-stage rat conceptuses.* Free Radical Biology and Medicine, 2013. **63**(0): p. 325-337.
31. Kiefer, J.C., *Epigenetics in development.* Developmental Dynamics, 2007. **236**(4): p. 1144-1156.

Chapter III

Mono-2-ethylhexyl phthalate disrupts neurulation and modifies the embryonic redox environment

Introduction

Development is a highly regulated process that relies on tightly controlled intra- and intercellular signaling for normal growth. Dysregulation of embryogenesis can be caused by a myriad of genetic, physiological, and environmental factors, and can alter specific signaling pathways to manipulate cell polarity and migration, membrane transport, and protein structure and function [1-4]. Ultimately, these changes may potentially manifest as spontaneous abortion, birth defects, or predispose individuals to diseases that arise during childhood and into adulthood. One such factor that may lead to this dysregulation is altered redox signaling and control, or perturbations of soluble thiol status from the steady state [5]. Classically, many teratogens, or compounds that produce congential malformations, were thought to act via classical oxidative stress: a change from a balanced and reducing intracellular redox environment to predominantly oxidizing conditions, concurrent with the generation of reactive oxygen species (ROS) [6]. An oxidizing environment during development has been associated with increased risk of diseases including neurodegeneration, hypertension, cancer, and Type II Diabetes [7-9]. However, ROS are now known to have a critical role in normal cell function, and redox potential may be a crucial indication of the steady state redox conditions that permit differentiation and tissue patterning during embryogenesis and organogenesis [5,10].

Altered redox potentials during embryonic development can range from mild to severe, leading to manifestations ranging from altered signal transduction to apoptosis and necrosis, respectively. Because these consequences are likely harmful, the body has an endogenous antioxidant system to prevent and protect against the more damaging consequences of oxidation. The reducing agent glutathione (GSH) and related enzymes glutathione reductase, glutathione peroxidase, and glutamate-cysteine ligase are primarily responsible for the maintenance of a balanced cellular redox potential. Production and recycling of these endogenous antioxidants is initiated through the induction of the Nrf2 antioxidant pathway. When this is insufficient to maintain a balanced environment during development, teratogenesis may occur [5].

It has been demonstrated that several chemical compounds have the ability to modify the embryonic redox environment, and that these changes may result in teratogenic outcomes [5,11-15]. Compounds such as ethanol, diamide, methylmercury, phenytoin, and L-buthionine-S,R-sulfoximine have been associated with oxidation of the various tissue and fluid compartments of the conceptus, including the visceral yolk sac (VYS), the yolk sac fluid, the amnion and amniotic fluid, and the embryo proper (EMB) (unpublished data) [14,16,17]. These compounds are able to decrease embryonic and fetal tissue glutathione concentrations, and co-treatment with antioxidants such as N-acetylcysteine and dithiole-3-thione (D3T) could prevent toxicant-induced injury [11,14,16,18-25]. The body of evidence for other toxicants altering redox signaling in the organogenesis-stage conceptus is growing, and many of these exposures are associated with adverse health outcomes and structural defects.

Mono-2-ethylhexyl phthalate (MEHP) is the primary metabolite of the common plasticizing agent, Di-2-ethylhexyl phthalate (DEHP). DEHP has been widely incorporated to products all over the world, especially including vinyl piping and medical tubing. Evidence of

phthalate transfer to the embryo and fetus has been evident through detection of MEHP in meconium, amniotic fluid, cord blood, rodent fetal tissues, and placental perfusate [26-34]. It has been previously demonstrated that MEHP can induce oxidative and inflammatory conditions in various reproductive tissues and developmental tissues, though these studies focus on other model organisms and different stages of development [35-38]. Thus, it is crucial to construct an ontogeny of redox potentials across the susceptible window of early organogenesis.

The goal of this study was to characterize MEHP-induced morphological changes in mouse whole embryo culture (mWEC), determine whether MEHP changes tissue and fluid antioxidant levels and alters redox potentials in embryonic tissues, and utilize gene expression profiles to identify pathways altered by MEHP treatment that may play a role in dysmorphogenesis.

Materials & Methods

Chemicals and reagents

Dioctyl phthalate (DEHP), dimethyl sulfoxide (DMSO), glutathione, glutathione disulfide, cysteine, cystine, γ-glutamyl-glutamate, iodoacetic acid, iodoacetamide, bicinchoninic acid, RNAlater®, Tyrode's balanced salt solution, and penicillin/streptomycin (10,000 units/ml penicillin, 10,000 μg/ml streptomycin sulfate) were obtained from Sigma/Aldrich (St. Louis, MO). Hanks balanced salt solution (HBSS) was purchased from GIBCO/Life Technologies (Grand Island, NY). Dansyl chloride was purchased from Fluka Chemie/Sigma-Aldrich (St. Louis, MO). Glacial acetic acid was obtained from Fisher Scientific (Waltham, MA). Mono-2-ethylhexyl phthalate was obtained from AccuStandard (New Haven, CT).

Mouse whole embryo culture

Mouse embryo culture was performed according to the procedures outlined in [39]. Briefly, female CD-1 mice were time-mated and obtained from Charles River (Portage, MI). The morning of discovery of a vaginal plug was designated as gestational day (GD) 0. Animals were maintained on a 12 h light-12h dark cycle and were supplied food and water *ad libitum*. On GD 8, female mice were euthanized with CO_2 and the uterus was removed. Culture-ready conceptuses were explanted from the uterus, removed from the decidual mass and freed from the Reichert's membrane, randomized, and placed into 10 ml culture bottles containing 5 ml of 75% heat-inactivated rat serum/25% Tyrode's balanced salt solution (TBSS) and 21.5 μl penicillin/streptomycin. Bottles were placed on a continuous-gassing carousel in an incubator held at 37°C and supplied with 5% O_2/5% CO_2/90% N_2. After 6 h in culture, the gas input was changed to 20% O_2/5% CO_2/75% N_2 to mimic the increased oxygenation of the *in utero* environment due to onset of embryonic heartbeat and active conceptal circulation.

Exposure and sample collection

DEHP and MEHP were suspended in DMSO to increase solubility in culture. DEHP and MEHP were added to the culture medium to bring the final concentration in culture to 100, 250, 500, or 1000 μg/ml. These concentrations were selected based upon concentrations utilized in other phthalate whole embryo culture studies [40,41]. DMSO was added to control bottles, and all DMSO concentrations were less than 1 μl/ml in culture. For morphology experiments, conceptuses were grown in culture for a total of 24 h before removal. For redox analysis, conceptuses were collected at 0 h before explant into culture, and following 1, 3, 6, 12, and 24 h in culture. Samples designated for RNA isolation were collected following 6 h in culture. At the time of removal from culture, all conceptuses were washed in Hank's balanced salt solution (2x) and ectoplacental cones

were removed. The EMB and VYS were manually separated using watchmaker's forceps. At this time, samples were either designated for morphology assessment or for redox analysis. Samples for redox analysis were placed into thiol preservation buffer (containing 5% perchloric acid, 0.2 M boric acid, and 10 μM γ-glutamylglutamate) snap frozen in liquid N_2, and stored at -76^0 C, as specified in [10]. Tissues collected for RNA isolation were placed into RNA later and stored at -76^0 C.

Morphology Assessment.

At the conclusion of the culture period, conceptuses for morphology assessement were removed from culture and washed thoroughly in HBSS without disruption. Once rinsed, conceptuses were placed into clean HBSS under a microscope for analysis and imaging. Images were taken before and after removal of the VYS. Morphological parameters were evaluated as specified in [39]. In short, we evaluated quality and developmental progress of the VYS, allantois, heart, flexion, caudal neural tube, forebrain, midbrain, hindbrain, otic vesicle, optic cups, forelimbs, mandible, maxillary process, and counted the number of somites. Additionally, crown-rump length, VYS diameter, and head length were measured [39]. Inviable conceptuses, characterized by a lack of heart beat, were excluded from the data set though the number of inviable embryos increased as the dose of MEHP increased. Protein quantification of tissue was done using bicinchoninic acid (BCA) assay on a microplate reader [42].

HPLC quantification of thiols and redox potentials.

Samples were thawed on ice and prepared for HPLC analysis of soluble thiols as previously described in [16,43]. Briefly, a Waters 2695 Alliance Separations module equipped with a

Supelcosil LC-NH_2 column (Sigma, St. Louis, MO) was coupled with a Waters 2475 Fluorescence Detector. Reverse-phase chromatography was used to measure reduced glutathione (GSH), oxidized glutathione disulfide (GSSG), reduced cysteine (cys), and oxidized cystine (cySS). Flow was set to 1 mL/min using a mobile phase gradient consisting of two mobile phases. Mobile phase A contained 80% methanol and mobile phase B consisted of 62.5% methanol, 12.5% glacial acetic acid, and 214 mg/ml CH_3COONa-3 H_2O. Peaks were evaluated (excitation 335 nm, emission 518 nm) using the Waters Empower software (Milford, MA). The Nernst equation (pH 7.4) was used for the calculation of redox potential (E_h) for both the cys/cySS and GSH/GSSG redox pairs: $E_h = -264 + 30 \log ([GSSG]/[GSH]^2)$, Cys/CySS, $E_h = -250 + 30 \log ([CySS]/[Cys]^2)$. Absolute concentrations of GSH, GSSG, cys, and cySS were calculated and normalized to tissue protein concentrations following BCA assay.

RNA isolation and Affymetrix microarray analysis of expression

Samples stored in RNAlater were thawed on ice and RNA was isolated following the instructions of the RNeasy Mini Kit (Qiagen). RNA was submitted for Affymetrix microarray processing at the University of Michigan Microarray Core Facility. Mouse MG-430 PM strip arrays were processed using the IVT Express Kit (Affymetrix). RNA purity and integrity were confirmed using the RNA 6000 Nano Kit for the Agilent 2100 Bioanalyzer. Raw data obtained for the array was further examined for quality and supported by satisfactory scores for PM chip density, RNA degradation, and standard errors. Robust multi-array average (RMA) was used for background correction, normalization, and quantification of $\log_2$ expression. Principle component analysis revealed distinctions between samples, confirming EMB and VYS tissue differences (Fig. 3.1).

Overall differences in expression between control and MEHP-treated EMB and VYS were examined using the *Limma* package in R 2.4.1. The *lmFit* function was used to downweight potential outliers. Raw p-values were obtained by t-test, and adjusted and ranked using an empirical Bayesian method (*eBayes* function in *Limma*). Enrichment was analyzed using LRpath, and biologically and statistically altered pathways were identified using the KEGG database [44]. Pathways containing genes were many statistical differences were considered "enriched". Highly conserved pathways containing fewer statistically altered genes than would be expected by random chance were considered "depleted".

Statistical Analysis

Values presented in this paper are means ± standard error of the mean. Statistical outliers were removed, identified as values 1.5 times the interquartile range outside of the first and third quartiles of the data. One-way ANOVA with Tukey posthoc tests and independent t-tests were used to assess statistical significance of differences between groups of data. A confidence level of 95% was used, and p-values <0.05 were deemed as statistically significant changes.

Results

Morphology Assessment

Following the culture period, dose-response examination of the morphological outcomes from both the parent compound and metabolite treatments was conducted, examining morphology in response to MEHP at concentrations of 100 μg/ml (M100), 250 μg/ml (M250), 500 μg/ml (M500), or 1000 μg/ml (M1000), or DEHP at concentrations of 100 μg/ml (D100), 500 μg/ml (D500), or 1000 μg/ml (D1000). Concentrations were selected based upon benchmark

concentrations obtained in another study [40], and confirmed following the initiation of this study [41]. In all, conceptuses treated with MEHP exhibited morphological changes, while conceptuses treated with DEHP remained similar morphologically to controls (Fig. 3.2). This is consistent with the likelihood that DEHP is metabolized maternally prior to conceptual exposure, and that MEHP is the active compound for teratogenesis. Conceptuses treated with MEHP were noticeably smaller than controls, and overall size decreased in a dose-dependent fashion (Fig. 3.3). Table 3.1 displays the average scores for all morphological parameters after MEHP treatment. Control conceptuses (n=17) had an average total morphology score of 86.6 ± 6.1. None had any notable defects, and they were fairly robust in size. Treatment significantly reduced many of the scores, though it seemed to have had little effect on the mandibular or forelimb scores. Of the affected developmental outcomes, the closure of the neural tube was particularly affected. Neural tube closure was significantly halted or delayed by MEHP treatment in the cephalic fore-, mid-, and hindbrain segments as well as in the caudal neuropore (Fig. 3.4).

MEHP morphology

The M100 group (n=7) had an average total morphology score of 73.8 ± 10.0, indicating a fair amount of morphological variability in these samples. Several of these M100 embryos were hypoplastic in the forebrain region, and 43% of the embryos had open neural tubes at least at one of the four neural tube regions examined (forebrain, midbrain, hindbrain, caudal neural tube). This is consistent with other concurrent studies being conducted in the laboratory, with open neural tubes occurring with an incidence of 33-45% in M100-treated conceptuses. One of the embryos developed a clear blister on the prosencephalon.

The M250 group (n=6) followed a similar pattern, with an average total morphology score of 72.9 ± 2.9. All but one of the embryos had an open neural tube at one or more of the neural tube regions scored. Though all of the caudal neural tubes were closed in the M250 group, all were highly hypoplastic at this locus.

The M500 group (n=16) had an average morphology score of 56.6 ± 3.3, and also showed hypoplasia of the caudal neural tube. About a third of the embryos possessed caudal neural tubes that were so necrotic that they could not be fully assessed due to the status of the caudal neuropore. In all of the embryos, the caudal region was truncated and hypoplastic. Allthe spinal columns of the M500 embryos had a 'zig-zag' pattern running dorsally along the neural tube. One of the embryos had complete dissociation of the neural epithelium, with large blisters and severe hypoplasia in the forebrain region. In approximately a third of the embryos, the pericardium was enlarged and fluid-filled, and these same embryos had blood pooling in the antimesometrial end of the VYS. One of the M500 embryos also had a very thin second branchial arch.

The M1000 group (n=5) was the first exposure that resulted in loss of viability in some of the conceptuses, with merely a 28.4 ± 0.8 morphology score. Nearly 30% of embryos lacked a heartbeat entirely, and those that survived had very weak heartbeats in terms of rate and apparent contractile force. All of the M1000 embryos were very hypoplastic at the caudal end, and had the 'zig-zag' pattern running along the dorsal side. All lacked a posterior neuropore, and had signs of necrosis. In one of the embryos, necrotic debris was visible within the hindbrain region. All of these M1000 embryos had blood pooling in the antimesometrial end of the VYS, and all had very thin second branchial arches.

DEHP morphology

Compared to the MEHP-treated conceptuses, the DEHP-treated conceptuses were normal morphologically. The D100 group (n=3) showed almost no signs of change relative to the morphology of the controls. The D500 (n=5) and D1000 (n=5) groups also showed little change, though the caudal neural tube and the forebrain regions were slightly hypoplastic.

Control EMB and VYS glutathione concentrations

Reduced glutathione, GSH, concentrations were measured in EMB and VYS tissues. Embryonic GSH rapidly increases after conceptal transfer into culture. At the time of placement into culture (t=0), control GSH concentrations are approximately 1188.1 ± 286.4 μM (n=5). After 1 h, control GSH concentrations rose to 1533.4 ±164.9 μM (n=4). After this time, GSH initially declines and then remains steady over the next 24 hours in controls (Fig. 3.5). After 3, 6, and 12 h, the concentrations decline to 777.3 ± 94.3 (n=4), 754.4 ± 174.9 (n=8), and 705.4 ± 16.4 (n=4) μM, respectively. After 24 h in culture, control EMB GSH concentrations decrease slightly to 620.1 ± 51.2 μM (n=6). GSH concentrations in the VYS follow a different pattern (Fig. 3.5). At the start of the culture period, control VYS GSH concentrations are 1272.1 ± 142.0 μM (n=4), which is similar to embryonic concentrations. Unlike in the EMB, GSH concentrations are reduced after 1 h to 1119.8 ± 31.0 (n=4). Concentrations steeply decrease after 3 h to 225.2 ± 43.3 μM (n=5), and then rise again at 6 h to 577.6 ± 46.3 (n=7). GSH remains fairly constant after 12 h (535.3 ± 6.4; n=4), but then increases by 50% to 804.8 ± 49.5 μM after 24 h (n=6).

Embryonic glutathione concentrations

MEHP treatment reduces GSH concentrations in the EMB after 1 h exposure in a dose-dependent manner, measuring 1014.3 ± 75.3 ($p=0.034$; n=3) and 539.3 ± 67.6 ($p<0.001$; n=5) μM

for the M100 and M250 groups, respectively. While the M250 group GSH concentrations continue to decline after 3 h exposures (634.2 ± 85.6; $p>0.1$; n=4), GSH concentrations increased in the M100 group to 1172.1 ± 139.3 μM ($p=0.07$; n=4). Though there was no statistically significant difference between controls and treated groups, GSH concentrations of the M100 group were significantly elevated compared to those of the M250 group ($p=0.017$). After 6 h in culture, the GSH concentrations of all exposure groups becomes fairly regular. The M100 concentrations are very similar to those of controls (754.2 ± 109.2; $p>0.99$; n=8). The M250 group appears to recover, and is slightly elevated (913.6 ± 125.5; $p>0.5$, n=8). After 6h in culture, gas concentrations are changed to mimic the *in utero* increased oxygen environment. While the control group was able to maintain a steady GSH concentration, the M100 and M250 groups were found to have decreased GSH concentrations in a dose-dependent manner. GSH concentrations were reduced in the M100 group to 337.7 ± 25.4 ($p<0.001$; n=3), and even more so by the 250 μg/ml exposure (153.0 ± 22.2; $p<0.001$; n=4). By 24h, all treatment groups had approximately the same GSH concentrations. GSH concentrations rose slightly to 612.9 ± 20.0 μM in the M100 exposure group ($p=0.983$; n=10) and to 651.1 ± 13.1 μM in the M250 exposure group ($p=0.758$, n=7).

Visceral yolk sac GSH concentrations

After 1 h in culture, VYS GSH concentrations in the M100 and M250 groups are both significantly lower than controls, with 477.6 ± 126.8 ($p=0.010$; n=5) and 637.2 ± 148.2 μM ($p=0.017$; n=5), respectively. Concentrations remain fairly stable at 490.3 ± 97.2 in the M100 group, but elevated compared to controls ($p=0.09$; n=3). The M250 group GSH concentrations decreased to 339.7 ± 95.7 μM after 3 h ($p=0.519$; n=4), remaining elevated compared to controls but depressed compared to the M100 exposure group. This relationship is still evident after 6 h of

exposure. The M250 VYS group had GSH concentrations lower than controls (p=0.515), but greater than the M100 VYSs (p=0.112). All of these concentrations were increased compared after 3 h exposures, with concentrations of 685.0 ±70.4 (n=7) and 458.4 ± 99.4 (n=7) μM for the M100 and M250 groups, respectively. Following the increased oxygenation of the environment and rapid morphological changes, all GSH concentrations decreased at the 12 h time point. Concentrations dropped to 350.7 ± 87.6 μM in the M100 group (n=4) and 524.9 ± 90.2 μM in the M250 group (n=6), and were similar to controls (p=0.291; p=0.897). All GSH concentrations were increased after 24 h, with concentrations of 816.3 ± 20.3 (n=10) and 906.8 ± 28.5 (n=8) μM for the M100 and M250 groups, respectively. There was a dose-dependent, slight increase in GSH concentrations compared to controls, though these differences were not statistically significant (M100: p=0.964; M250: p=0.096).

Overall, MEHP exposure decreases EMB GSH concentrations in a dose-dependent manner at crucial windows of EMB development, but the EMB and VYS are capable of restoring GSH concentrations after 24 h.

Control EMB and VYS cysteine concentrations

Reduced cysteine, cys, was measured in EMB and VYS tissues. Cysteine concentrations progressively decrease over the first 6 hours in control EMB and VYS. In the EMB, cys concentrations start at 234.2 ± 96.1 μM prior to the culture period (n=5). After 1, 3, and 6 h, cys decreases to 211.3 ± 53.6 (n=4), 159.1 ± 26.6 (n=4), and 46.7 ± 10.5 (n=7) μM, respectively. After introduction of the higher oxygen environment and entrance into a stage of rapid embryogenesis, embryonic cysteine concentrations climb to 224.6 ± 29.4 μM by 12 h (n=5), and then drops again by 24 h to 86.2 ± 6.6 μM (n=6). Concentrations of cys in the VYS are slightly elevated compared

to the EMB at t=0, measuring at 374.2 ± 152.3 μM (n=5). Unlike the EMB, cys is increased in the control VYSs to 1990.0 ± 804.5 after 1 h in culture (n=4). Concentrations rapidly drop to 136.4 ± 25.5 μM after 3 h (n=4), and then to 52.8 ± 9.1 after 6 h (n=6). Like in the EMB, the numerous changes that occur between 6 and 12 h are pronounced at the 12 h time point by a rapid increase in cys to 467.4 ± 111.2 μM (n=4), and this is succeeded by a 75% decrease in cys to 118.5 ± 13.5 μM at 24 h (n=6).

Embryonic cysteine concentrations

After 1 h of exposure, embryonic cysteine concentrations are slightly elevated in the M100 group to 221.0 ± 28.1 μM (n=5) and decreased in the M250 group to 144.4 ± 9.4 μM (n=3), but neither change was statistically significant ($p>0.05$ for all relationships; Fig. 3.6). After 3 h exposure, a dose-dependent decrease in cysteine concentrations is evident, dropping to 87.2 ± 31.3 μM for the 100 μg/ml exposure group (n=4) and 32.1 ± 2.8 μM for the 250 μg/ml group (n=3). Though this decrease compared to controls is not statistically significant in the M100 group ($p=0.169$), it is significant for the M250 group ($p=0.03$). Low- and high-dose exposures to MEHP are fairly similar to controls following 6 h in culture ($p=0.651$ and $p=0.653$, respectively). The M100 group cysteine concentrations dropped further to 37.7 ± 4.3 μM (n=7), and the M250 group to 37.7 ± 4.8 μM (n=7). Following the morphological and environmental oxygen changes in culture, the 12 h time point results in decreased cysteine concentrations in both the M100 and M250 groups though neither is statistically significant ($p=0.338$ and $p=0.960$, respectively). The low-dose exposure results in an average cysteine concentration of 177.4 ± 9.0 μM (n=4), while the M250 group cysteine concentrations were 216.0 ± 18.6 μM (n=4) after 12 h. All cysteine concentrations decrease leading up to the 24 h time point, though all concentrations are fairly

similar ($p>0.4$ for all relationships). The M100 group concentration was 73.3 ± 6.1 μM (n=10), and the M250 group concentration was found to be 73.6 ± 7.6 μM (n=8).

Yolk sac cysteine concentrations

Following 1 h exposure, control and exposed VYSs all had similar cys concentrations ($p>0.99$ for all relationships). Yolk sac cys concentrations for the M100 group were highly variable, averaging 1978.7 ± 986.8 μM (n=5), while the M250 group had average cys concentrations of 1902.4 ± 34.5 μM (n=3). After 3 h exposure, the M100 group has significantly greater cysteine than the control or high-dose group, though these relationships are not statistically significant ($p>0.07$). Cysteine concentrations from the M100 group were highly variable and average at 329.4 ± 138.1 μM (n=3), while M250 concentrations drop to 82.5 ± 15.0 μM (n=4). Concentrations all remain low at the 6 h time point, with M100 VYSs dropping cysteine concentrations further to 55.9 ± 18.6 μM (n=6) and M250 concentrations rising slightly to 103.5 ± 26.2 μM (n=7), though no statistically significant relationships were observed at the 6 h time point ($p>0.2$). After 12 h in culture, MEHP-exposed VYSs had significantly lower cys concentrations than controls ($p=0.003$ for both relationships). M100 (n=3) and M250 group (n=6) cys concentrations rose to 196.3 ± 12.5 and 275.5 ± 29.2 μM, respectively. Cysteine concentrations all drop at the 24 h time point, though this is exacerbated in the M100 group. The M100 group cys concentrations in the VYS drop to a mere 11.5 ± 1.3 μM (n=8), significantly lower than control ($p<0.001$) and M250 cys concentrations (92.2 ± 16.2 μM; $p<0.001$; n=8).

Total glutathione and cysteine concentrations

Total glutathione concentrations are shown for the EMB (Fig. 3.7A) and VYS (Fig. 3.7B), as well as total cysteine concentrations in the EMB (Fig. 3.7C) and VYS (Fig. 3.7D). Total glutathione is defined as the sum of the reduced fraction concentration and two times the disulfide concentration. No obvious trends were observed in the VYS for either total cys or total GSH. Total GSH in the EMB follows two interesting profiles: one occurring between t=0-6, and another between t=12-24. Between 0-6 hours, each treatment group has peak total GSH concentrations at different time points, suggesting that biosynthesis may play a role in this measure. Control total GSH concentration peaks at 1 h in culture, and is significantly greater than the treated EMBs ($p=0.002$). Total GSH then decreases progressively until the t=6 point. The M100 total GSH concentration peaks at 3 hours, and is elevated compared to the dwindling control ($p=0.073$) and M250 ($p<0.001$) total GSH measures. After 6 h, total GSH peaks for the M250 group, though it is not statistically different ($p>0.6$). Because the amount of bioactive GSH is dependent on both the utilization and biosynthesis of GSH, it is likely that this may be time- and dose-dependent oxidation of the EMB due to MEHP as well as decreased capacity to reduce and synthesize new GSH. At 12 h, total GSH in the EMB significantly decreases in a dose-dependent manner compared to controls (M100: $p=0.035$; M250: $p<0.001$). However, all embryonic total GSH concentrations are almost identical after 24 h exposures ($p>0.28$). This suggests that MEHP may reduce the embryonic antioxidant capabilities during significant windows of development including the peak of morphological and *in utero* environmental change. Embryonic total cys measures also follow a dose-dependent pattern over the first 6 h of exposure on GD8. However, a great deal of variability was observed in these samples. Because GSH is synthesized from cys, it is possible that in addition to the influence of MEHP on uptake and utilization of cys itself, the increased GSH demand of the EMB requires increased utilization of cys for GSH.

Redox Profiles

Control redox profiles at the 24h time point match control redox profiles from the same stage of development (GD9) in prior *in vivo* and WEC studies (unpublished data). After 6 h in culture, EMB GSH/GSSG redox potentials are reduced in a dose-dependent manner, though these observations are not statistically significant (Fig. 3.8). After 6 h in culture, control EMB redox potentials were -193.4 ± 11.7 mV (n=8), and was reduced to -198.8 ± 9.3 (n=8) and -208.8 ± 9.1 (n=8) mV by MEHP concentrations of 100 and 250 μg/ml, respectively. It is likely that GSH biosynthesis has been increased in MEHP-exposed conceptuses, as MEHP itself would not be expected to reduce cellular redox environment. After 12 h, control samples are significantly more reduced than M100 ($p=0.009$) and M250 ($p<0.001$) EMB, and increasing dose significantly oxidizes the EMB. Control EMB GSH/GSSG redox potentials were -176.9 ± 1.6 mV (n=4), and the M100 and M250 groups were -158.3 ± 1.4 (n=3) and -138.2 ± 4.5 mV (n=4), respectively. After 24 h, all samples are much more reduced than at previous time points, but this dose-dependent oxidation in the EMB is still apparent. This also supports that MEHP induces embryonic oxidation during the most active window of embryogenesis. The EMB cys/cySS redox potential follows a similar trend. After 1 h, MEHP treatments reduced the environment, though only the 100 μg/ml induces a significant change ($p=0.014$). After 1 h, control EMB cys/cySS redox potentials were -158.6 ± 1.0 mV (n=3), and were reduced in M100 and M250 EMB to -177.6 ± 4.5 (n=5) and -165.8 ± 2.6 mV (n=5), respectively. After 3 h, EMB are oxidized by MEHP in a dose-dependent fashion though only the 250 μg/ml dose was statistically significant ($p=0.009$). Control potentials were -165.3 ± 7.1 mV (n=5) and reduced to -145.7 ± 4.4 (n=3) and -132.4 ± 9.8 mV (n=4), respectively. This dose-dependent decrease is continued to the 6 h time point, with cys/cySS

potentials of -138.8 ± 5.3 (n=6), -131.7 ± 5.8 (n=8), and -130.1 ± 2.7 (n=7) for control, M100, and M250 groups, respectively. EMB cys redox potentials are similar for all groups at 12 h, and only the 250 μg/ml EMB are significantly oxidized at 24 h compared to controls ($p=0.04$).

In the VYS, GSH/GSSG redox potentials were oxidized by MEHP treatment at the 1 h and 12 h time points ($p>0.05$). At 12 h, this oxidation results in a near 15 mV change in redox potential. At 3 h, redox potentials are more reduced with increasing doses of 100 and 250 μg/ml MEHP ($p=0.06$ and $p=0.04$, respectively). These 3 h redox potentials were -145.4 ± 4.9 (n=3), -162.2 ± 5.2 (n=3), -164.5 ± 1.1 mV (n=3) for control, M100 and M250 groups, respectively. After 24 h, GSH/GSSG redox potentials are fairly similar across treatment groups, though EMB are slightly reduced in the MEHP-treated groups ($p>0.05$). The cys/cySS redox potentials are also reduced at the 3 h time point, though the 100 μg/ml MEHP-treated VYS are most significantly reduced ($p=0.014$). At 12 h, increasing dose of MEHP increases oxidization of the VYS ($p>0.05$). At the 24 h time point, the controls and 250 μg/ml MEHP-treated VYS have similar redox potentials, but the 100 μg/ml MEHP-treated VYS are significantly oxidized after 24 h ($p<0.001$).

Pathways enriched by MEHP treatment

Pathways significantly enriched or depleted by 6 h MEHP treatment are shown in Table 3.2. “Enriched” pathways are those that contain many significantly changed genes. “Depleted” pathways have fewer changed genes than would be expected by chance, indicating conservation of these pathways. Several similarities were noted in EMB and VYS in response to MEHP. The most significantly enriched pathway in both EMB and VYS was oxidative phosphorylation ($p\leq0.001$). Expression of several NADH dehydrogenase genes was significantly decreased, including Ndufa3, Ndufs5, Ndufa6, and especially Ndufa7 in both EMB and VYS. In EMB,

expression of several ATPases and ATP synthases was also significantly altered by MEHP treatment—primarily those of lysosomal and mitochondrial origin. ATPases were primarily upregulated, while ATP synthases were primarily downregulated. Expression of Uqcr11, part of the ubiquinol-cytochrome c reductase complex crucial for cellular respiration, was increased in the VYS but decreased in the EMB.

The majority of enriched pathways in both tissues were, in general, metabolic pathways, namely xenobiotic response and amino acid metabolic pathways. The drug metabolism - cytochrome P450 (CYP450) and the glutathione metabolism pathways were significantly enriched in the VYS. The constituents of these pathways, consisting mostly of CYP450 isozymes, glutathione-S-transferases, and glutathione peroxidases were significantly increased in expression. The occurrence of these changes in the VYS and not the EMB confirm that the VYS is a metabolic barrier that serves to protect the developing EMB from chemical and environmental insults.

Amino acid metabolic pathways including histidine metabolism, arginine and proline metabolism, and alanine, aspartate and glutamate metabolism were all enriched in both EMB and VYS. Starch and sucrose metabolism was also enriched in the EMB. Synergistically, these alterations are likely indicative of decreased nutrient availability to the EMB, and have numerous downstream consequences affecting signal transduction and energy biosynthesis.

Retinol metabolism was enriched in the EMB, namely with regards to non-optic pathways. Though involved in the metabolism of Vitamin A, the genes most affected by MEHP treatment were mostly involved in the xenobiotic response and direct signal transduction during embryogenesis. Retinol dehydrogenase 1 (Rdh1), the enzyme responsible for the rate-limiting step of retinaldehyde biosynthesis, was significantly decreased in the EMB following MEHP treatment. As previously mentioned, several CYP450 genes were upregulated by treatment—including

CYP26 family variants. The function of the CYP26 family is to convert retinaldehyde into retinoic acid, and is essential for guiding posterior tissue patterning by directing Hox genes for hindbrain formation. Interestingly, Hox gene expression was significantly reduced in several Hoxb, Hoxc, and Hoxd variants.

1.2% of significantly affected genes were members of the solute carrier (SLC) gene families, which are evolutionarily well-conserved across the animal kingdom [45] (Table 3.3). Although no single family was specifically altered in the pathway analysis, the collective volume of significantly altered SLC genes was notable. Though SLCs have a diverse array of functions, all are involved in the transport of important cellular substrates across cellular membranes [46]. The largest group of transporters significantly impacted by MEHP treatment were involved in the mitochondrial transport of solutes. These mitochondrial transporters are important for metabolism, namely in oxidative processes [47]. Expression of SLC7A9, involved in cySS absorption, was significantly decreased in EMB [48]. In addition to regulating cys/cySS redox balance, SLC7A9 is crucial for proper kidney development and defects in the gene have been associated with increased risk for chronic cystinuria later in life [49,50]. Significant expression changes to members of the SLC6 family, involved in neurotransmission, appear only in the EMB tissue. Decreased expression was observed in several of these genes, crucial for glycine, noradrenaline, and methionine homeostasis. Several patterns were observed in the overall expression of these genes. Though there was a mixture or upregulated and downregulated SLC family expression in the EMB, there was a strong pattern of downregulation in the VYS.

Pathways depleted due to MEHP treatment

Though depleted pathways are not significantly altered, they are of interest because they are more heavily conserved. Pathways depleted in EMB and VYS by MEHP treatment are also listed in Table 3.2. Many signal transduction pathways essential for tissue patterning are conserved, including Wnt, Jak-STAT, ErbB, calcium, and VEGF signaling pathways. Neuronal function pathways including neuroactive ligand-receptor interaction and axon guidance pathways are also conserved, which is surprising due to the morphological findings of this work. Though these pathways were conserved, specific genes in these pathways may still be significantly altered. Several genes involved in these pathways are significantly upregulated, including EphB4 in the VYS and Ngef in the EMB. Additionally, conservation of expression in these pathways does not necessarily mean that there are no changes to the functional product. It is possible that regulation of these pathways is occurring at the translational or post-translational level.

Discussion

Development is a tightly regulated process, governed by combinations of genetic and environmental cues. These environmental cues come from a myriad of sources, including nutrient availability, maternal hormones, extracellular ligands, and redox environment. Redox environment in particular is crucial in the determination of cell fates. Oxidation of protein thiol residues, including those of the early EMB, can serve as a sensitive switch, indicative of disruption of redox steady state. The consequences that accompany altered redox potentials may guide cell fate towards proliferation, differentiation, apoptosis, or necrosis [51,52]. Typically, more reducing environments are correlated with cells undergoing proliferation, while more oxidative environments are associated with differentiation or ultimately cell death. For these reasons, protein thiol oxidation and ROS have been implicated in the pluripotency of stem cells and in the formation

of cancers [53-56]. The coordination of redox signals is crucial for normal growth and development, and dysregulation of redox environment may largely contribute to teratogenesis [5,51,57].

The EMB is sensitive to changes in redox potential. An E_h shift of merely 20 mV as measured for the GSH/GSSG redox couple may alter cell fate from proliferation to differentiation, while a 50 mV increase may permit conditions favorable toward death [58]. In this study, changes in redox environment were measured following MEHP treatment with 100 or 250 μg/ml in culture. After 12 h in culture, the 100 and 250 μg/ml MEHP treatments resulted in nearly 20 and 40 mV potential increases, respectively, in the EMB for the GSH/GSSG redox couple. Thus, it is possible that exposure to MEHP is inducing changes in cell fate and has the potential to alter tissue patterning via abnormal differentiation and even cell death. However, we have yet to characterize the individual proteins, pathways and signaling nodes involved.

The EMB undergoes many phenotypic and physiological changes at this time point in development. The 12-h time point in culture coincides with GD 8.5 in development, a very dynamic window of embryonic change. At this time, the EMB heart begins to beat, and conceptal circulation via the vitelline vasculature commences. Also at this time, the EMB flexion rotates, and the neural tube begins to close [59]. By 24 h, on GD 9, the anterior neural tube is expected to be fully closed. After 24 h in culture, the number of defectively open neural tubes was significantly increased with increasing dose of MEHP in culture. It is possible that the increased E_h and probable increased generation of ROS altered the migration and proliferation of the ectodermal germ layer. Future work should investigate whether oxidation of specific protein thiols and the consequences related to altered redox potentials may contribute to the teratogenic potential of MEHP in the EMB, especially focused on the tissues of the developing CNS.

The balance of the GSH/GSSG redox couple is built upon coordinated cellular efforts to reduce and recycle existing GSH, as well as to synthesize additional GSH. Both GSH biosynthesis and enzymatic reduction processes are mediated by the induction of the Nrf2 antioxidant response pathway. Nrf2 serves as a transcription factor that binds to the antioxidant response element (ARE) of promoters for genes involved in cellular redox balance [60,61]. As a result, enzymes and cofactors involved in reducing oxidized glutathione species are increased, and GSH can be recycled. GSH biosynthesis is also crucial to the GSH/GSSG balance. GSH is a tripeptide, created from cysteine, glutamate, and glycine building blocks. Decreased nutritional supply of amino acids, namely cysteine, have been associated with decreased GSH concentrations and increased oxidative stress [62-64]. It is additionally possible that glutamate may also be rate limiting under conditions of nutrient starvation.

Histiotrophic nutrition pathways (HNPs) are the processes by which nutrients and other substrates are transported from the maternal uterine environment to the conceptus, via the receptor-mediated endocytosis (RME) and subsequent proteolysis of the substrate-containing vesicles [65-67]. During this time, the placenta is not functional and the conceptus replies solely on HNPs for nutrient uptake. Thus, the VYS serves an important role in providing critical nutrients to the developing EMB. Because of the expected depletion of amino acids and observed general decrease in expression of SLCs in the VYS induced by MEHP treatment, it is possible that MEHP may be disrupting HNPs. Therefore, it is probable that decreased expression of SLCs in the VYS may have numerous downstream consequences affecting signaling and overall growth and differentiation. The decreased size of embryos exposed to MEHP raises questions regarding the implications of phthalates in both growth and also potentially metabolic disease later in life.

HNPs are believed to be evolutionarily adaptive, as they limit the oxygenation and resultant generation of teratogenic ROS during the first, and most sensitive, trimester [68]. At the end of the first human trimester of gestation, implementation of conceptal and then maternal circulation steeply increases the oxygenation of the embryonic environment [69,70]. At the 12-h time point, the oxygenation of the culture environment was increased to mimic the implementation of circulation in the conceptuses, and then from maternal circulation [39]. At this point in the culture period, MEHP caused oxidation and depleted GSH concentrations in the EMB. The end of the first trimester marks a sensitive period of development. Even though teratogenesis typically originates earlier during embryogenesis, chemically-induced susceptibility during this time may lead to functional rather than structural deficits [68].

Because HNPs are responsible for the uptake of amino acids and other micro- and macronutrients crucial for growth and development, decreased HNP function may result conditions akin to in amino acid starvation. In this study, numerous pathways involved in amino acid metabolism were disrupted, such as the metabolism of alanine, aspartate, glutamate, arginine, proline, and histidine. Additional indirect amino acid metabolic pathways, such as GSH metabolism and TCA cycle were also affected. Because all of these pathways rely on the supply of amino acids, it is possible that MEHP treatment is inducing amino acid starvation via decreased HNP activity. Amino acid starvation has been discovered to have numerous physiological and metabolic consequences, namely effects on energy metabolism including oxidative phosphorylation (unpublished data) [71].

Oxidative phosphorylation was the most significant pathway for both EMB and VYS due to phthalate treatment. The changes in oxidative phosphorylation processes observed are indicative of MEHP-induced dysregulation of energy metabolic processes. Increases in the expression of

ATPases, some of the most redox-sensitive proteins in the cell, suggest the necessity to maintain cellular homeostasis and potentially mitochondrial ion gradients during toxicant-induced physiological changes in the cell [72-77]. Likewise, decreases in the expression of ATP synthases may be indicative of decreased substrates available for energy production (ATP-form) in the cell. This suggests that the ability to produce ATP is compromised, and yet the energy demands are growing.

Oxidative phosphorylation, generation of mitochondrial ROS, and resultant changes to redox potentials have been associated with the induction of autophagy [78]. Autophagy is the process by which cellular proteins and even organelles are vesicle-bound and tagged for lysosomal proteolysis, in order to recycle cellular substrates to maintain viability under starvation conditions [78]. In autophagy, other processes are halted in order to conserve energy and resources and to preserve those of utmost importance. Proteins from these non-essential processes are often degraded to preserve a reservoir of amino acids for synthesis of proteins and enzymes for essential processes. Often, processes governing mitochondrial function are stimulated or supported at the expense of cytosolic processes [79]. Expression changes to enzymes involved with amino acid metabolism, GSH metabolism, TCA cycle, and oxidative phosphorylation, coupled to the expression changes observed in the SLC25 mitochondrial transporters class suggest that this shunting and prioritization of the maintenance of mitochondrial functions is beginning to occur at this 6 h time point.

The brain has very high energy demands, and relies heavily on oxidative phosphorylation and mitochondrial function [80]. It is not surprising that this time in development would be very susceptible to changes in oxidative phosphorylation, since large increases in mitochondrial density and mitochondrial proteins are initiated at the beginning of neurogenesis [81]. Changes to the

oxidative phosphorylation pathway have been previously demonstrated to be altered by exposures in the brain and NTDs [82,83]. Because oxidative phosphorylation requires the coordination of numerous enzymes and energy substrates, as well as maintenance of a high-energy proton gradient, these processes are often decreased in starved cells. These cells then rely on the more efficient but lower energy payout process of glycolysis. While autophagy may be able to prolong cell growth and function in times of distress, this would likely be unsustainable over longer periods of time. Studies have associated decreased autophagic capacity with increased apoptosis and increased risk for NTDs [84-87]. More work is necessary to determine whether MEHP treatment is resulting in amino acid starvation, and whether or not these conditions may induce autophagy if prolonged. It is possible that these factors may play a role in the etiology of NTDs.

In summary, this work suggests a novel mechanism by which MEHP treatment elicits developmental malformations in mWEC and that NTD incidence increases with increasing doses of MEHP. Dose-dependent oxidation of the GSH and cys redox couples and resultant disruption of steady state redox potentials were present at the 12-h time point—a period of rapid growth and metabolic change during early organogenesis. This suggests that MEHP may increase susceptibility to damage and dysfunction during sensitive windows of development. Altered metabolic capabilities suggest the MEHP induces conditions akin to amino acid starvation, yet more work is needed to characterize the role of amino acid supply, HNPs, and nutrition in these metabolic changes. Dysregulation of oxidative phosphorylation and energy metabolism in this study suggests the possible initiation of cell survival and potentially autophagy activities at the 6-h time point due to MEHP treatment in culture. Future work should characterize expression changes in oxidative phosphorylation, autophagy, and apoptosis pathways in order to discern

whether MEHP-induced alterations in amino acid availability and metabolism may be contributing the NTD phenotypes.

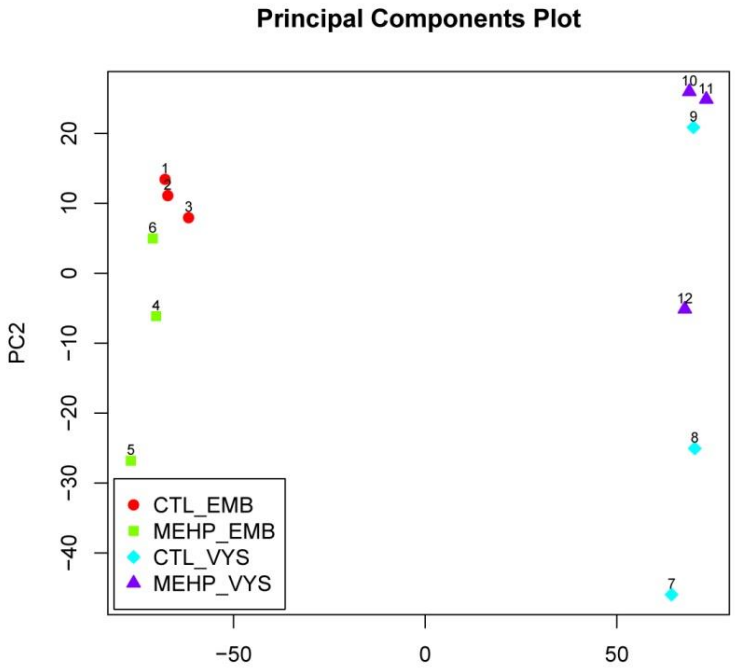

Figure 3.1. Principle components analysis (PCA) of Affymetrix data. The PCA plot reveals distinct differences in expression patterns between the EMB and VYS tissues. There is greater variability in the VYS samples. There is some distinction between control and MEHP-treated samples as well.

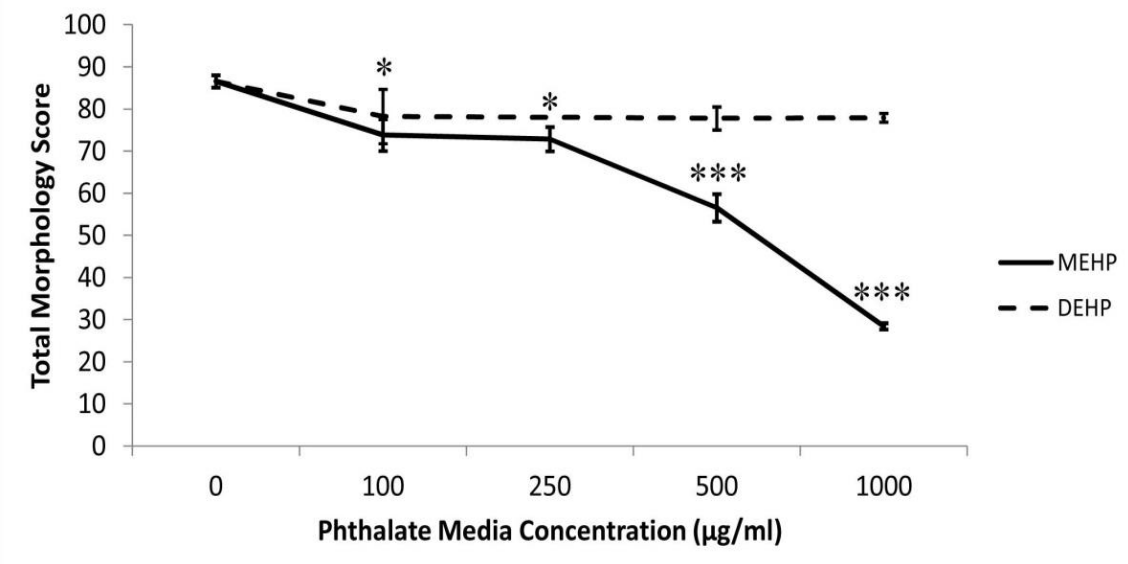

Figure 3.2. MEHP treatment reduces overall morphological score. Unlike the parent compound DEHP, metabolite MEHP is able to reduce overall morphological scores in a dose-dependent manner after 24 h treatment in WEC. * indicates a significant change ($p<0.05$) in the MEHP group from the control at this dose. *** indicates a very significant change ($p<0.001$) in the MEHP group from the control at this dose.

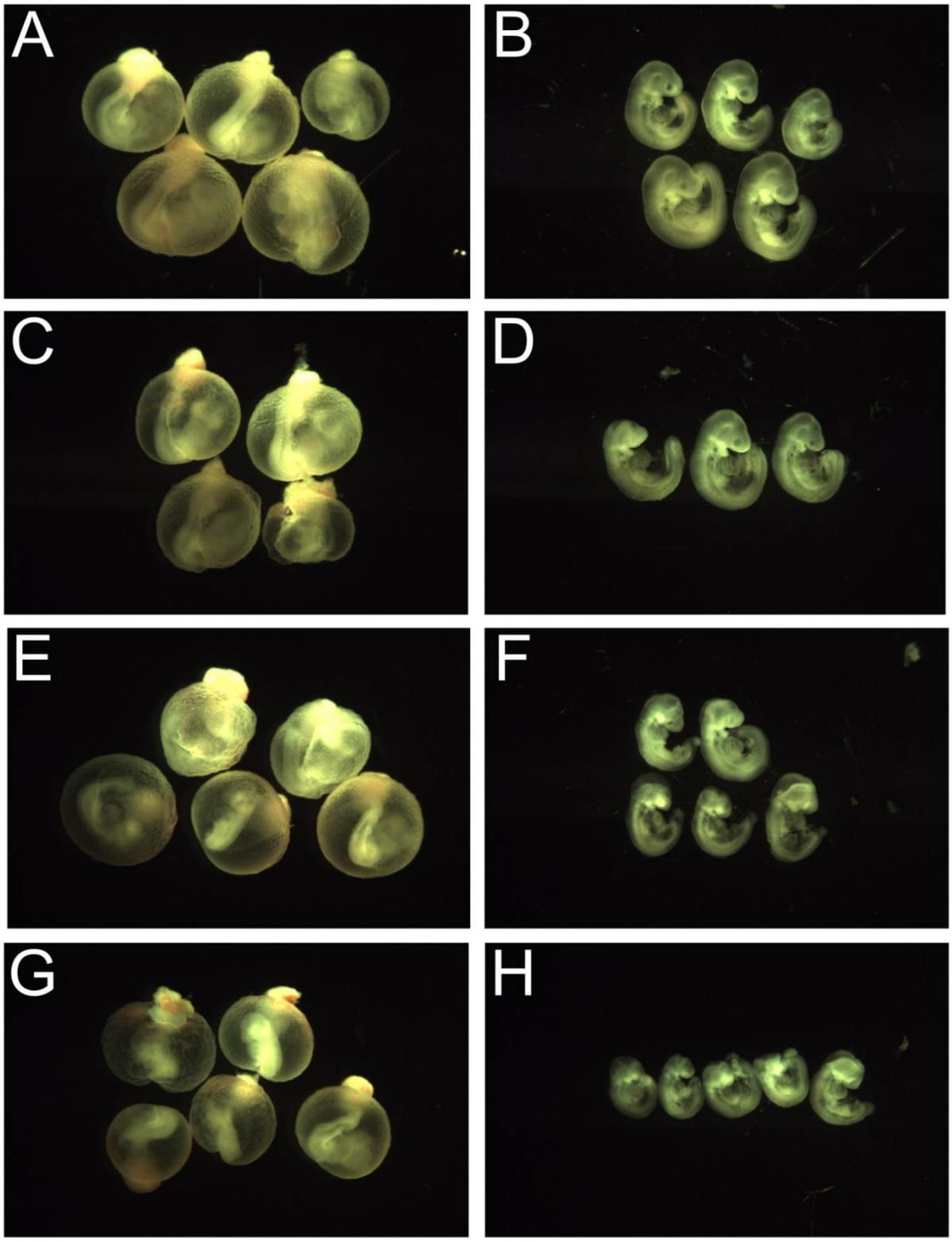

Figure 3.3. MEHP decreases embryonic size and induces malformations. Images taken of the exposed conceptuses reveals a gradual decrease in overall size and an increase in malformations as media MEHP concentrations were increased. Image key: control (A&B), MEHP 100μg/ml (C&D), MEHP 500μg/ml (E&F), MEHP 1mg/ml (G&H).

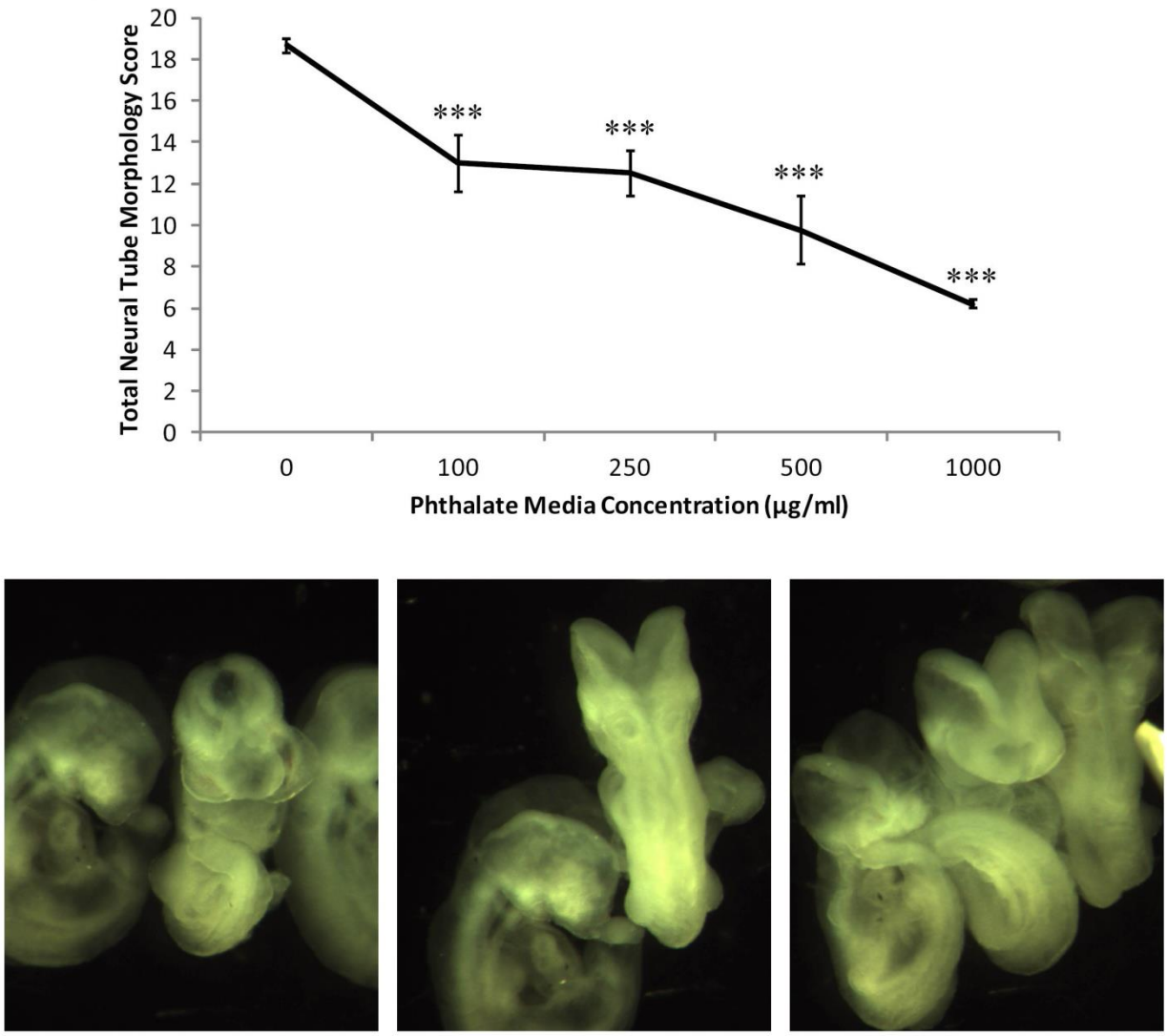

Figure 3.4. MEHP treatment impairs neural tube closure in WEC. An unusually high number of open neural tubes were observed in the MEHP-treated groups after 24 h treatment. Some of those malformations are shown above. Overall, with increased concentration of MEHP in the culture media, there is a reduction of neural tube scores. The highest possible total neural tube score attainable is 20, and scores are reduced by characteristics such as an open neural tube, necrotic debris present in the neural tube, and hypoplastic tissues around the brain regions. *** indicates a very significant change ($p<0.001$) in the MEHP group from the control at this dose.

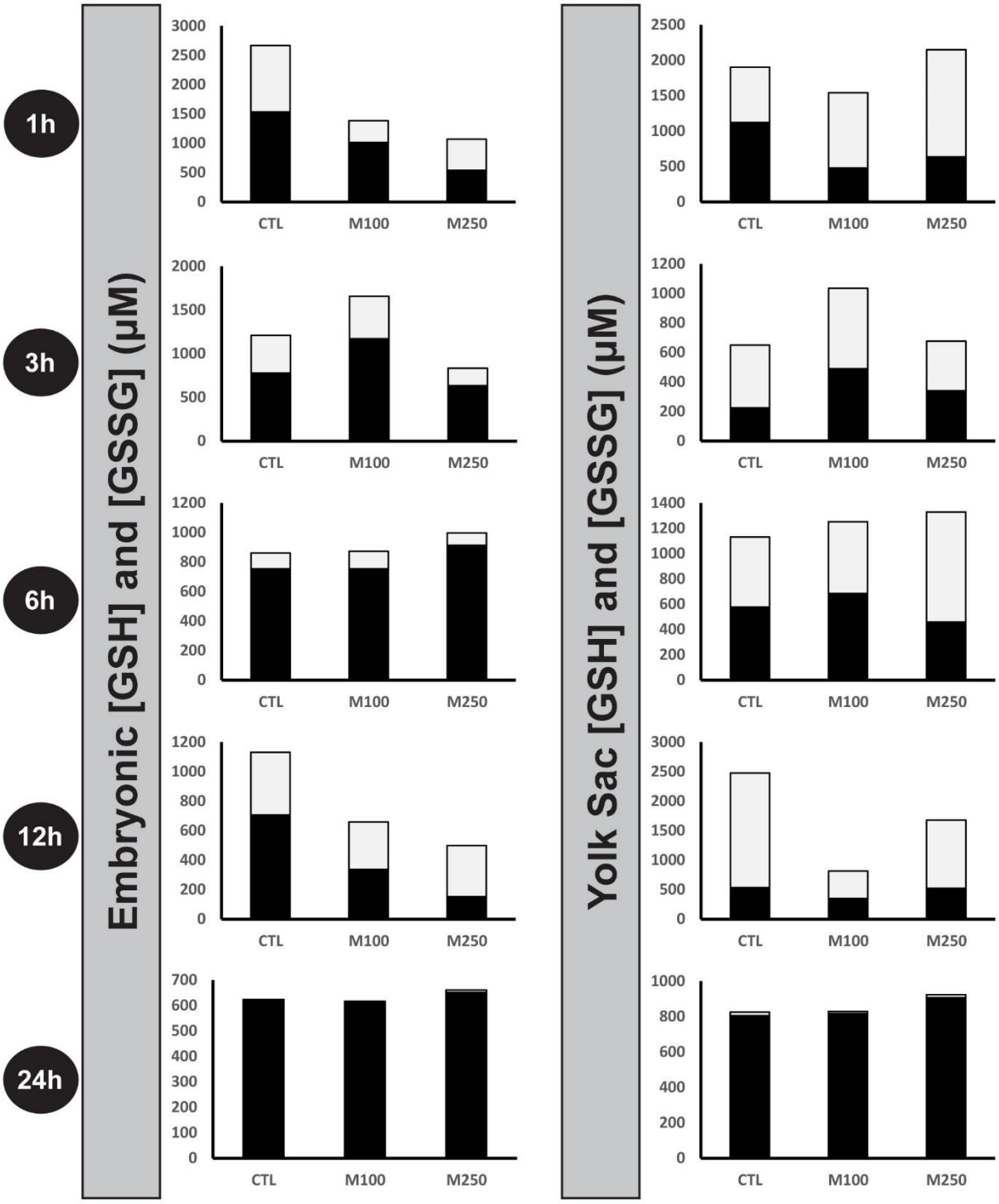

Figure 3.5. Ontogeny of reduced and oxidized glutathione measurements in EMB and VYS following MEHP treatment. Black fractions represent the concentrations (µM) of reduced glutathione (GSH), and gray fractions represent the concentrations (µM) of oxidized glutathione (GSSG).

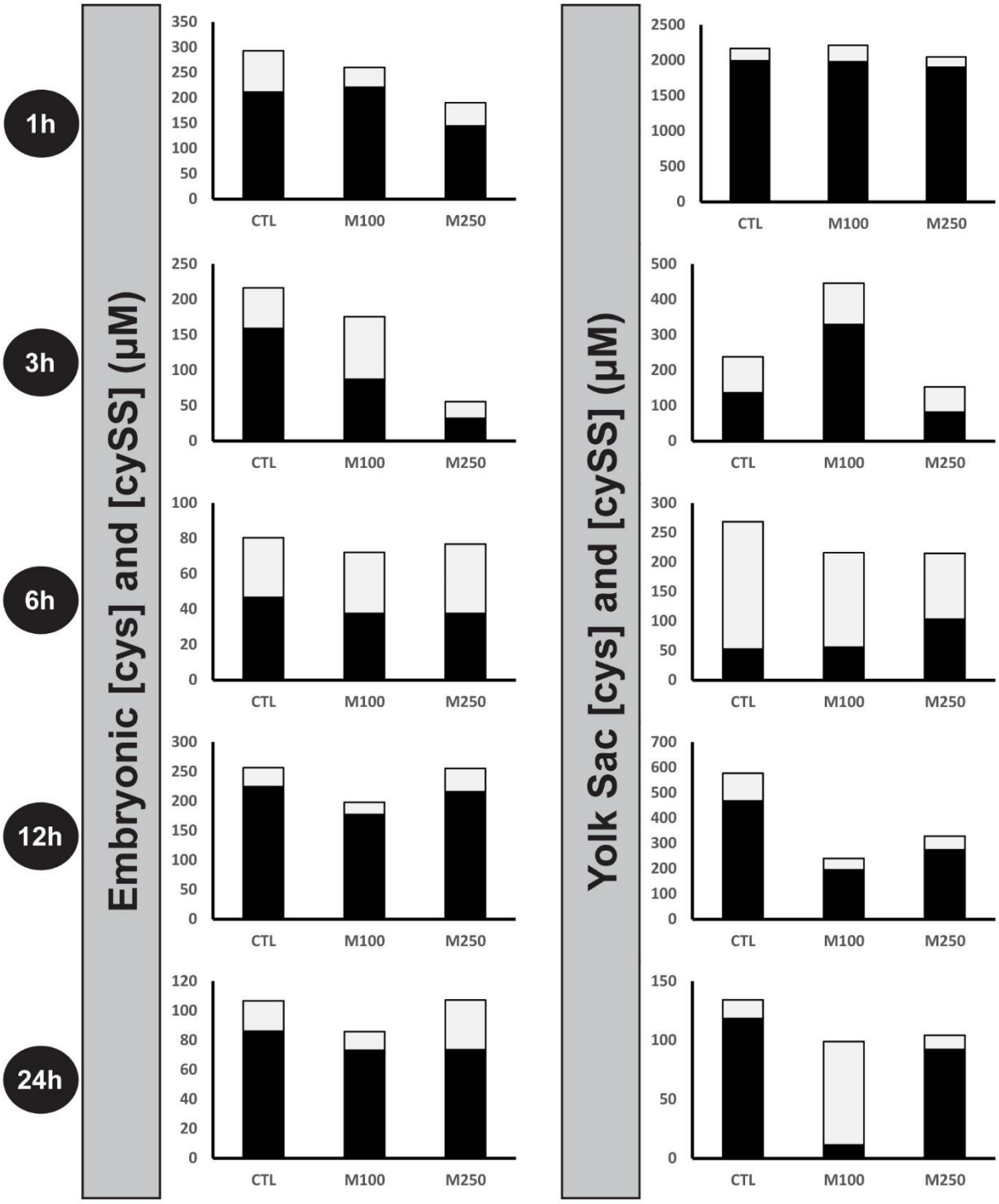

Figure 3.6. Ontogeny of reduced and oxidized cysteine measurements in EMB and VYS following MEHP treatment. Black fractions represent the concentrations (µM) of reduced cysteine (cys), and gray fractions represent the concentrations (µM) of oxidized cystine (cySS).

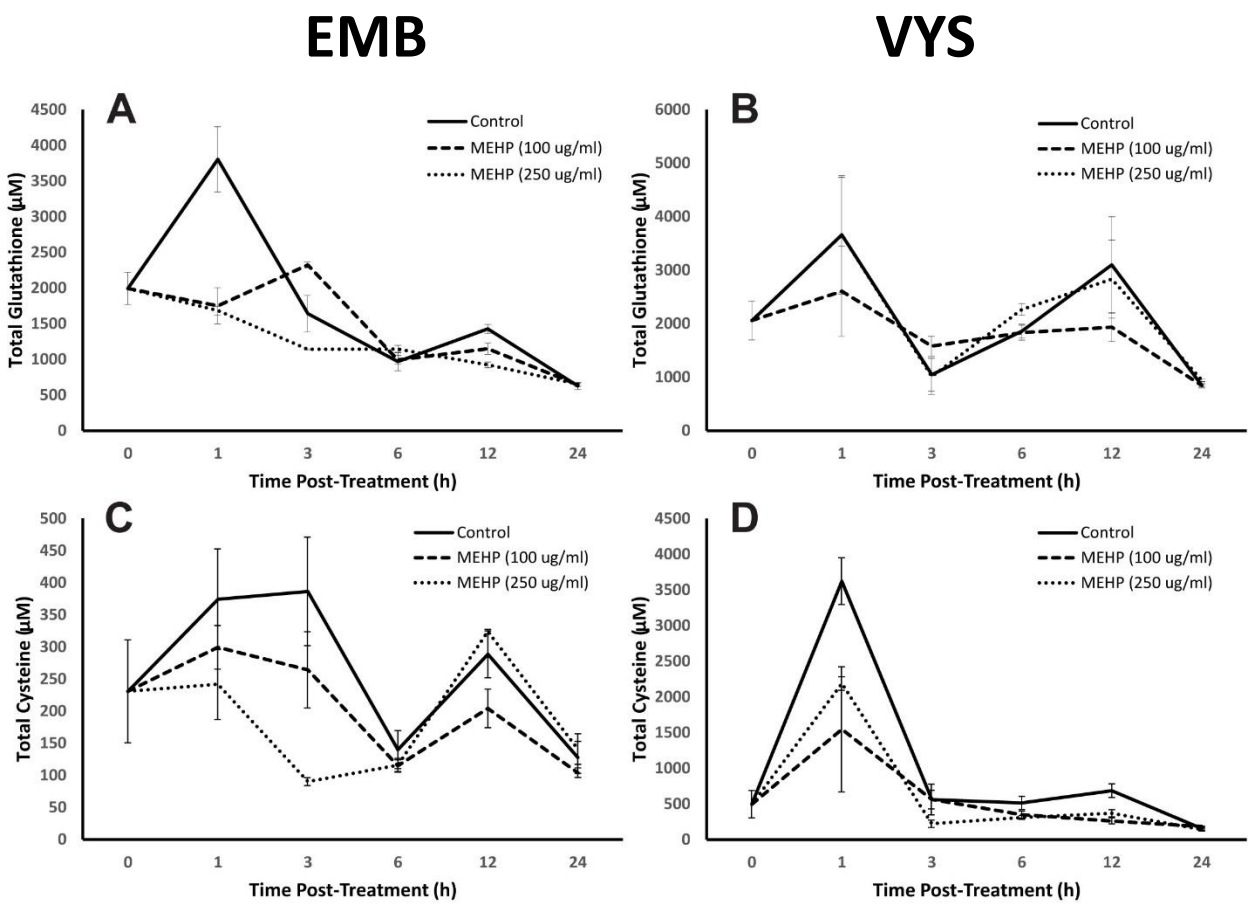

Figure 3.7. Ontogeny of total thiol measurements in EMB and VYS following MEHP treatment. Total concentrations are equal to the sum of the reduced and 2x the oxidized fractions of the thiol, since disulfides were measured. Image key: (A) total glutathione concentrations measured in EMB, (B) total glutathione concentrations measured in VYS, (C) total cysteine concentrations measured in EMB, and (D) total cysteine concentrations measured in VYS.

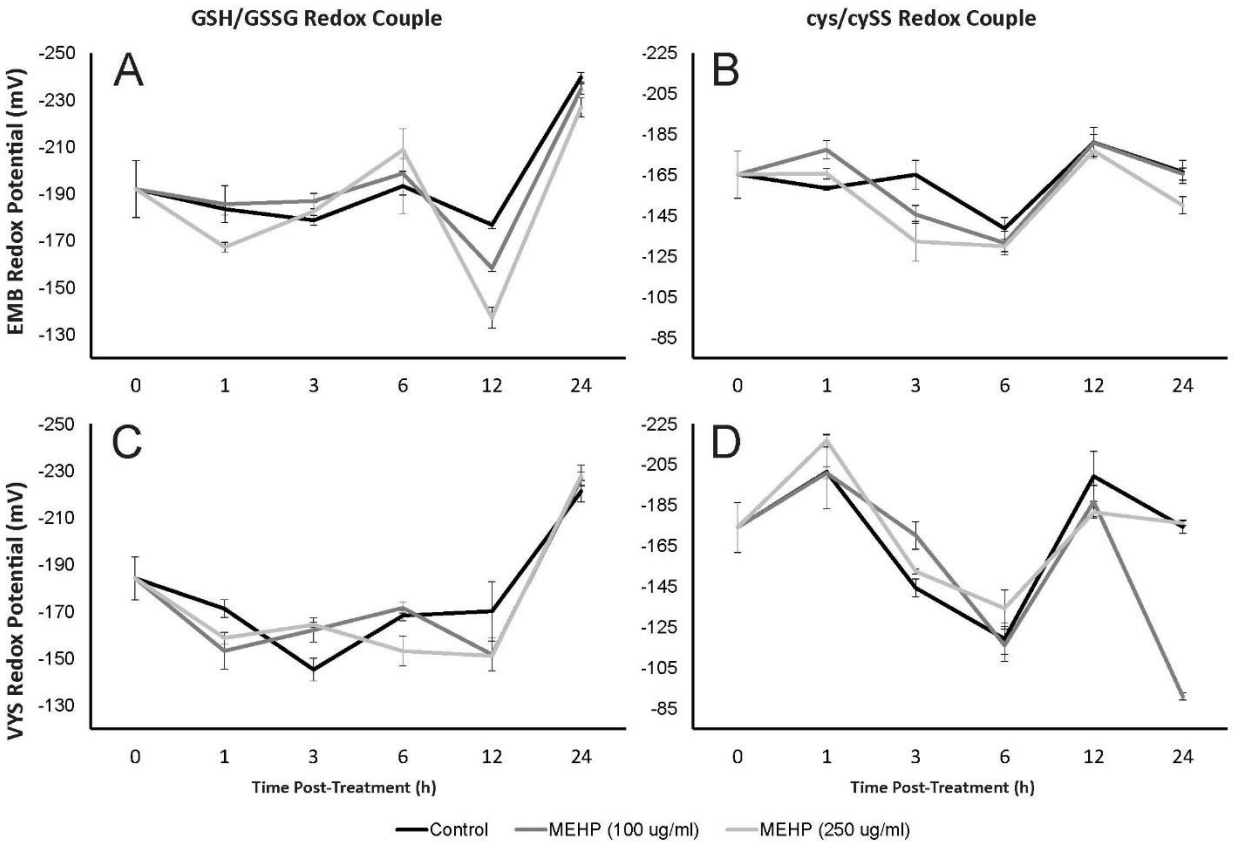

Figure 3.8. Ontogenies of redox profiles in conceptal tissues following treatment MEHP treatment. Embryonic redox profiles for glutathione (A) and cysteine (B) redox couples are shown left. VYS redox profiles for glutathione (C) and cysteine (D) redox couples are shown right.

Table 3.1. MEHP treatment significantly alters developmental progress in WEC. Though DEHP treatment produced little change in most measurable developmental parameters, the metabolite MEHP significantly altered many defect scores. Values presented are the means ± standard error of the mean. *p<0.05, **p<0.01, ***p<0.001, --- indicates that the specimen were too necrotic to accurately assess this parameter.

	Control (n=17)	MEHP (100 μg/ml) (n=7)	MEHP (250 μg/ml) (n=6)	MEHP (500 μg/ml) (n=16)	MEHP (1 mg/ml) (n=5)
Yolk Sac	5.0 ± 0	4.6 ± 0.3	5.0 ± 0	2.1 ± 0.3	0.4 ± 0.2
Allantois	3.0 ± 0	2.6 ± 0.2	3.0 ± 0	1.8 ± 0.2	1.2 ± 0.4
Flexion	4.7 ± 0.1	3.9 ± 0.4	4.3 ± 0.2	4.0 ± 0.1	4.0 ± 0
Heart	3.8 ± 0.1	3.7 ± 0.2	3.5 ± 0.2	3.3 ± 0.1	2.6 ± 0.2
CaudalNT	4.2 ± 0.1	3.7 ± 0.2	4.0 ± 0	1.3 ± 0.5	--
HindB	4.9 ± 0.1	3.6 ± 0.4	2.8 ± 0.3	3.0 ± 0.3	2.0 ± 0
MidB	4.9 ± 0.1	3.6 ± 0.5	2.8 ± 0.4	2.6 ± 0.3	2.0 ± 0
ForeB	4.6 ± 0.2	3.3 ± 0.5	2.8 ± 0.5	2.9 ± 0.2	2.2 ± 0.2
Otic Ves.	4.5 ± 0.2	3.3 ± 0.3	2.5 ± 0.2	2.7 ± 0.3	2.4 ± 0.2
Optics	4.6 ± 0.2	3.7 ± 0.4	2.8 ± 0.5	1.9 ± 0.3	1.0 ± 0
Branchial	2.7 ± 0.1	2.6 ± 0.2	2.7 ± 0.2	2.0 ± 0.1	2.0 ± 0
Maxillary	3.0 ± 0	1.9 ± 0.1	2.0 ± 0	1.7 ± 0.1	1.0 ± 0
Mandible	2.0 ± 0	2.0 ± 0.2	2.0 ± 0	1.9 ± 0.1	2.0 ± 0
Forelimbs	2.1 ± 0.2	1.9 ± 0.3	2.2 ± 0.2	2.0 ± 0.2	1.6 ± 0.2
Somites	24.6 ± 0.4	21.0 ± 0.8	23.7 ± 0.8	18.8 ± 1.5	--
VYS volume	17.9 ± 1.4	13.8 ± 1.4	17.1 ± 0.8	13.8 ± 1.1	10.2 ± 0.9
Crown Rump	2.9 ± 0.1	2.7 ± 0.1	2.9 ± 0.1	2.5 ± 0.1	1.7 ± 0.2
Head Length	1.5 ± 0	1.2 ± 0.1	1.4 ± 0.1	1.2 ± 0	1.0 ± 0.1
TOTAL SCORE	86.6 ± 1.5	73.8 ± 3.8	72.9 ± 2.9	56.6 ± 3.3	28.4 ± 0.8

P>0.05	
P<0.05	
P<0.01	
P<0.001	

Table 3.2. EMB pathways significantly altered by 6h MEHP treatment in WEC. Significantly enriched KEGG pathways (shown left) include many metabolic pathways and those dependent upon the redox environment. Significantly depleted pathways (shown right) include pathways involved in signal transduction, including several crucial for neurodevelopment.

Pathways significantly *enriched* in EMB tissue	Odds Ratio	P-value	Pathways significantly *depleted* in EMB tissue	Odds Ratio	P-value
Oxidative phosphorylation	4.136	0.001	Fc gamma R-mediated phagocytosis	0.032	0.001
Alanine, aspartate and glutamate metabolism	8.517	0.002	Ribosome	0.022	0.003
Retinol metabolism	5.637	0.005	Pathways in cancer	0.322	0.005
Phagosome	3.060	0.008	Intestinal immune network for IgA production	0.008	0.007
Proteasome	5.231	0.010	Calcium signaling pathway	0.217	0.009
Rheumatoid arthritis	3.816	0.011	Wnt signaling pathway	0.215	0.013
Collecting duct acid secretion	6.880	0.012	Axon guidance	0.203	0.017
Purine metabolism	2.679	0.014	Prostate cancer	0.140	0.021
Arginine and proline metabolism	4.135	0.023	Amoebiasis	0.173	0.024
Vasopressin-regulated water reabsorption	4.610	0.024	Pancreatic cancer	0.118	0.028
Starch and sucrose metabolism	4.713	0.028	Pyruvate metabolism	0.042	0.032
Histidine metabolism	5.117	0.040	ABC transporters	0.045	0.032
Parkinson's disease	2.633	0.047	Adherens junction	0.155	0.042
			Arrhythmogenic right ventricular cardiomyopathy (ARVC)	0.158	0.043
			T cell receptor signaling pathway	0.245	0.047

Table 3.3. VYS pathways significantly altered by 6h MEHP treatment in WEC. Significantly enriched KEGG pathways (shown left) are similar to EMB, including pathways central to metabolism, and adaptation of redox environment. Significantly depleted pathways (shown right) are also similar for both tissues, including pathways involved in signal transduction, including several crucial for neurodevelopment.

Pathways significantly *enriched* in VYS tissue	Odds Ratio	P-value	Pathways significantly *depleted* in VYS tissue	Odds Ratio	P-value
Oxidative phosphorylation	8.109	0.000	Neuroactive ligand-receptor interaction	0.127	0.000
Parkinson's disease	7.795	0.000	Tight junction	0.059	0.001
Glutathione metabolism	13.522	0.000	Axon guidance	0.108	0.005
Alzheimer's disease	5.166	0.000	Fc gamma R-mediated phagocytosis	0.068	0.007
Aminoacyl-tRNA biosynthesis	11.307	0.000	Leukocyte transendothelial migration	0.093	0.007
Histidine metabolism	11.235	0.002	Cell adhesion molecules (CAMs)	0.105	0.007
N-Glycan biosynthesis	8.051	0.002	Long-term depression	0.037	0.007
Antigen processing and presentation	7.024	0.003	Hypertrophic cardiomyopathy (HCM)	0.057	0.008
Drug metabolism - cytochrome P450	6.644	0.004	Arrhythmogenic right ventricular cardiomyopathy (ARVC)	0.049	0.008
Selenocompound metabolism	14.129	0.006	Wnt signaling pathway	0.158	0.009
Huntington's disease	3.321	0.007	Jak-STAT signaling pathway	0.160	0.014
Alanine, aspartate and glutamate metabolism	8.852	0.007	Dilated cardiomyopathy	0.089	0.015
Arginine and proline metabolism	5.335	0.015	Pathways in cancer	0.345	0.016
Ribosome biogenesis in eukaryotes	4.276	0.022	Osteoclast differentiation	0.145	0.017
Complement and coagulation cascades	3.972	0.039	ECM-receptor interaction	0.095	0.019
			ErbB signaling pathway	0.105	0.020
			Hepatitis C	0.176	0.022
			T cell receptor signaling pathway	0.151	0.023
			Regulation of actin cytoskeleton	0.293	0.028
			Amoebiasis	0.153	0.030
			Fc epsilon RI signaling pathway	0.117	0.034
			Glioma	0.088	0.038
			VEGF signaling pathway	0.119	0.039

Table 3.4. Solute carrier (SLC) family genes are significantly impacted by 6h MEHP treatment in WEC. The mitochondrial transport family (SLC25) represents the most significantly altered family of transporters, crucial for the catabolic processes of the cell.

		# genes sig. changed		
SLC family	Function	EMB	VYS	TOTAL
1	glial high affinity glutamate/neutral amino acid transporter	1	2	3
4	bicarbonate transporters	6	2	8
5	inositol/sodium-dependent glucose transporters	2	1	3
6	neurotransmitter transporters	3	0	3
7	cationic/L-type amino acid transporters	3	2	5
8	sodium/calcium exchangers	1	1	2
9	sodium/hydrogen exchangers	3	3	6
10	sodium/bile salt exchangers	0	1	1
11	proton-coupled divalent metal ion transporters	1	0	1
12	electroneutral cation-coupled chloride cotransporters	2	1	3
13	sodium sulphate/carboxylate exchangers	0	1	1
16	monocarboxylic acid transporters	6	2	8
17	phosphate/organic anion transporters	2	1	3
19	folate/thiamine transporters	1	1	2
21	organic anion transporters	4	3	7
22	organic cation/anion transporters	4	0	4
23	ascorbate/nucleobase transporters	1	1	2
24	sodium/potassium/calcium exchangers	1	0	1
25	mitochondrial transporters	9	6	15
26	sulfate/anion transporters	2	2	4
29	nucleoside transporters	1	0	1
30	zinc transporters	2	2	4
31	copper transporters	1	0	1
33	acetyl-CoA transporters	0	1	1
35	nucleotide sugar transporters	8	1	9
36	proton-coupled amino acid transporters	0	1	1
37	sugar phosphate exchangers	1	0	1
38	sodium-amino acid cotransporters	1	0	1
39	zinc/metal ion transporters	1	3	4
44	choline transporter-like family	1	2	3
45	putative sugar transporters	2	1	3
46	folate transporters	1	1	2

References

1. Cai, J., et al., *Membrane properties of rat embryonic multipotent neural stem cells.* J Neurochem, 2004. **88**(1): p. 212-26.
2. Cove, D.J., *The generation and modification of cell polarity.* Journal of Experimental Botany, 2000. **51**(346): p. 831-838.
3. Thiery, J.P., J.L. Duband, and G.C. Tucker, *Cell Migration in the Vertebrate Embryo: Role of Cell Adhesion and Tissue Environment in Pattern Formation.* Annual Review of Cell Biology, 1985. **1**(1): p. 91-113.
4. Tsujioka, M., *Cell migration in multicellular environments.* Dev Growth Differ, 2011. **53**(4): p. 528-37.
5. Hansen, J.M. and C. Harris, *Redox control of teratogenesis.* Reproductive Toxicology, 2013. **35**(0): p. 165-179.
6. Jones, D.P., *Redefining oxidative stress.* Antioxid Redox Signal, 2006. **8**(9-10): p. 1865-79.
7. Ornoy, A., *Prenatal origin of obesity and their complications: Gestational diabetes, maternal overweight and the paradoxical effects of fetal growth restriction and macrosomia.* Reproductive Toxicology, 2011. **32**(2): p. 205-212.
8. Wan, J. and L.M. Winn, *In utero–initiated cancer: The role of reactive oxygen species.* Birth Defects Research Part C: Embryo Today: Reviews, 2006. **78**(4): p. 326-332.
9. Jeng, W., et al., *Methamphetamine-enhanced embryonic oxidative DNA damage and neurodevelopmental deficits.* Free Radical Biology and Medicine, 2005. **39**(3): p. 317-326.
10. Harris, C. and J. Hansen, *Oxidative Stress, Thiols, and Redox Profiles*, in *Developmental Toxicology*, C. Harris and J.M. Hansen, Editors. 2012, Humana Press. p. 325-346.
11. Hansen, J.M., et al., *Misregulation of gene expression in the redox-sensitive NF-κb-dependent limb outgrowth pathway by thalidomide.* Developmental Dynamics, 2002. **225**(2): p. 186-194.
12. Hansen, J.M., E.W. Carney, and C. Harris, *Altered differentiation in rat and rabbit limb bud micromass cultures by glutathione modulating agents.* Free Radical Biology and Medicine, 2001. **31**(12): p. 1582-1592.
13. McNutt, T.L. and C. Harris, *Lindane embryotoxicity and differential alteration of cysteine and glutathione levels in rat embryos and visceral yolk sacs.* Reproductive Toxicology, 1994. **8**(4): p. 351-362.
14. Hiranruengchok, R. and C. Harris, *Glutathione Oxidation and Embryotoxicity Elicited by Diamide in the Developing Rat Conceptus in Vitro.* Toxicology and Applied Pharmacology, 1993. **120**(1): p. 62-71.
15. Sahambi, S.K. and B.F. Hales, *Exposure to 5-Bromo-2'-deoxyuridine induces oxidative stress and activator protein-1 DNA binding activity in the embryo.* Birth Defects Research Part A: Clinical and Molecular Teratology, 2006. **76**(8): p. 580-591.
16. Harris, C., et al., *Inhibition of glutathione biosynthesis alters compartmental redox status and the thiol proteome in organogenesis-stage rat conceptuses.* Free Radical Biology and Medicine, 2013. **63**(0): p. 325-337.
17. Thompson, S.A., et al., *Modulation of Glutathione and Glutamate-L-cysteine Ligase by Methylmercury during Mouse Development.* Toxicological Sciences, 2000. **57**(1): p. 141-146.
18. Harris, C. and J.M. Hansen, *Nrf2-Mediated Resistance to Oxidant-Induced Redox Disruption in Embryos.* Birth Defects Research Part B: Developmental and Reproductive Toxicology, 2012. **95**(3): p. 213-218.
19. Akella, S.S. and C. Harris, *Pyridine nucleotide flux and glutathione oxidation in the cultured rat conceptus.* Reproductive Toxicology, 1999. **13**(3): p. 203-213.
20. Winn, L.M. and P.G. Wells, *Evidence for embryonic prostaglandin H synthase-catalyzed bioactivation and reactive oxygen species-mediated oxidation of cellular macromolecules in phenytoin and benzo[a]pyrene teratogenesis.* Free Radical Biology and Medicine, 1996. **22**(4): p. 607-621.

21. Dreosti, I.E., *Micronutrients, superoxide and the fetus.* Neurotoxicology, 1987. **8**(3): p. 445-9.
22. Dreosti, I.E., S.J. Manuel, and R.A. Buckley, *Superoxide dismutase (EC 1.15.1.1), manganese and the effect of ethanol in adult and foetal rats.* British Journal of Nutrition, 1982. **48**(02): p. 205-210.
23. Dreosti, I. and E. Partick, *Zinc, ethanol, and lipid peroxidation in adult and fetal rats.* Biological Trace Element Research, 1987. **14**(3): p. 179-191.
24. Devi, B.G., et al., *Effect of ethanol on rat fetal hepatocytes: Studies on cell replication, lipid peroxidation and glutathione.* Hepatology, 1993. **18**(3): p. 648-659.
25. Henderson, G.I., et al., *In Utero Ethanol Exposure Elicits Oxidative Stress in the Rat Fetus.* Alcoholism: Clinical and Experimental Research, 1995. **19**(3): p. 714-720.
26. Erkekoglu, P., et al., *Evaluation of cytotoxicity and oxidative DNA damaging effects of di(2-ethylhexyl)-phthalate (DEHP) and mono(2-ethylhexyl)-phthalate (MEHP) on MA-10 Leydig cells and protection by selenium.* Toxicology and Applied Pharmacology, 2010. **248**(1): p. 52-62.
27. Lin, S., et al., *Phthalate exposure in pregnant women and their children in central Taiwan.* Chemosphere, 2011. **82**(7): p. 947-955.
28. Lin, L., *[Levels of environmental endocrine disruptors in umbilical cord blood and maternal blood of low-birth-weight infants].* Zhōnghuá yùfáng-yīxué zázhì, 2008. **42**(3): p. 177-80.
29. Huang, P.-C., et al., *Association between prenatal exposure to phthalates and the health of newborns.* Environment International, 2009. **35**(1): p. 14-20.
30. Mose, T., et al., *Phthalate monoesters in perfusate from a dual placenta perfusion system, the placenta tissue and umbilical cord blood.* Reproductive Toxicology, 2007. **23**(1): p. 83-91.
31. Stroheker, T., et al., *Effect of in utero exposure to di-(2-ethylhexyl)phthalate: Distribution in the rat fetus and testosterone production by rat fetal testis in culture.* Food and Chemical Toxicology, 2006. **44**(12): p. 2064-2069.
32. Calafat, A.M., et al., *Urinary and amniotic fluid levels of phthalate monoesters in rats after the oral administration of di(2-ethylhexyl) phthalate and di-n-butyl phthalate.* Toxicology, 2006. **217**(1): p. 22-30.
33. Latini, G., et al., *In Utero Exposure to Di-(2-Ethylhexyl)phthalate and Duration of Human Pregnancy.* Environmental health perspectives, 2003. **111**(14): p. 1783-1785.
34. Latini, G., et al., *Exposure to Di(2-ethylhexyl)phthalate in Humans during Pregnancy.* Neonatology, 2003. **83**(1): p. 22-24.
35. Tetz, L.M., et al., *Mono-2-ethylhexyl phthalate induces oxidative stress responses in human placental cells in vitro.* Toxicology and Applied Pharmacology, 2013. **268**(1): p. 47-54.
36. Chu, D.-P., et al., *Abnormality of maternal-to-embryonic transition contributes to MEHP-induced mouse 2-cell block.* Journal of Cellular Physiology, 2013. **228**(4): p. 753-763.
37. Erkekoğlu, P., et al., *Induction of ROS, p53, p21 in DEHP- and MEHP-exposed LNCaP cells-protection by selenium compounds.* Food and Chemical Toxicology, 2011. **49**(7): p. 1565-1571.
38. Onorato, T.M., P.W. Brown, and P.L. Morris, *Mono-(2-ethylhexyl) Phthalate Increases Spermatocyte Mitochondrial Peroxiredoxin 3 and Cyclooxygenase 2.* Journal of Andrology, 2008. **29**(3): p. 293-303.
39. Harris, C., *Rodent Whole Embryo Culture*, in *Developmental Toxicology*, C. Harris and J.M. Hansen, Editors. 2012, Humana Press. p. 215-237.
40. Janer, G., et al., *Use of the rat postimplantation embryo culture to assess the embryotoxic potency within a chemical category and to identify toxic metabolites.* Toxicology in Vitro, 2008. **22**(7): p. 1797-1805.
41. Robinson, J.F., et al., *Dose–response analysis of phthalate effects on gene expression in rat whole embryo culture.* Toxicology and Applied Pharmacology, 2012. **264**(1): p. 32-41.
42. Stoscheck, C., *Quantification of Protein.* Methods in Enzymology, 1990. **182**: p. 50-69.
43. Jones, D.P., et al., *Glutathione measurement in human plasma: Evaluation of sample collection, storage and derivatization conditions for analysis of dansyl derivatives by HPLC.* Clinica Chimica Acta, 1998. **275**(2): p. 175-184.

44. Sartor, M.A., G.D. Leikauf, and M. Medvedovic, *LRpath: a logistic regression approach for identifying enriched biological groups in gene expression data.* Bioinformatics, 2009. **25**(2): p. 211-217.
45. Hoglund, P.J., et al., *The solute carrier families have a remarkably long evolutionary history with the majority of the human families present before divergence of Bilaterian species.* Mol Biol Evol, 2011. **28**(4): p. 1531-41.
46. Institute of Biochemistry and Molecular Medicine, *SLC Tables*, in *Bioparadigms.org*, 2004, University of Bern: Bern, Switzerland
47. Palmieri, F., *The mitochondrial transporter family SLC25: Identification, properties and physiopathology.* Molecular Aspects of Medicine, 2013. **34**(2–3): p. 465-484.
48. *SLC7A9*, in *Gene Database*2014, National Center for Biotechnology Information.
49. Rogers, A., et al., *Management of Cystinuria.* Urologic Clinics of North America, 2007. **34**(3): p. 347-362.
50. Feliubadalo, L., et al., *Slc7a9-deficient mice develop cystinuria non-I and cystine urolithiasis.* Hum Mol Genet, 2003. **12**(17): p. 2097-108.
51. Hansen, J.M., *Oxidative stress as a mechanism of teratogenesis.* Birth Defects Res C Embryo Today, 2006. **78**(4): p. 293-307.
52. Aw, T.Y., *Cellular Redox: A Modulator of Intestinal Epithelial Cell Proliferation*. Vol. 18. 2003. 201-204.
53. Droge, W., *Free radicals in the physiological control of cell function.* Physiol Rev, 2002. **82**(1): p. 47-95.
54. Shi, X., et al., *Reactive oxygen species in cancer stem cells.* Antioxid Redox Signal, 2012. **16**(11): p. 1215-28.
55. Pervaiz, S., R. Taneja, and S. Ghaffari, *Oxidative stress regulation of stem and progenitor cells.* Antioxid Redox Signal, 2009. **11**(11): p. 2777-89.
56. Acharya, A., et al., *Redox regulation in cancer: a double-edged sword with therapeutic potential.* Oxid Med Cell Longev, 2010. **3**(1): p. 23-34.
57. Kovacic, P. and R. Somanathan, *Mechanism of teratogenesis: electron transfer, reactive oxygen species, and antioxidants.* Birth Defects Res C Embryo Today, 2006. **78**(4): p. 308-25.
58. Harris, C. and J.M. Hansen, *Oxidative stress, thiols, and redox profiles.* Methods Mol Biol, 2012. **889**: p. 325-46.
59. Hill, M., *Mouse Timeline Detailed*, in *UNSW Embryology*2000. p. ISBN: 978 0 7334 2609 4.
60. Harris, C. and J.M. Hansen, *Nrf2-mediated resistance to oxidant-induced redox disruption in embryos.* Birth Defects Res B Dev Reprod Toxicol, 2012. **95**(3): p. 213-8.
61. Nguyen, T., P. Nioi, and C.B. Pickett, *The Nrf2-antioxidant response element signaling pathway and its activation by oxidative stress.* J Biol Chem, 2009. **284**(20): p. 13291-5.
62. Mannery, Y.O., et al., *Oxidation of plasma cysteine/cystine and GSH/GSSG redox potentials by acetaminophen and sulfur amino acid insufficiency in humans.* J Pharmacol Exp Ther, 2010. **333**(3): p. 939-47.
63. Mani, S., G. Yang, and R. Wang, *A critical life-supporting role for cystathionine gamma-lyase in the absence of dietary cysteine supply.* Free Radic Biol Med, 2011. **50**(10): p. 1280-7.
64. Jahoor, F., *Effects of decreased availability of sulfur amino acids in severe childhood undernutrition.* Nutr Rev, 2012. **70**(3): p. 176-87.
65. Ambroso, J. and C. Harris, *Assessment of Histiotrophic Nutrition Using Fluorescent Probes*, in *Developmental Toxicology*, C. Harris and J.M. Hansen, Editors. 2012, Humana Press. p. 407-423.
66. Moestrup, S.K. and P.J. Verroust, *Megalin- and Cubilin-Mediated Endocytosis of Protein-Bound Vitamins, Lipids, and Hormones in Polarized Epithelia.* Annual Review of Nutrition, 2001. **21**(1): p. 407-428.
67. Fisher, C.E. and S.E.M. Howie, *The role of megalin (LRP-2/Gp330) during development.* Developmental Biology, 2006. **296**(2): p. 279-297.

68. Burton, G.J., J. Hempstock, and E. Jauniaux, *Nutrition of the human fetus during the first trimester--a review.* Placenta, 2001. **22 Suppl A**: p. S70-7.
69. Jauniaux, E., et al., *Onset of maternal arterial blood flow and placental oxidative stress. A possible factor in human early pregnancy failure.* Am J Pathol, 2000. **157**(6): p. 2111-22.
70. Jauniaux, E., A. Watson, and G. Burton, *Evaluation of respiratory gases and acid-base gradients in human fetal fluids and uteroplacental tissue between 7 and 16 weeks' gestation.* American Journal of Obstetrics and Gynecology, 2001. **184**(5): p. 998-1003.
71. Johnson, M.A., et al., *Amino Acid Starvation Has Opposite Effects on Mitochondrial and Cytosolic Protein Synthesis.* PLoS ONE, 2014. **9**(4): p. e93597.
72. Petrushanko, I.Y., et al., *S-glutathionylation of the Na,K-ATPase catalytic alpha subunit is a determinant of the enzyme redox sensitivity.* J Biol Chem, 2012. **287**(38): p. 32195-205.
73. Liu, J., et al., *Reactive Oxygen Species Modulation of Na/K-ATPase Regulates Fibrosis and Renal Proximal Tubular Sodium Handling.* Int J Nephrol, 2012. **2012**: p. 381320.
74. Petrushanko, I., et al., *Na-K-ATPase in rat cerebellar granule cells is redox sensitive.* Am J Physiol Regul Integr Comp Physiol, 2006. **290**(4): p. R916-25.
75. Comellas, A.P., et al., *Hypoxia-Mediated Degradation of Na,K-ATPase via Mitochondrial Reactive Oxygen Species and the Ubiquitin-Conjugating System.* Circulation Research, 2006. **98**(10): p. 1314-1322.
76. Liu, J., et al., *Ouabain interaction with cardiac Na+/K+-ATPase initiates signal cascades independent of changes in intracellular Na+ and Ca2+ concentrations.* J Biol Chem, 2000. **275**(36): p. 27838-44.
77. Formentini, L., et al., *The mitochondrial ATPase inhibitory factor 1 triggers a ROS-mediated retrograde prosurvival and proliferative response.* Mol Cell, 2012. **45**(6): p. 731-42.
78. Mizushima, N., *Autophagy: process and function.* Genes Dev, 2007. **21**(22): p. 2861-73.
79. Lin, T.C., et al., *Autophagy: resetting glutamine-dependent metabolism and oxygen consumption.* Autophagy, 2012. **8**(10): p. 1477-93.
80. Kann, O. and R. Kovacs, *Mitochondria and neuronal activity.* Am J Physiol Cell Physiol, 2007. **292**(2): p. C641-57.
81. Cordeau-Lossouarn, L., et al., *Mitochondrial maturation during neuronal differentiation in vivo and in vitro.* Biol Cell, 1991. **71**(1-2): p. 57-65.
82. Hong, Y., et al., *Subchronic exposure to arsenic decreased Sdha expression in the brain of mice.* Neurotoxicology, 2009. **30**(4): p. 538-43.
83. Wlodarczyk, B.J., et al., *Arsenic-induced gene expression changes in the neural tube of folate transport defective mouse embryos.* Neurotoxicology, 2006. **27**(4): p. 547-57.
84. Maria Fimia, G., et al., *Ambra1 regulates autophagy and development of the nervous system.* Nature, 2007. **v447**(n7148): p. 1121-1125.
85. Cecconi, F., et al., *A novel role for autophagy in neurodevelopment.* Autophagy, 2007. **3**(5): p. 506-8.
86. Xu, C., et al., *Trehalose prevents neural tube defects by correcting maternal diabetes-suppressed autophagy and neurogenesis.* Am J Physiol Endocrinol Metab, 2013. **305**(5): p. E667-78.
87. Walls, K.C., et al., *Lysosome dysfunction triggers Atg7-dependent neural apoptosis.* J Biol Chem, 2010. **285**(14): p. 10497-507.

Chapter IV

Mono-2-ethylhexyl phthalate (MEHP) alters histiotrophic nutrition pathways and epigenetic processes in the developing conceptus

Introduction

The processes by which mammalian embryos obtain nutrients and substrates for growth and development during embryogenesis and early organogenesis are known as histiotrophic nutrition pathways (HNPs). Because the placenta has not yet become fully functional, active maternal-embryonic supply of substrates and metabolic cofactors from maternal circulation is not yet available. HNPs involve the receptor-mediated endocytosis (RME) of proteins and their bound nutrient and cofactor cargoes through the visceral yolk sac (VYS) brush border, and subsequent proteolysis of the proteins in the vesicles to release nutrients for cellular processes in the VYS and the embryo proper (EMB). During HNPs, RME of whole, bulk proteins and their cargos followed by their subsequent proteolysis maintains an amino acid and nutrient pool to provide substrates for protein biosynthesis and enzymatic function.

HNPs are responsible for providing and transporting many substrates to the EMB, including methyl donors for one-carbon (C_1) metabolism such as methionine and folate. C_1 metabolism is the process by which dietary methyl donors are utilized to synthesize S-adenosylmethionine (SAM), the primary molecular methyl donor for cells. Through C_1 metabolism, SAM is made available for numerous processes, including post-translational

modifications and epigenetic regulation. Thus, the nutritional state of the conceptus may govern epigenetic regulation of genetic processes [1].

During the first trimester of pregnancy, cells are rapidly dividing to facilitate overall growth and anatomical form in order to complete embryogenesis. During this time, DNA undergoes substantial epigenetic remodeling, from near-complete loss of methylation marks after fertilization to reprogramming of methylation marks during embryogenesis and early organogenesis [2,3]. Histone methylation, on the other hand, is variable; methylation increases over developmental time at the H3K4 locus and decreases at the H3K27 locus [4]. Because these processes occur during the phase of HNP-supplied nutrition and this process provides the necessary methyl donors for epigenetic marks, it is possible that perturbation of HNPs may result in abnormal epigenetic programming. Previous work has demonstrated that inhibition of HNP lysosomal function with leupeptin resulted in decreased DNA methylation in the EMB and VYS during early organogenesis [5].

Common dietary methyl donors and cofactors for C_1 metabolism, including folate, betaine, choline, and vitamin B_{12}, are required for normal growth and development. Maternal deficiencies in folate and choline during pregnancy have been associated with increased risk for neural tube defects (NTDs) [6-8]. Previous studies have demonstrated that exposure to mono-2-ethylhexyl phthalate (MEHP), the primary metabolite of the ubiquitous plasticizing agent di-2-ethylhexyl phthalate, increased the number of embryos with NTDs (Chapter 3). Thus, the purpose of this work is to identify whether this increased number of NTDs is concordant with decreased nutrient bioavailability to the EMB, and whether this may have epigenetic consequences. It is hypothesized that MEHP exposure will reduce the efficacy of HNPs, reducing availability of methyl donors and C_1 metabolism, and that these changes will result in decreased DNA and histone methylation.

Materials & Methods

Chemicals and Reagents

Bicinchoninic acid, dimethyl sulfoxide (HPLC grade), Tyrode's balanced salt solution (TBSS), penicillin/streptomycin (10,000 units/ml penicillin, 10,000 μg/ml streptomycin sulfate), N,N,N-Trimethyl-d_9-Glycine HCl (Betaine-d_9), Homocysteine-d8 were obtained from Sigma/Aldrich (St. Louis, MO). Hanks balanced salt solution (HBSS) was purchased from GIBCO/Life Technologies (Grand Island, NY). Mono-2-ethylhexyl phthalate was obtained from AccuStandard (New Haven, CT). L-Methionine (methyl-d3) and D,L-cysteine (3,3-d2) were purchased from Cambridge Isotope Laboratories (Andover, MA, USA), and S-Adenosyl-L-methionine-d3 (S-methyl-d3) tetra (p-toluenesulfonate) salt was from C/D/N Isotopes (Pointe-Claire, Quebec, Canada).

Mouse whole embryo culture

Mouse embryo culture (mWEC) was performed following the conditions outlined in [9], and described in Chapter 3. Briefly, female CD-1 mice were time-mated and obtained from Charles River (Portage, MI). The morning of discovery of a vaginal plug was designated as gestational day (GD) 0. Animals were maintained on a 12 h light-12h dark cycle and were supplied food and water *ad libitum*. Pregnant mice were euthanized with CO_2 on GD 8 and the uterus was removed. Conceptuses were explanted from the uterus, randomized, and placed into 10 ml culture bottles. Each culture bottle contained 5 ml of 75% heat-inactivated rat serum/25% Tyrode's balanced salt solution (TBSS), and 21.5 ul penicillin/streptomycin. Bottles were placed on a continuous-gassing

carousel supplied with 5% O_2/5% CO_2/90% N_2, and the gas mixture was changed after 6 hours to 20% O_2/5% CO_2/75% N_2 to mimic *in utero* circulatory changes.

Exposures and Sample Collection

MEHP was suspended in DMSO to increase solubility, and stored at a concentration of 1 mg/ml. This MEHP mixture was diluted in DMSO and added to each treatment culture bottle to produce a final concentration of 100 or 250 µg/ml. These concentrations were optimized from previous experiments (Chapter 3), accounting for viability and morphology, as well as reproducibility from other phthalate WEC experiments [10,11]. Control bottles received an equivalent volume of DMSO only, and the total volume added was no greater than 1 µl/ml culture medium. Conceptuses remained in culture for 24 h.

Following the culture period, conceptuses for DNA and histone analysis were thoroughly rinsed in HBSS and briefly inspected, at which time malformations and delayed closure of the embryonic neural tube were noted. EMB with closed neural tubes were denoted as NTD-, while those with open neural tubes were denoted as NTD+ (Fig. 4.1). At the time of collection, no control samples had notable defects to the neural tube. Conceptuses providing tissues for DNA isolation were dissected into EMB and VYS, snap frozen, and stored at -76^{0}C until use. Conceptuses for histone isolation were also dissected into EMB and VYS, but histone proteins were immediately extracted using the EpiQuik™ Total Histone Extraction Kit (Epigentek). Following extraction, proteins were stored at -20^{0}C overnight until completion of histone methylation experiments the following day.

Conceptuses for histiotrophic nutrition analysis were untreated for the first 24 h in culture, before beginning histiotrophic nutrition protocols outlined in [12,13]. After 24 h (GD 9),

fluorescently tagged FITC-albumin was added to the culture media at a nontoxic, total concentration of 100 µg/ml. At this time, 100 or 250 µg/ml MEHP treatment was added. Ethanol treatment was also performed as a positive control, as it is a known inhibitor of endocytosis and histiotrophic nutrition processes (unpublished data) [14]. These treatment conditions occurred in complete darkness for 3 h. At the conclusion, conceptuses were removed from culture and thoroughly rinsed in HBSS. They were then pooled in duplicate and transferred into a 150 µl drop containing 50 mM sodium phosphate buffer (pH=6.0) for dissection. The VYS was removed and collected into 0.1% Triton X-100, followed by the EMB. The extra-embryonic fluids (EEF) were thus remaining in the sodium phosphate buffer and also collected.

Whole conceptuses for analysis for C_1 component quantification or quantification of methyl donors were treated with 100 or 250 µg/ml MEHP for 24 h in culture. At the conclusion of the culture period, whole conceptuses were carefully rinsed and kept intact. Samples for C_1 component quantification were collected in reducing agent containing dithiothreitol and sodium hydroxide and incubated at room temperature for 15 min. Conceptuses for quantification of choline and betaine were collected into 100 µl acetonitrile, and conceptuses for quantification of folate and vitamin B_{12} were collected into 500 µl 6% trichloroacetic acid (TCA).

Histiotrophic Nutrition Assay

Histiotrophic nutrition assays were conducted using a modified version of the protocol outlined in [12]. Though its contribution to total fluorescence is minimal, fluorescence in the EMB fraction of the conceptus was also measured. After tissue separation and collection, samples were sonicated. A 20 µl aliquot of each sample and of culture media were immediately collected and set aside for measurement of total fluorescence, following addition of 230 µl of Triton X-100 and 750

ml of 6% TCA with 1% SDS. 750 µl of 6% TCA was added to the remainder of each sample, followed by vortexing and precipitation at 4°C overnight.

The next morning, samples were centrifuged at 9,500 x *g* for 10 min. The supernatant of each sample was transferred to a new tube for quantification of soluble fraction fluorescence. One ml of 500 mM and 150 µl of 1N sodium hydroxide were added to each tube, before setting aside for fluorescence quantification. The insoluble fractions were precipitated in 150 µl of 1N NaOH at room temperature for 1 h, prior to addition of Tris buffer, sodium hydroxide, and 6% TCA in equivalent amounts to the soluble fractions.

Soluble, insoluble, and total fluorescence were quantified by fitting sample fluorescence to a standard curve, ranging from 1-250 µg/ml FITC-albumin. Samples were plated onto opaque, black 96-well plates in triplicate replicates of 200 µl for each sample. Plates were read by spectrofluorometer, with excitation and emission wavelengths set at 495 and 520 nm, respectively. Normalization of results to sample protein concentrations was performed following bicinchoninic acid (BCA) assay.

C_1 Metabolism Component Quantification

Quantification of C_1 components was performed as previously described in [5]. Liquid chromatography-tandem mass spectrometry was performed using a TSQ Quantum Ultra AM triple quadrupole mass spectrometer (Thermo Scientific, Rockford, IL) coupled to a Water 2695 Separations Module (Waters, Milford, MA). These were fitted with a Luna C18(2) 5-µM 250 x 4.6-mm column and 4 mm C18 guard column (Phenomenex, Torrence, CA). All data was recorded using Xcalibur software (Thermo).

Briefly, isotopic standards for SAM, methionine, cysteine, and homocysteine were added to each sample in known quantities following the incubation in reducing agent. To precipitate the samples, 0.1% formic acid and 0.05% trifluoroacedtic acid were added to the samples before centrifugation and transfer of the supernatant to high-performance liquid chromatographic (HPLC) vials for analysis. The pellet was resolubilized in 0.25M sodium hydroxide, and total protein was quantified using BCA assay. A gradient method was programmed to conduct linear transitions between mobile phases containing water and 0.1% formic acid (mobile phase A) and acetonitrile and 0.1% formic acid (mobile phase B). All transitions, flow rate, and injection volume were optimized through direct tuning. Concentrations of each analyte were calculated by ratio of the measured analyte to the known quantity of the isotopic standard in each sample. All data was normalized to the total protein concentration of the conceptus to account for the differences in size and morphology due to MEHP treatment (Chapter 3).

Quantification of Choline and Betaine

Quantification of choline and betaine was performed using a modified version of the protocol outlined in [15]. The same instrumentation used to measure C_1 components was utilized, but outfitted with an Atlantis HILIC Silica 3-µm 4.6 x 30-mm column (Waters) and 4-mm guard column. Samples collected in acetonitrile were centrifuged and the supernatant was removed. The pellet was reconstituted in 0.25M sodium hydroxide and used to determine total protein concentration using BCA assay. Choline-d_9 and betaine-d_9 isotopic standards were added to supernatants at final concentrations of 0.4 µM, and the samples were transferred to HPLC vials prior to injection. The concentration of choline and betaine was a response factor, calculated as the ratio of the analyte to the known quantity of isotopic standard, and normalized to total protein

concentration. Culture medium was also sampled, and there were no differences in the amounts of choline and betaine between culture bottles.

Quantification of Folate and Vitamin B_{12}

Samples collected in 6% TCA were briefly sonicated, and centrifuged at 9,500 x *g* for 5 minutes. The supernatant was transferred to a new tube, snap frozen, and shipped to the Gastrointestinal Laboratory at the Texas A&M University Department of Veterinary Small Animal Clinical Sciences. Immunoassays for folate and vitamin B_{12} were conducted using the IMMULITE 2000 system (Siemens Healthcare). The pellet was re-suspended in 0.25M sodium hydroxide, and total protein was determined using BCA assay. Folate and vitamin B_{12} measures concentrations were reported after normalization to total conceptal protein. No differences in the amounts of folate and vitamin B_{12} were detected between culture bottles.

A linear gradient method flowing at 2.0 ml/min was programmed for mobile phases. Mobile phase A was comprised of water, 10 mM ammonium acetate, and 0.15% formic acid. Mobile phase B was 100% acetonitrile. The gradient began at 20% A:80% B for 1 min, ramped to 60% A from 1 to 2 min, and then held until 2.3 min until returning to initial conditions at 2.4 min. Flow was split 4:1, sending 500 ul/min to the mass spectrometer set to ESI positive ion mode. The injection volume was 2 µl. The following settings were applied: 3500 spray voltage, 55 units sheath gas, 30 units auxillary gas, capillary 300 C and 35 V, and 1.5 mtorr collision pressure. The needle wash used was 9:1 methanol:water, and carryover was very minimal. *m/z* transitions were optimized for detection of analytes and isotopic standards as follows: choline 104-60+, choline-d_9 113-69+ (collision energy 16V, tubelens 62 V), betaine 118-59+ and betaine-d_9 127-68 (collision energy 21V, tubelens 75 V).

Global Histone Methylation

Total histone protein was quantified using bicinchoninic acid assay, and equivalent amounts of histone protein were used for methylation analysis. Histone methylation at the H3K4 and H3K27 loci was probed using EpiQuik™ Global Pan-Methyl Histone Quantification Kits (Epigentek). Fluorescence associated with methyl markers at the loci was detected and used to quantify percent methylation. H3K4 histone methylation is typically associated with activation of genes, making chromatin more accessible, and H3K27 methylation is typically considered a repressive marker, encouraging the tight packaging of chromatin [4]. These pan-methyl kits were selected to probe the effects of altered nutrition on histone methylation, instead of specifically investigating the effects on tri-methylation at these loci.

DNA Isolation

Genomic DNA from EMB and VYS samples exposed for 24 h to MEHP (100 or 250 µg/ml) or controls (DMSO) was isolated using phenol-chloroform extraction. Briefly, thawed samples were sonicated in Buffer ATL (Qiagen), and digested overnight at 50^0C after addition of Proteinase K (Qiagen). The following morning, RNase A was added before repeated phenol-chloroform isoamyl alcohol extractions in phase-lock gel tubes (5 PRIME). A choloroform-only wash was performed, followed by repeated ethanol precipitations. The DNA pellet was then dried before storage in Tris buffer (pH 8.0) until use.

LUmiometric Methylation Assay (LUMA)

LUMA was utilized as explained in [16,17] and previously performed in [5]. Briefly, DNA isolated from EMB and VYS samples was subjected to restriction enzyme digestion for 4 hours at 37^0C. Samples were separately digested with either methylation-sensitive HpaII or methylation–insensitive MspI restriction enzymes (Invitrogen), which both cleave genomic DNA at CCGG sites. EcoRI (Invitrogen) was also added to each digest to function as an internal control. Following digestion, Annealing buffer (Qiagen) was added to the products and these were analyzed using the PyroMark™ Q96 MD system (Qiagen). Samples were run in triplicate to account for variation. Ratios for MspI and HpaII relative to their internal EcoRI controls were used to quantify overall percent methylation, using the following equation: 1-[(HpaII/EcoRI)/(MspI/EcoRI)]x100.

Statistical Analysis

Results presented are presented as mean ± SEM. Unpaired t-tests and ANOVA with Tukey's post-hoc test were used to probe statistical significance. A confidence level of 95% was used throughout the study, and all tests were performed using SPSS. Statistical outliers were removed if data points fell at least 1.5 times the interquartile range outside of the first and third quartile values.

Results

Histiotrophic Nutrition Assay

Total clearance, defined as the cumulative clearance from the culture medium into the VYS, EEF, and EMB, was quantified to determine whether MEHP could reduce histiotrophic uptake of proteins (Fig. 4.2). Clearance is expressed as the volume of culture media cleared of FITC-albumin per min per mg of conceptal protein. Immediately upon inspection, the insoluble

fraction clearance was less than 10% of the soluble fraction clearance. This is indicative of inhibition of RME rather than inhibition of proteolytic processes. For this reason, ethanol was selected as an appropriate positive control because it is a known inhibitor of RME (unpublished data) [14]. Soluble control histiotrophic clearance (54.6 ± 4.3 ml media/mg protein/h; n=9) and total (soluble + insoluble) FITC-albumin clearance (59.8 ± 5.2; n=9) was significantly greater than the clearance of ethanol-exposed conceptuses for both the soluble (34.5 ± 3.9; n=9) and total (35.5 ± 3.3; n=9) fractions (p=0.001). No significant changes were observed due to any MEHP or ethanol treatment for the insoluble fractions (p>0.05). Exposure to MEHP at the 100 µg/ml dose significantly decreased clearance as measured by the soluble fraction (38.9 ± 2.7; n=8; p=0.018), though only slightly decreased FITC-albumin clearance of the total fraction (48.8 ± 2.7; n=8; p=0.28). Exposure to MEHP at the 250 µg/ml dose significantly reduced both soluble (31.3 ± 2.5; n=9) and total (33.1 ± 4.7; n=9) fraction clearance (p<0.001). These decreases in clearance for the high MEHP exposure group were even greater than those of the ethanol positive control. Overall, MEHP can effectively reduce histiotrophic nutrient uptake of the conceptus, and this is most likely due to inhibition of RME.

Quantification of Methyl Donors and C_1 Metabolism Components

C_1 metabolism components and dietary methyl group donors were quantified to determine whether these decreases in HNPs translate to functional methyl group deficiencies (Table 4.1). SAM concentrations were variable across samples, and thus no statistically significant differences were observed (p>0.05). However, there was an obvious increase in SAM concentrations with increasing MEHP dose. Control SAM concentrations (820.9 ± 87.3 ng/mg protein; n=4) were lower than those from conceptuses exposed to 100 µg/ml MEHP in culture (1487.4 ± 358.6; n=5;

p>0.5), and this increased further for those exposed at the 250 μg/ml dose (2380.1 ± 659.5; n=5; p=0.129).

This same increasing trend was evident for cysteine and methionine. Though control conceptal cysteine measurements (1467.4 ± 192.0 ng/mg protein; n=5) are lower than those of the 100 μg/ml group (2338.4 ± 378.0; n=5), this relationship was not statistically significant (p=0.125). Cysteine was further increased in the 250 μg/ml group (2506.9 ± 265.2; n=5; p=0.062). Methionine concentrations increased with increasing MEHP dose from controls (635.1 ± 44.0 ng/mg protein; n=4) to 956.5 ± 171.8 (n=5; p=0.16) for the 100 μg/ml group and to 1427.0 ± 235.6 (n=5; p=0.031).

Homocysteine does not follow the same pattern as the other C_1 metabolic components. The control (70.1 ± 5.1 ng/mg protein; n=5) and 100 μg/ml (63.8 ± 3.4; n=4) groups do not significantly differ (p>0.9). However, the 250 μg/ml group has significantly elevated homocysteine concentrations (97.4 ± 8.5; n=4; p=0.031).

Folate does not significantly change due to MEHP treatment after 24 h. Control folate concentrations (0.66 ± 0.04 ng/mg protein; n=4) were similar to those exposed at the 100 μg/ml dose (0.51 ± 0.03; n=4; p=0.4). At the 250 μg/ml dose, however, folate concentrations are slightly greater than the 100 μg/ml concentrations (0.74 ± 0.08; n=5; p=0.07). Choline also follows this pattern. Choline concentrations in control conceptuses (2.15 ± 0.41 ng/mg protein; n=5) are similar to 100 μg/ml dosed conceptuses (1.35 ± 0.54; n=5; p=0.18), and is slightly elevated in the 250 μg/ml group (3.04 ± 0.87; n=4; p=0.15 compared to controls). The 250 μg/ml exposed conceptuses had significantly greater choline concentrations that the 100 μg/ml group (p=0.004).

Vitamin B_{12} control concentrations (17.00 ± 0.09 pg/mg protein; n=3) are significantly elevated compared to the 100 μg/ml MEHP dose (12.25 ± 0.41; n=3; p<0.001). Similarly to folate and choline, the 250 μg/ml MEHP dose concentration (15.23 ± 0.47; n=5) is significantly elevated

compared to the 100 μg/ml dose (p=0.003), but unlike folate and choline, this still remains decreased compared to the control measure (p=0.046). Betaine also follows this pattern. Control betaine concentrations (4.23 ± 0.39 ng/mg protein; n=4) are significantly greater than conceptuses exposed to 100 μg/ml MEHP (2.13 ± 0.95; n=5; p=0.002). Betaine concentrations are similar in the 250 μg/ml conceptuses (2.95 ± 0.42; n=4) compared to the 100 μg/ml group (p=0.3), but still slightly reduced compared to controls (p=0.056).

Global Histone Methylation

Global histone pan-methylation was measured in both control and MEHP-exposed (100 μg/ml) EMB and VYS, also stratified by NTD status (Fig. 4.3). Pan methylation is defined as the cumulative mono-, di-, and tri-methylation at a locus. Pan-methylation was examined at the H3K4 and H3K27 loci after 24 h in culture to determine whether nutritional modifications may result in methylation changes. H3K4 methylation was significantly increased in MEHP-treated, NTD+ EMB (55.1 ± 4.5; n=4) compared to MEHP-treated NTD- EMB (41.3 ± 1.9; n=6; p=0.01), and was also elevated compared to the controls (42.3 ± 4.5; n=6; p=0.08), though this increase was not statistically significant (Fig. 4.3A). No significant H3K4 methylation changes were observed between control (23.7 ± 2.8; n=5), MEHP-treated, NTD-negative (29.1 ± 5.3; n=8), or MEHP-treated, NTD-positive (30.4 ± 8.0; n=4) VYS (p>0.05).

H3K27 pan methylation was also measured in the EMB and VYS (Fig. 4.3B). No statistically significant changes in H3K27 methylation were observed in the EMB or VYS (p>0.05). H3K27 methylation was unchanged between control (58.2 ± 0.8; n=6), MEHP-treated and NTD-negative (56.7 ± 0.7; n=7), and MEHP-treated and NTD-positive (57.9 ± 2.5; n=4) EMB. H3K27 methylation was slightly increased in the VYS by MEHP treatment (64.6 ± 1.2; n=8)

compared to controls (62.7 ± 0.5; n=5), though this change was not statistically significant (p=0.18). H3K27 methylation was further increased in the NTD-positive, MEHP-treated VYS (66.4 ± 1.7; n=4), though this change was also not statistically significant (p=0.1).

LUminometric Methylation Assay (LUMA)

Global DNA methylation was measured in both control and MEHP-exposed (100 μg/ml) EMB and VYS following stratification by NTD status (Fig. 4.4A). MEHP exposure in the absence of NTD significantly reduced (p=0.03) DNA methylation in the EMB (54.7 ± 1.8; n=10) after 24 h when compared to controls (61.9 ± 2.2; n=5). DNA methylation was further reduced in MEHP-treated EMB with NTD (43.3 ± 7.7; n=3) compared to both controls (p=0.02) and MEHP-treated NTD negative EMB (p=0.04). In the VYS, there methylation was much lower than EMB DNA methylation and had the inverse response to treatment and NTD, though these changes were not statistically significant. MEHP exposure (37.7 ± 4.4; n=10) produced a trend of increased global DNA methylation in the VYS compared to controls (32.4 ± 3.8; n=4; p=0.4) but this was not significant. MEHP-treated VYS from conceptuses with NTDs also showed a mild trend but was not significant (p=0.08).

The effect of treatment concentration was further examined by treating conceptuses with 250 μg/ml MEHP (Fig. 4.4B). Again, regardless of NTD status, 100 μg/ml MEHP treatment significantly reduced global DNA methylation in the EMB (55.4 ± 1.9; n=13; p=0.01) compared to controls (61.9 ± 2.2; n=5). High variability of global DNA methylation was observed in EMB treated with 250 μg/ml MEHP, so no statistically significant further decrease was observed (p=0.4). No statistically significant changes were observed in the VYS (p=0.1-0.4), though there was a general trend of increased methylation with increasing MEHP dose. These changes are

consistent with methylation changes previously observed due to ethanol treatment, an inhibitor of RME (unpublished data).

Discussion

The relationship between prenatal nutrition and growth and development has been well studied, though the long-term consequences of nutritional deficiencies are highly variable. Previous work has demonstrated that exposure to MEHP during early organogenesis may result in stunted growth and delayed or halted neurulation (Chapter 3). Here, a nutritional deficiency is observed after exposure to MEHP, suggesting that embryonic exposures to toxicants may reduce nutrition and produce a canonical stunting of growth. The primary focus of this work was to examine these relationships during embryogenesis and early organogenesis, and does not make any conclusions about the long-term fetal and child consequences of this deficiency. A growing body of epidemiological studies have suggested that *in utero* deficiencies may result in the programming of a thrifty phenotype, resulting in predispositions to metabolic syndromes later in life [18]. Though this work suggests that growth is immediately stunted, it is possible that adaptation to these deficiencies may result in a thrifty phenotype.

This is further supported by measurements of C_1 components. In a previous study, it was demonstrated that decreases in HNPs result in C_1 deficiencies 6 h after initial exposure [5]. Here, however, C_1 metabolic components are increased with increasing MEHP concentrations in culture after 24 h. Because HNP activity is reduced in a dose-dependent fashion after 3 h, these results were surprising. It is hypothesized that methyl donors and C_1 components are actually decreased in the short run, but the conceptuses are able to adapt and compensate by 24 h post-initial exposure. Future studies investigating the ontogeny of nutritional environmental changes following

exposures should be performed to probe the short-term nutritional consequences of MEHP treatment and the potential compensatory mechanisms by which the conceptus may adapt.

Many studies have utilized toxicological and pharmacological agents to modify RME [19], though relatively few studies have demonstrated a link between toxicological or pharmacological agents and disruption of HNPs during development [14,20-27]. These studies encompass a wide range of chemical agents, with diverse structures and functions, and yet many of these exposures have the same outcomes. In this study, both ethanol and MEHP have been characterized to disrupt the RME portion of HNPs, but it is unknown whether or not they are acting via the same mechanism. Comparative toxicant studies should be done to characterize which classes of persistent compounds may directly affect HNPs, and to compare and contrast similarities in structure and function to predict HNP-mediated toxicity of other environmental agents. Additionally, an ontogeny of HNP clearance profiles would provide information about the compartmental differences in nutrient availability. In this study, total HNP clearance was measured, representing the total amount of media clearance to the VYS, EEF, and to the EMB. However, very little of the media had been cleared to the EMB during the 3-h window of investigation. By examining clearance over a greater time frame in the different conceptal compartments, it would be possible to understand the specificity and extent of reduced nutrition.

Megalin and cubilin, known as the multiligand endocytotic receptor complex (MERC), are major receptors involved in HNPs are which are localized to polarized epithelia such as the VYS [28-30]. Though rodent VYS are inverted, both rodent and human VYS both highly express megalin and cubilin [31]. These receptors are also found on neuroepithelia, and have been implicated in neurulation and neurodevelopment [32-35]. The MERC is responsible for the uptake of a vast array of nutrients, including various proteins and their cargoes, cholesterol, vitamins,

lipids, iron, and calcium [29,34,35]. It is also a major transporter of the developmental ligands Sonic Hedgehog (Shh) and retinoic acid, which are crucial for neurulation [33,36-39]. Vitamin B_{12} and folate are also co-transported across epithelia via the MERC by carrier proteins, suggesting a link between methyl donor metabolism and the MERC [29,40]. Future studies are required to discern whether MEHP acts through the MERC, and whether this response may be time-dependent. Work with transgenic Lrp2-deficient or Cubn-deficient models could provide insight into this mechanism, as well as an ontogeny of Lrp2 and Cubn expression following MEHP exposure.

In addition to the MERC, the solute carrier (SLC) families of transporters are also crucial for the transport of hormones, ligands, and nutrients across membranes. Several SLC families are responsible for the transport of choline, betaine, folate, and amino acids required for C_1 metabolism, and there are tissue- and organelle-specific transporters to allow for specific action. In particular, several SLC families are responsible for neurotransmitter transport and catabolism and cholinergic activity in the brain [41-44]. Studies have demonstrated that choline transporters and uptake are susceptible to chemical modulation of expression in the brain, including in fetal brain [45,46]. The relationship between embryonic toxicant exposures and molecular impacts on other transporters such as SLCs should be further characterized.

Previous survey of epigenetic literature has typically correlated increased methyl donor supplementation and availability with increased global methylation measures [1]. Pharmacological inhibition of HNPs was associated with decreased EMB and VYS SAM concentrations after 6 h and decreased global DNA methylation at both 6- and 24-h post initial treatment [5]. Here, 24 h treatment with increasing concentrations of MEHP increased C_1 component concentrations but had varying effects on methyl donor concentrations. As a result, VYS DNA methylation was

increased as would be expected, but EMB DNA methylation was decreased. However, the concentrations of methyl donors and C_1 metabolic components were measured in whole conceptuses inclusive of the VYS, EMB and all EEF. Further examination of compartmental C_1 components and methyl donors would provide more information about the bioavailability of these methylation substrates throughout the conceptus. It is probable that there are compensatory responses to nutrient deficits that may recycle and restore C_1 function, due to its metabolic importance. An ontogeny of C_1 component concentrations over this range of time would provide novel insight into the mechanisms by which decreased nutritional clearance may not alter C_1 component concentrations.

During embryogenesis, histone methylation is reprogrammed. H3K4 methylation is absent in the zygote and increases through to organogenesis, while H3K27 methylation becomes progressively demethylated between the zygote and organogenesis stages [4]. In the VYS, both treatment with MEHP and presence of NTD are associated with increased H3K27 methylation. It is possible that treatment with MEHP or presence of NTD prevent the demethylation processes required for normal methylation programming at the H3K27 locus. H3K4 global histone methylation was increased by both MEHP treatment and presence of NTD in both EMB and VYS, though most significantly in NTD+ EMB. Because H3K4 methylation is an activating epigenetic mark, it is possible that this is a mechanism of gene dysregulation that leads to teratogenesis.

Pan methylation of H3K4 and H3K27 histone loci was assayed, rather than tri-methylation, in order to establish a nutritional framework. It was expected that decreased HNPs would result in decrease SAM biosynthesis and decreased methylation of histones and DNA. However, this was not the case at the time point examined. It is likely that the tight control of gene regulation during embryonic development is prioritized and more conserved. Though there were slight modifications

to histone methylation, it is unknown whether these changes will lead to altered epigenetic regulation. Future work should investigate tri-methylation at these loci, since these measures are most closely associated with epigenetic gene regulation. ChIP-seq could also be conducted to determine whether or not these methylation alterations would affect chromatin structure via histone binding.

Like histone methylation, DNA methylation also undergoes substantial reprogramming during the first trimester of development. After fertilization, DNA is substantially demethylated and then remethylated later during embryogenesis and early organogenesis [2-4]. In this study, treatment with MEHP was initiated and continued during this *de novo* remethylation phase of development. It was expected that MEHP would decrease HNP activity and deplete methyl donor availability, and that this would lead to decreased SAM generation and resultant decreased methylation. This is concordant with findings of a previous study [5], but was not entirely the case here. MEHP did in fact reduce EMB DNA methylation, but DNA methylation was increased in MEHP-treated VYS. These findings are consistent with previous studies conducted in EMB and VYS treated with ethanol, another inhibitor of endocytosis. It is unknown why DNA methylation would increase in the VYS if HNP function is reduced, though it is possible that increased DNA methylation due to treatment in the terminally-differentiated VYS could be a mechanism to conserve other cellular resources for the developing EMB. Separate quantification of methyl donors and C_1 metabolic components should be done in order to determine whether the nutritional consequences observed in the whole conceptus are consistent with each compartment of the conceptus. It is possible that nutrient concentrations are maintained in the VYS and potentially even the EEF, but that these are not properly taken up by the EMB.

It is also possible that this effect is due to lineage-specific effects of phthalate exposure, since VYS is primarily paternally-imprinted [47,48]. It has been previously demonstrated that impaired activity of the *de novo* DNA methyltransferase (Dnmt) enzyme, Dnmt3a, results in EMB with open neural tubes, loss of maternal imprints throughout the genome, and yet most of the paternal imprints and methylation at repetitive elements were maintained [49]. It is possible that the increase in NTD, loss of methylation in the EMB, and increase of methylation in the VYS that follow MEHP-treatment may be related to the function of Dnmt3a. In a previous study, an inhibitor of the proteolysis stage of HNPs was unable to modify Dnmt3a expression in the EMB or VYS [5]. However, it is possible that inhibitors of endocytosis may result in differential expression of Dnmts. It is also possible that the relationship between decreased HNP function and Dnmts does not exist on the expression level and that there is potential for post-translational modulation of Dnmt activity. More work is needed to characterize the specific activities of Dnmts after disruption of HNPs during development.

The use of WEC in this study provided unique tools for the investigation of nutrient uptake. Though WEC conditions mimic many of the *in utero* conditions, the translation of this work to *in vivo* studies would allow further examination of the link between nutrition and epigenetic regulation with a more complex environment. The uterine glands secrete nutrients which are transported through the trophoblast to the coelomic fluid and ultimately undergo the HNPs via the VYS [50,51]. *In vivo* studies of these relationships would also provide insight into the effects of MEHP treatment on the function of the uterine glands, and intermediate transport steps before entering the conceptal HNPs. Because conceptuses must share these nutrients with litter mates in the same uterus, *in vivo* studies would also provide information about the potential for resource competition due to altered nutrition pathways.

In summary, this study has demonstrated the ability of MEHP to modify the conceptal nutrition environment and ultimately the epigenetic landscape of the developing embryo. Histiotrophic clearance of nutrients was decreased with increasing MEHP treatment concentrations after 3 h, though measured conceptal methyl donor concentrations were variable and relatively unchanged after 24 h. C_1 metabolism components were increased with increasing MEHP concentration in culture after 24 h, including increased SAM. DNA methylation of the EMB was increased at 24 h, though increased in the VYS. Histone methylation at the H3K27 locus was decreased in MEHP-treated VYS, though H3K4 methylation was increased in EMB with NTDs. HNP sensitivity to toxicants during this window of development may be a mechanism by which developmental susceptibility is induced. Toxicants may disrupt HNPs in either the endocytosis or proteolysis stage, and these modulations of nutrient environment may manifest as different epigenetic patterns. Further characterization of the mechanisms by which toxicants may alter HNPs is necessary, and may provide predictive models of toxicant-nutrient disruption for future compounds.

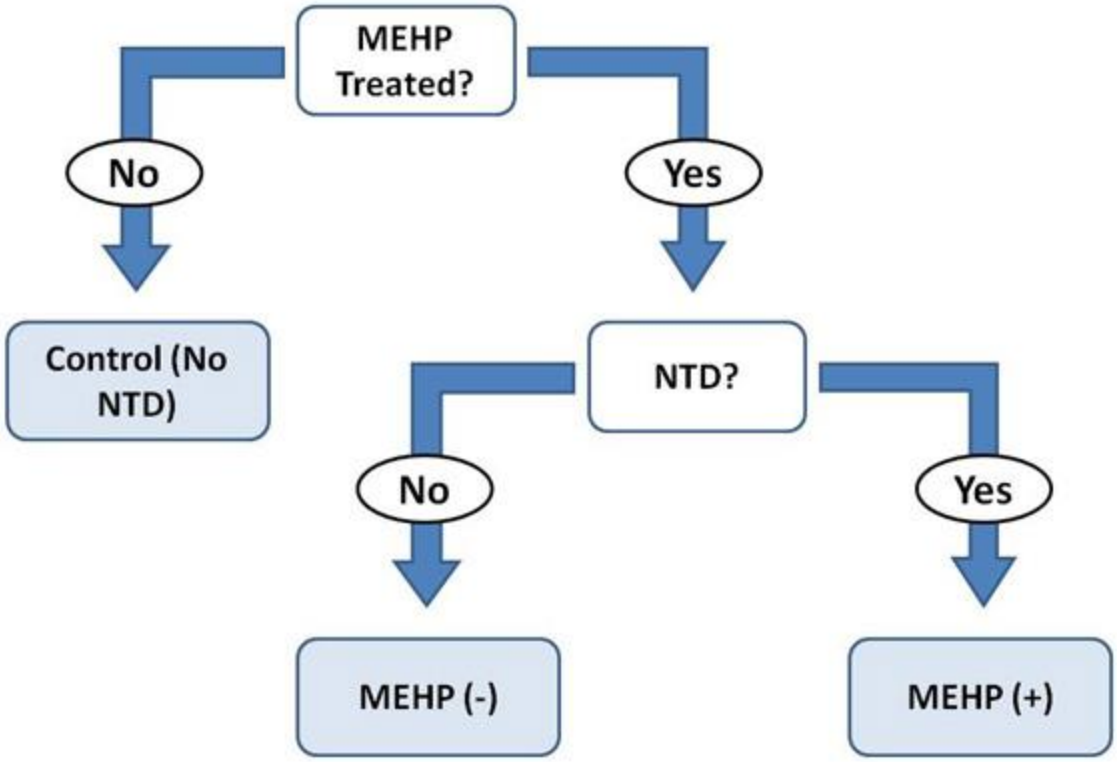

Figure 4.1. Schematic representing the sampling strategy utilized in this study. Samples were characterized by both treatment with MEHP as well as by NTD status (-) or (+).

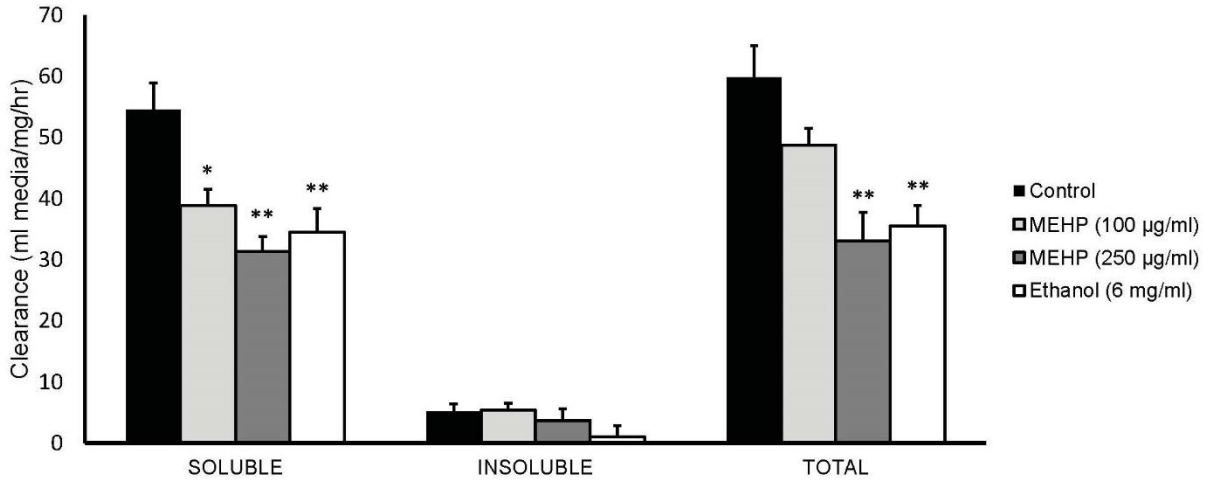

Figure 4.2. Histiotrophic nutrient uptake is hindered by MEHP treatment. Clearance is measured as µl media cleared into conceptus per mg protein per hour, and thus is the rate of uptake. Ethanol was used as a positive control, as it has been previously demonstrated to decreased endocytotic processes. *$p<0.05$, **$p<0.01$.

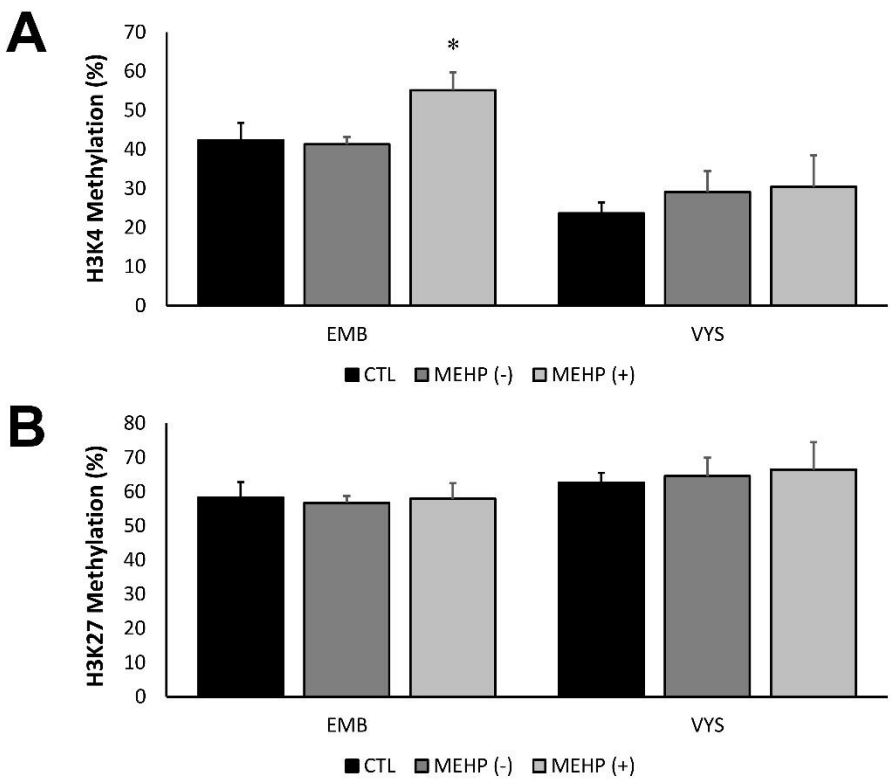

Figure 4.3. Global histone H3K4 and H3K27 methylation percentages in the EMB and VYS. MEHP-treated (100 μg/ml) and NTD positive EMB have elevated H3K4 methylation compared to controls and MEHP-treated NTD negative EMB (A). No significant changes in H3K4 methylation were observed in the VYS. No significant changes in H3K27 methylation were observed in EMB or VYS (B). *$p<0.05$

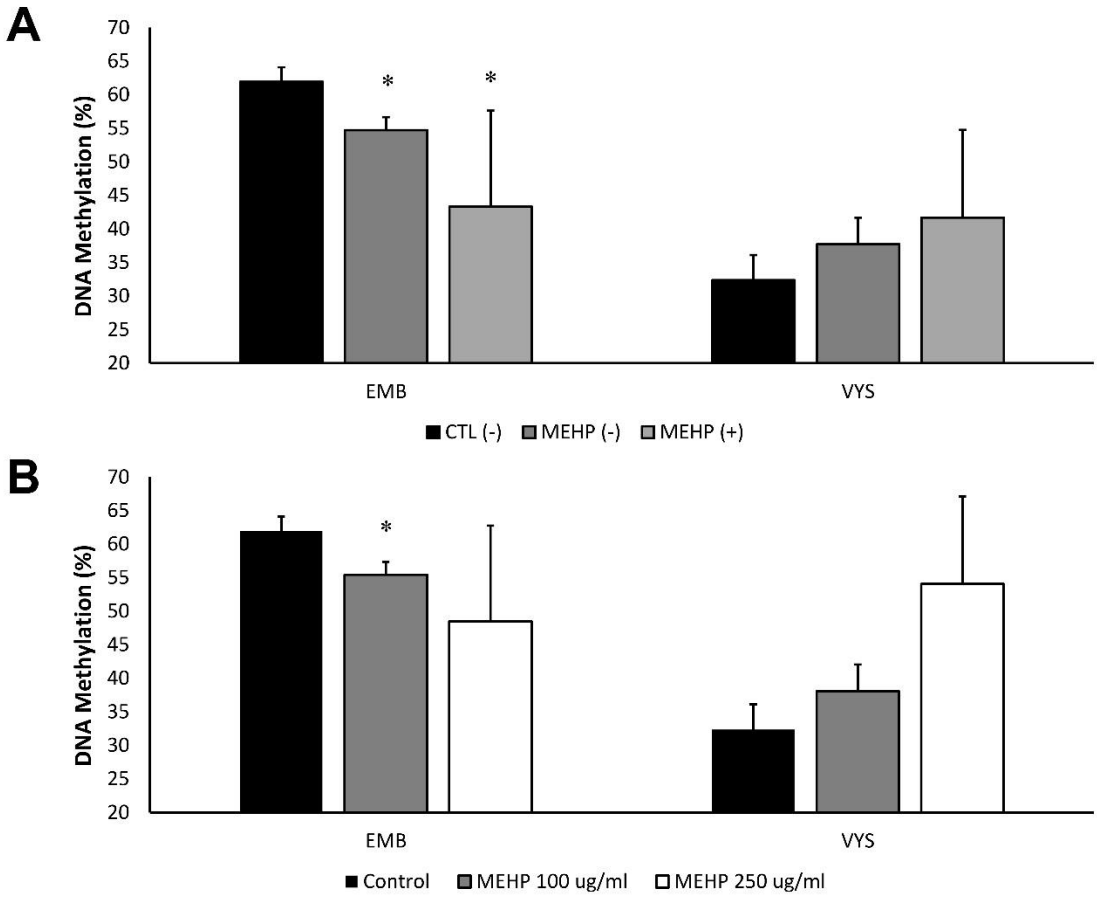

Figure 4.4. Global DNA methylation is modified by MEHP treatment and in conceptuses with NTDs. EMB exposed to MEHP at 100 μg/ml concentrations in culture had significantly lower global DNA methylation percentages than controls, regardless of NTD status (A). EMB that were MEHP treated and NTD+ had further reduced DNA methylation. In the VYS, MEHP treatment and NTD status did not significantly alter DNA methylation, though there was an increasing trend. DNA methylation decreases in the EMB and increases in the VYS with increasing MEHP dose (B). *$p<0.05$

Table 4.1. Measurements of dietary methyl donors and C_1 metabolism components in whole conceptuses following 24 h in WEC. All measurements were normalized, and are reported as the concentration of each nutrient per mg total protein. Comparisons between treatments and controls: *p<0.05, **p<0.01, ***p<0.001. Comparisons between low- and high-dose groups: $^{\$}$p<0.05, $^{\$\$}$p<0.01.

	Control	MEHP (100 μg/ml)	MEHP (250 μg/ml)
Folate (ng/mg protein)	0.66±0.04 (n=4)	0.51±0.03 (n=4)	0.74±0.08 (n=5)
Vitamin B12 (pg/mg protein)	17.00±0.09 (n=3)	12.25±0.41*** (n=3)	15.23±0.47*$^{\$\$}$ (n=5)
Choline (ng/mg protein)	2.15±0.41 (n=5)	1.35±0.54 (n=5)	3.04±0.87$^{\$\$}$ (n=4)
Betaine (ng/mg protein)	4.23±0.39 (n=4)	2.13±0.95** (n=5)	2.95±0.42 (n=4)
SAM (ng/mg protein)	820.93±87.27 (n=4)	1487.44±358.57 (n=5)	2380.10±659.50 (n=5)
Cysteine (ng/mg protein)	1467.39±192.00 (n=5)	2338.37±377.96 (n=5)	2506.89±265.18 (n=5)
Homocysteine (ng/mg protein)	70.10±5.07 (n=5)	63.75±3.36 (n=4)	97.37±8.50*$^{\$\$}$ (n=4)
Methionine (ng/mg protein)	635.06±43.95 (n=4)	956.51±171.79 (n=5)	1426.98±235.62* (n=5)
Total protein (mg/sample)	2.68±0.09 (n=5)	2.84±0.09 (n=5)	2.40±0.11$^{\$}$ (n=5)

References

1. Anderson, O.S., K.E. Sant, and D.C. Dolinoy, *Nutrition and epigenetics: an interplay of dietary methyl donors, one-carbon metabolism and DNA methylation.* The Journal of Nutritional Biochemistry, 2012. **23**(8): p. 853-859.
2. Reik, W., W. Dean, and J. Walter, *Epigenetic Reprogramming in Mammalian Development.* Science, 2001. **293**(5532): p. 1089-1093.
3. Faulk, C. and D.C. Dolinoy, *Timing is everything: The when and how of environmentally induced changes in the epigenome of animals.* Epigenetics, 2011. **6**(7): p. 791-797.
4. Reik, W., *Stability and flexibility of epigenetic gene regulation in mammalian development.* Nature, 2007. **447**(7143): p. 425-432.
5. Sant, K.E., et al., *Inhibition of proteolysis in histiotrophic nutrition pathways alters DNA methylation and one-carbon metabolism in the organogenesis-stage rat conceptus.* The Journal of Nutritional Biochemistry, 2013. **24**(8): p. 1479-1487.
6. Zeisel, S.H., *Importance of methyl donors during reproduction.* Am J Clin Nutr, 2009. **89**(2): p. 673S-7S.
7. Imbard, A., J.F. Benoist, and H.J. Blom, *Neural tube defects, folic acid and methylation.* Int J Environ Res Public Health, 2013. **10**(9): p. 4352-89.
8. Osterhues, A., N.S. Ali, and K.B. Michels, *The role of folic acid fortification in neural tube defects: a review.* Crit Rev Food Sci Nutr, 2013. **53**(11): p. 1180-90.
9. Harris, C., *Rodent Whole Embryo Culture*, in *Developmental Toxicology*, C. Harris and J.M. Hansen, Editors. 2012, Humana Press. p. 215-237.
10. Robinson, J.F., et al., *Dose–response analysis of phthalate effects on gene expression in rat whole embryo culture.* Toxicology and Applied Pharmacology, 2012. **264**(1): p. 32-41.
11. Janer, G., et al., *Use of the rat postimplantation embryo culture to assess the embryotoxic potency within a chemical category and to identify toxic metabolites.* Toxicology in Vitro, 2008. **22**(7): p. 1797-1805.
12. Ambroso, J. and C. Harris, *Assessment of Histiotrophic Nutrition Using Fluorescent Probes*, in *Developmental Toxicology*, C. Harris and J.M. Hansen, Editors. 2012, Humana Press. p. 407-423.
13. Ambroso, J.L., et al., *Fluorometric analysis of endocytosis and lysosomal proteolysis in the rat visceral yolk sac during whole embryo culture.* Teratology, 1997. **56**(3): p. 201-209.
14. Steventon, G.B. and K.E. Williams, *Ethanol-induced inhibition of pinocytosis and proteolysis in rat yolk sac in vitro.* Development, 1987. **99**(2): p. 247-53.
15. Holm, P.I., et al., *Determination of choline, betaine, and dimethylglycine in plasma by a high-throughput method based on normal-phase chromatography-tandem mass spectrometry.* Clin Chem, 2003. **49**(2): p. 286-94.
16. Karimi, M., S. Johansson, and T. Ekström, *Using LUMA: a Luminometric-Based Assay for Global DNA-Methylation.* Epigenetics, 2006. **1**(1): p. 45-48.
17. Karimi, M., et al., *LUMA (LUminometric Methylation Assay)—A high throughput method to the analysis of genomic DNA methylation.* Experimental Cell Research, 2006. **312**(11): p. 1989-1995.
18. Hales, C.N. and D.J. Barker, *The thrifty phenotype hypothesis.* Br Med Bull, 2001. **60**: p. 5-20.
19. Ivanov, A.I., *Pharmacological inhibition of endocytic pathways: is it specific enough to be useful?* Methods Mol Biol, 2008. **440**: p. 15-33.
20. Claussen, U., et al., *The embryotoxicity of cyclophosphamide in rabbits during the histiotrophic phase of nutrition.* Teratog Carcinog Mutagen, 1985. **5**(2): p. 89-100.
21. Beck, F., *Induced cell injury and cell death as a cause of congenital malformations in rats.* Histochem J, 1981. **13**(4): p. 667-79.
22. Holson, J.F., et al., *Mode of action: yolk sac poisoning and impeded histiotrophic nutrition--HBOC-related congenital malformations.* Crit Rev Toxicol, 2005. **35**(8-9): p. 739-45.
23. Ambroso, J. and C. Harris, *In vitro embryotoxicity of the cysteine proteinase inhibitors benzyloxycarbonyl-phenylalanine-alanine-diazomethane (Z-Phe-Ala-CHN2) and*

benzyloxycarbonyl-phenylalanine-phenylalanine-diazomethane (Z-Phe-Phe-CHN2). Teratology, 1994. **50**(3): p. 214-228.
24. Ambroso, J.L. and C. Harris, *Chloroquine accumulation and alterations of proteolysis and pinocytosis in the rat conceptus in vitro.* Biochemical Pharmacology, 1994. **47**(4): p. 679-688.
25. Hunter, E.S., 3rd, et al., *Altered visceral yolk sac function produced by a low-molecular-weight somatomedin inhibitor.* Teratology, 1991. **43**(4): p. 331-40.
26. Brent, R.L., et al., *Experimental yolk sac dysfunction as a model for studying nutritional disturbances in the embryo during early organogenesis.* Teratology, 1990. **41**(4): p. 405-13.
27. Balkan, W., et al., *Role of the mouse visceral yolk sac in nutrition: inhibition by a somatomedin inhibitor.* J Exp Zool, 1989. **249**(1): p. 36-40.
28. Christensen, E. and P. Verroust, *Megalin and cubilin, role in proximal tubule function and during development.* Pediatric Nephrology, 2002. **17**(12): p. 993-999.
29. Moestrup, S.K. and P.J. Verroust, *Megalin- and Cubilin-Mediated Endocytosis of Protein-Bound Vitamins, Lipids, and Hormones in Polarized Epithelia.* Annual Review of Nutrition, 2001. **21**(1): p. 407-428.
30. Muller, D., A. Nykjaer, and T.E. Willnow, *From holoprosencephaly to osteopathology: role of multifunctional endocytic receptors in absorptive epithelia.* Ann Med, 2003. **35**(5): p. 290-9.
31. Burke, K.A., et al., *Expression and immunolocalisation of the endocytic receptors megalin and cubilin in the human yolk sac and placenta across gestation.* Placenta, 2013. **34**(11): p. 1105-9.
32. Willnow, T.E., et al., *Defective forebrain development in mice lacking gp330/megalin.* Proc Natl Acad Sci U S A, 1996. **93**(16): p. 8460-4.
33. Fisher, C.E. and S.E.M. Howie, *The role of megalin (LRP-2/Gp330) during development.* Developmental Biology, 2006. **296**(2): p. 279-297.
34. Zohn, I.E. and A.A. Sarkar, *The visceral yolk sac endoderm provides for absorption of nutrients to the embryo during neurulation.* Birth Defects Research Part A: Clinical and Molecular Teratology, 2010. **88**(8): p. 593-600.
35. Kozyraki, R. and F. Gofflot, *Multiligand endocytosis and congenital defects: roles of cubilin, megalin and amnionless.* Curr Pharm Des, 2007. **13**(29): p. 3038-46.
36. Duester, G., *Retinoic acid synthesis and signaling during early organogenesis.* Cell, 2008. **134**(6): p. 921-31.
37. Maden, M., *Retinoids and spinal cord development.* J Neurobiol, 2006. **66**(7): p. 726-38.
38. Copp, A.J. and N.D. Greene, *Neural tube defects--disorders of neurulation and related embryonic processes.* Wiley Interdiscip Rev Dev Biol, 2013. **2**(2): p. 213-27.
39. Shimamura, K., et al., *Longitudinal organization of the anterior neural plate and neural tube.* Development, 1995. **121**(12): p. 3923-33.
40. Gelineau-van Waes, J., et al., *Microarray analysis of E9.5 reduced folate carrier (RFC1; Slc19a1) knockout embryos reveals altered expression of genes in the cubilin-megalin multiligand endocytic receptor complex.* BMC Genomics, 2008. **9**(1): p. 156.
41. Okuda, T., et al., *Substrate-induced internalization of the high-affinity choline transporter.* J Neurosci, 2011. **31**(42): p. 14989-97.
42. Haga, T., *Molecular properties of the high-affinity choline transporter CHT1.* J Biochem, 2014.
43. Pramod, A.B., et al., *SLC6 transporters: structure, function, regulation, disease association and therapeutics.* Mol Aspects Med, 2013. **34**(2-3): p. 197-219.
44. Broer, S. and U. Gether, *The solute carrier 6 family of transporters.* Br J Pharmacol, 2012. **167**(2): p. 256-78.
45. Mao, C., et al., *The effect of prenatal nicotine on mRNA of central cholinergic markers and hematological parameters in rat fetuses.* Int J Dev Neurosci, 2008. **26**(5): p. 467-75.
46. Silva, V.S., et al., *Comparative effects of aluminum and ouabain on synaptosomal choline uptake, acetylcholine release and (Na+/K+)ATPase.* Toxicology, 2007. **236**(3): p. 158-177.
47. Rastan, S. and B.M. Cattanach, *Interaction between the Xce locus and imprinting of the paternal X chromosome in mouse yolk-sac endoderm.* Nature, 1983. **303**(5918): p. 635-7.

48. Davis, T.L., K.D. Tremblay, and M.S. Bartolomei, *Imprinted expression and methylation of the mouse H19 gene are conserved in extraembryonic lineages.* Dev Genet, 1998. **23**(2): p. 111-8.
49. Kaneda, M., et al., *Essential role for de novo DNA methyltransferase Dnmt3a in paternal and maternal imprinting.* Nature, 2004. **429**(6994): p. 900-3.
50. Burton, G.J., J. Hempstock, and E. Jauniaux, *Nutrition of the human fetus during the first trimester--a review.* Placenta, 2001. **22 Suppl A**: p. S70-7.
51. Burton, G.J., et al., *Uterine glands provide histiotrophic nutrition for the human fetus during the first trimester of pregnancy.* J Clin Endocrinol Metab, 2002. **87**(6): p. 2954-9.

Chapter V

Integrated Epigenomic and Transcriptomic Profiles of Early Organogenesis-Stage Mouse Conceptuses after Exposure to Mono-2-Ethylhexyl Phthalate: Effects in the Absence and Presence of Neural Tube Defects

Introduction

Despite recent intervention efforts, neural tube defects (NTDs) remain one of the most prevalent birth defects worldwide. Folate supplementation of foods has reduced but not eradicated the prevalence of NTDs, and the mechanism by which this occurs is controversial. Folate and other dietary methyl donors are responsible for supplying substrates necessary for cellular methylation processes, including epigenetic modifications [1]. An association between neural tube defects, central nervous system (CNS) defects, and various epigenetic modifications has been suggested, including disruption of methyl group donors [2-4].

Mono-2-ethylhexyl phthalate (MEHP) is the primary metabolite of di-2-ethylhexyl phthalate, a ubiquitously used plasticizing agent that has been widely found as an environmental contaminant. Phthalates are xenoestrogens, and are well-known and best characterized for their endocrine-disrupting function in reproduction. However, previous studies have demonstrated other mechanisms by which MEHP may alter embryogenesis and early organogenesis, including

decreased overall growth, disruption of redox signaling, decreased nutrient uptake, and alteration of epigenetic marks (Chapters 2 and 3).

Previous work demonstrated that increasing dose of MEHP for 24 h between GD 8-9 in mouse whole embryo culture (mWEC) significantly increased the prevalence of NTDs in mouse conceptuses (Chapter 3). Here, we try to identify the pathways 1) that are most significantly impacted by MEHP treatment and 2) that are amplified in conceptuses with open neural tubes compared to those with normal neural tube closure in order to understand processes that may contribute to the development of NTDs.

Materials & Methods

Chemicals & Reagents

HPLC-grade dimethyl sulfoxide (DMSO), Tyrode's balanced salt solution (TBSS), and penicillin/streptomycin (10,000 units/ml penicillin, 10,000 μg/ml streptomycin sulfate) were obtained from Sigma/Aldrich (St. Louis, MO). Mono-2-ethylhexyl phthalate was obtained from AccuStandard (New Haven, CT). Hanks balanced salt solution (HBSS) was purchased from GIBCO/Life Technologies (Grand Island, NY).

Mouse whole embryo culture

Mouse whole embryo culture was performed following the conditions outlined in [5] and described previously (Chapters 3 and 4). Briefly, time-mated female CD-1 mice were obtained from Charles River (Portage, MI). The morning of the discovery of a vaginal plug was designated

as gestational day (GD) 0. Food and water were supplied *ad libitum*, and animals were kept on a 12 h light:dark cycle. On the morning of GD 8, pregnant mice were euthanized with CO_2, and the gravid uterus was removed. Conceptuses were explanted from the uterus, removed from their decidual masses, pooled, and randomized into 10 ml culture bottles containing 5 ml of 75% heat-inactivated rat serum/25% TBSS, and supplemented with penicillin/streptomycin. Bottles were placed in a rotating incubator that supplied continuous gas to conceptuses during the culture period. The intial gas mizture was low-oxygen to mimic the uterine conditions, containing only 5% O_2/5% CO_2/90% N_2. After 6 h in culture, the gas mixture was adjusted to contain 20% O_2/5% CO_2/75% N_2 to mirror the increased oxygenation of the environment due to implementation of circulation.

Exposure & sample collection

MEHP was suspended and stored in dimethyl sulfoxide (DMSO) at a concentration of 1 mg/ml. MEHP was added to culture bottles containing GD 8 conceptuses at a final concentration of 100 μg/ml in culture. DMSO was added to control bottles at an equal volume (<1 μl/ml), which is below the toxic concentration in culture. Conceptuses grew overnight in culture before sampling 24 h later, on GD 9. At the conclusion of the culture period, conceptuses were removed and thoroughly washed in HBSS. EMB and VYS were manually separated using watchmakers' forceps. EMB and VYS were classified by their treatment status as either control or MEHP-treated. At this time, a brief morphological assessment was performed. If the neural tube of an EMB was open, these EMB and their corresponding VYS were designated as NTD positive (Fig. 5.1).

RNA isolation was performed immediately upon sampling using the RNeasy Mini Kit (Qiagen), and isolated RNA was stored at -80°C until use. DNA was performed using a phenol-

chloroform extraction method. Briefly, EMB or VYS tissue were each individually collected into 540 µl Buffer ATL lysis buffer (Qiagen) and sonicated. Proteinase K (Qiagen) was added, and samples were incubated overnight at 50°C. RNase A was added to each sample before repeated phenol-chloroform isoamyl alcohol extractions in phase-lock gel tubes (5 PRIME). One chloroform only extraction was performed prior to repeated ethanol precipitations. Pellets were dried and genomic DNA was suspended in Tris buffer (pH 8.0). To ensure purity for future applications, DNA clean-up was performed using the DNA Clean & Concentrator-25 Kit (Zymo Research). DNA was stored at -20°C until use.

Affymetrix microarray analysis of expression

RNA for Affymetrix microarray processing were submitted to the University of Michigan Microarray Core Facility, and analyzed as described previously (Chapter 3). Briefly, Affymetrix Mouse MG-430 PM strip arrays were processed using the IVT Express Kit (Affymetrix), and RNA purity and integrity were confirmed using the RNA 6000 Nano Kit for the Agilent 2100 Bioanalyzer. Other quality controls including PM chip density, RNA degradation, and standard error analyses were performed on the raw data. Background correction, normalization, and quantification of $\log_2$ expression was performed within-array using RMA, and quantile normalization was used across-arrays. Principle component analysis revealed distinctions between samples, confirming EMB and VYS tissue differences (Fig. 5.2).

First, differences in expression between control (n=4) and MEHP-treated tissues (n=6), regardless of NTD status, were examined in both EMB and VYS using the *Limma* package in R 2.4.1. Potential outliers were downweighted using the *lmFit* function, and raw p-values were

calculated by t-test. These p-values were adjusted and ranked using an empirical Bayesian method (*eBayes* function in *Limma package*). LRpath software was utilized to identify significantly altered (enriched) and conserved (depleted) concepts, as annotated by the Kyoto Encyclopedia of Genes and Genomes (KEGG) database [6]. Differences in expression between NTD negative (n=6) and positive (n=4) EMB and VYS, regardless of treatment, were also examined using the same methodologies. Validation of candidate genes *Dnmt3b, Mat2a, Lrp2,* and *SLC25a32* was performed by qPCR. Proprietary primers and complimentary SYBR green master mix (Qiagen) were utilized. All samples were run in triplicate at the University of Michigan Microarray Core facility using the PRISM 7900HT Sequence Detection System (Applied Biosystems).

NimbleGen DNA promoter methylation tiling array

Genomic DNA from each sample was divided into two aliquots and sheared to 200-1000 bp fragment sizes using sonication (Episonic). Fragment sizes were confirmed using gel electrophoresis, and one aliquot from each sample was set aside as control DNA for each sample. Methyl-CpG binding domain-based capture (MBD-cap) was utilized to enrich the methylated fractions of each sample, using the protocols outlined by the Methylated DNA Enrichment Kit (Epimark). Whole genome amplification of the methylation-enriched samples was performed by using the GenomePlex Complete Whole Genome Amplification Kit (Sigma). These methylation-rich samples were labeled with Cy5 cyanine dye and the control fractions were labeled with Cy3 cyanine dye, using the NimbleGen Dual-Color DNA Labeling Kit (Roche). Both labeled fractions were pooled for each sample, and hybridized to NimbleGen Mouse DNA Methylation 3x720K CpG Island Plus RefSeq Promoter Arrays (Roche). After the 20 h hybridization period, arrays were

washed and then scanned in the Glover laboratory in the University of Michigan Department of Human Genetics using the NimbleGen MS 200 Microarray Scanner (Roche).

Microarray images were obtained and analyzed using the NimbleGen DEVA Software v2.3 (Roche). Raw Cy5 and Cy3 signal intensities for each aligned and analyzed array were exported for analysis. Within-array normalization of the raw data was performed using LOESS on each array using the *Limma* package in R 2.4.1. These were then converted to $\log_2$ ratios (Cy5/Cy3) for each sample, mean-centered, and quantile normalization was used for across-array normalization. Like the expression array data, promoter methylation was analyzed for changes between control (n=3) and MEHP-treated (n=6) tissues, regardless of NTD status, and changes in NTD negative (n=6) and positive (n=3) tissues, regardless of treatment. Data was analyzed using the *Limma* package in R, using the *lmFit* function and *eBayes*. LRpath software was used to identify significantly enriched and depleted pathways.

Results

Expression profiles of functional pathways

Overall functional pathways for which gene expression was affected by MEHP treatment or in NTDs are shown in Fig. 5.3. Significantly affected pathways, as identified by LRpath, were organized and grouped according to KEGG BRITE pathway hierarchies [7]. In the VYS, MEHP treatment mostly impacted metabolic pathways, though key regulatory pathways involved in genetic information processing, cellular process, and organismal systems were also impacted (Fig. 5.3C). In the EMB, MEHP treatment had more diverse effects (Fig. 5.3A). Pathways involved in the etiology of human diseases were impacted, along with substantial changes to metabolic and

systemic pathways. A smaller percentage of pathways involving the processing of environmental information as well as governing cellular processes also were affected.

In EMB with NTDs, the majority of affected pathways were involved in metabolic processes, though several pathways involved in environmental information processing were also impacted (Fig. 5.3B). In the VYS of conceptuses with NTDs, changes in metabolic pathways accounted for approximately 50% of affected pathways, and pathways involved in human disease accounted for most of the remaining fraction (Fig. 5.3D). Secondary functional pathway clusters observed in each of these groups are shown in Table 5.1. It is interesting to note that several of these hierarchical pathways involved in the etiology of human disease appear as those affecting immune and infection response. Most of the affected genes in these pathways govern inflammatory processes, such as cytokine function.

Promoter methylation profiles of functional pathways

Overall functional pathways for which promoter methylation was affected by MEHP treatment or in NTDs in EMB and VYS are shown in Fig. 5.4. KEGG BRITE pathway hierarchies were interrogated after analysis in LRpath, as performed for expression. In the EMB, MEHP treatment induced methylation changes primarily in metabolic pathways, though changes in organismal systems and environmental information processing pathways were also observed (Fig. 5.4A). In the VYS, methylation of genes involved in organismal systems was most significantly affected, though environmental information processing, metabolism and human disease pathways were also represented (Fig. 5.4C).

In EMB and VYS from conceptuses with NTDs, methylation of genes in pathways involved in the etiology of human disease represent the largest percentages of affected pathways.

Changes to promoter methylation in EMB with NTDs occurred in pathways of diverse functions (Fig. 5.4B). Though human disease pathways were most impacted in NTDs in the VYS, environmental and genetic information processing pathways were also affected (Fig. 5.4D). Secondary functional pathway clusters observed in each of these groups are also shown in Table 5.1.

Expression pathways altered by MEHP treatment

Analysis of significantly affected gene expression pathways was performed using LRpath and interrogating the KEGG pathway database. Pathways significantly enriched by MEHP-treatment in VYS and EMB are shown in Table 5.2. In the VYS, few pathways were significantly enriched. These pathways were primarily metabolic, though cytokine-cytokine receptor interaction was also enriched. Metabolism of xenobiotics by cytochrome P450 was the most enriched pathway induced by MEHP-treatment in the VYS. *Cyp1a1* was one of the most significantly altered genes (p=1.427E-07), as expression was increased more than 3-fold in VYS due to MEHP-treatment.

In the EMB, pathways involved in xenobiotic metabolism were also enriched. Numerous pathways involved in the metabolism and biosynthesis of lipids were also affected, including linoleic acid and arachidonic acid metabolism. Regulation of autophagy was also enriched by MEHP-treatment after 24 h, which is consistent with findings from 6 h MEHP-treatment data (Chapter 3). Numerous interferons and insulin II (*Ins2*) in this pathway were downregulated by MEHP-treatment in the EMB, and several PI3K subunits were upregulated. The autophagy/beclin 1 regulator 1 (*Ambra1*) gene, a known contributor to autophagic processes in the early CNS, was increased in EMB treated with MEHP. A large number of the pathways significantly impacted by MEHP-treatment in the EMB surround the function of the immune system, namely pathways

involved in the inflammatory response. Such pathways include cytokine interactions, and those involved in the progression of autoimmune and inflammatory disorders.

Expression pathways altered in NTDs

Pathway analysis was similarly performed for genes differentially expressed in VYS and EMB from conceptuses with NTDs compared to controls (Table 5.3). In EMB, NTDs were associated with altered signaling in pathways primarily involved in amino acid metabolism and biosynthesis, including valine, leucine, isoleucine, arginine, proline, glycine, serine, and threonine. Again, *Ambra1* was increased in expression. In the VYS, NTDs were associated with changes to a diverse array of pathways, including those involved in amino acid and other nutrient metabolism, inflammatory response, and the development of Type I diabetes and maturity onset diabetes of the young. Similar to the MEHP-treated EMB, *Ins2* expression was altered in VYS with NTDs. Genes involved in the anti-inflammtory and antioxidant responses of cells were heavily impacted. Expression of thioredoxin reductase 1 (*Txnrd1*) was the most significantly change observed (p=1.106E-05), with a nearly 40% decrease in gene expression.

Methylation pathways altered by MEHP treatment

Analysis of pathways containing genes with significantly altered promoter methylation was similarly performed for EMB and VYS treated with MEHP (Table 5.4). In the EMB, inositol phosphate metabolism and phosphatidylinositol signaling system pathways were most significantly altered, including the hypermethylation of several Pi3k catalytic and regulatory subunits. Other metabolic pathways were affected, such as propanoate metabolism, though hypermethylation of lactate dehydrogenase gene promoters account for several of these changes.

In the VYS, the Jak-STAT signaling pathway was most significantly altered by MEHP-treatment, as were two related pathways, B cell receptor signaling and natural killer cell cytotoxicity. These pathways are directly related to autophagic and apoptotic potential of cells, and have several genes in common.

Methylation pathways altered in NTDs

Pathway analysis was also performed in significantly altered genes based upon the NTD status of the tissue (Table 5.5). In EMB with NTDs, several pathways involved with cell fate and proliferation were significantly enriched, including the mTOR and Jak-STAT signaling pathways, and numerous pathways involved in cancers. *Cyp11a1* was the most impacted gene, significantly hypermethylated in its promoter. Very few pathways were enriched in VYS with NTDs compared to normal VYS. Only methylation of pancreatic cancer, primary immunodeficiency, and recombination pathways was enriched.

Overall profiles for expression and methylation changes

Log_2 fold change ratios for expression and promoter methylation were matched for each gene within each tissue and treatment or NTD status. Genes for which both expression and promoter methylation data were not available were excluded. Data sets were merged, and the distributions were plotted (Fig. 5.5). Because of the assumption that most points would be centered around a log_2 fold change of zero, a diamond shape would be expected as a normal distribution. When comparing EMB with and without NTDs (Fig. 5.5B), this diamond shape was evident. This was also similar for VYS from conceptuses with and without NTDs (Fig. 5.5D), though there was a slightly greater degree of variability of promoter methylation. Log_2 fold change ratios for EMB

and VYS based upon exposure to MEHP showed a greater degree of variability in expression. In the VYS (Fig. 5.5C), the distribution was fairly normal with a slightly higher degree of variability in expression ratios due to treatment. In both the VYS and the EMB (Fig. 5.5A), hypomethylation was more variable than hypermethylation due to MEHP treatment, though the data is mean-centered. In EMB treated with MEHP, the range of $\log_2$ expression ratios is great. Though variability is high, expression changes due to MEHP treatment are skewed toward increased expression. Overall, MEHP treatment more significantly affects expression and promoter methylation profiles than NTD status, and these effects are more exaggerated in the EMB.

Canonical changes in expression and methylation

After analysis, genes that were either hypomethylated and over-expressed or hypermethylated and under-expressed due to MEHP treatment or NTD status in the EMB and VYS were identified. Only genes for which treatment or NTD status produced significant p-values were included. Log_2 fold change values of less than 0.5 in either direction were excluded, and genes were only included in the canonical sets if change in methylation and in expression were in opposing directions. The number of genes meeting these criteria ranged from 53-575 genes, with the most canonical changes in MEHP-treated EMB and the fewest in NTD+ EMB. Of these changes, several genes were consistently altered in both tissues by both MEHP treatment and in NTDs.

The gene D-3-phosphoglycerate dehydrogenase (*Phgdh*) was hypomethylated and had increased expression in MEHP-treated EMB and VYS, as well as in EMB and VYS with NTDs. Studies have demonstrated a correlation between decreased *Phgdh* expression and brain malformations, and these malformations were followed by lethality in knockout models [8-12].

Increased expression of *Phgdh* has been implicated in numerous cancers [13-19]. *Phgdh* is an oxidoreductase involved in energy metabolism and additionally is crucial for the biosynthesis of serine, which is elevated in many cancers. The mechanism by which increased serine induces oncogenesis is unknown, but increased cellular serine increases proliferation of cells and can increase the one-carbon pool [19]. Because conceptal tissues are undergoing extensive epigenetic remodeling that is dependent upon the one-carbon pool, it is no surprise that the increased demand solicits increased *Phgdh* expression. Likewise, because growth of the conceptus requires proliferation, *Phgdh* is essential. The hypomethylation of the *Phgdh* promoter and increased expression in EMB and VYS due to MEHP treatment and also in NTDs suggests that *Phgdh* overexpression may play an important role in dysmorphogenesis.

Also of interest was the hypermethylation and underexpression of somatostatin in EMB treated with MEHP and in EMB with NTDs. Somatostatin has been previously shown to be hypermethylated and underexpressed in cancers [20-23]. Somatostatin is an important endocrine signaling molecule, inhibiting the release of hormones such as insulin, glucagon, and thyroid-stimulating hormone. Thus, it is possible that exposure to MEHP during early organogenesis may alter the metabolic programming of the EMB.

Similarities in observed expression and promoter methylation changes

Comparisons were made to identify genes that are commonly altered across tissues, treatments, and NTD states. To identify genes for which expression changes are common, all genes for which at least one probe was significantly changed at the $p<0.05$ level were included in the data set and collapsed. Figure 5.6 shows the percent of the total number of genes significantly changed in each categorization. In EMB with NTDs, 7.6% of total genes were significantly altered,

and 12.1% were significantly changed in VYS from conceptuses with NTDs. MEHP-treatment more significantly altered expression, affecting 48.1% of genes in the EMB and 32.9% in the VYS. 21.6% of genes were commonly changed in the MEHP-treated tissues. In EMB with NTDs, 7.6% of genes are significantly changed, and 12.1% in the VYS are impacted by NTD state. 1.6% of total genes were commonly altered in both EMB and VYS from conceptuses with NTDs. In all, 0.5% of total genes were affected by treatment and NTD state in both the EMB and VYS.

Because of the large number of probes on the promoter methylation arrays, a confidence level of 99.9% ($p<0.001$) was used to identify commonly affected gene promoters (Fig. 5.7). In the EMB, 5.8% of total genes had altered promoter methylation due to MEHP-treatment, and 2.8% were significantly changed in NTDs. In the VYS, 1.1% of gene promoters had aberrant methylation due to MEHP-treatment, and 3.3% were altered in VYS with NTDs. Only 0.1% of gene promoters were commonly affected by treatment in both the EMB and VYS, and only 0.2% were common to both the EMB and VYS from conceptuses with NTDs. No gene promoters had altered methylation for all tissues, treatments, and NTD states.

Expression changes in candidate pathways

The solute carrier (SLC) families of genes represent membrane transporters integral to cellular processes across tissues and organelles. Though numerous SLC genes were significantly increased or decreased in expression, a heatmap was constructed on all SLC genes in order to visualize overall effects of treatment and in NTDs for EMB and VYS (Fig. 5.8). Array expression values were median-centered, and arrays were hierarchically clustered by Euchlidean distance using Cluster 3.0 software [24]. Results were visualized using Java TreeView [25]. Arrays were statistically clustered by treatment, rather than by NTD status. Overall, no trends were obvious in

the VYS (Fig. 5.8B). However, there was notably decreased expression of SLC genes in MEHP-treated EMB (Fig. 5.8A). The same pattern was observed when examining genes in glutathione (GSH) metabolism and thioredoxin-response (Fig. 5.9). Again, hierarchical clustering of arrays reveals that treatment, rather than NTD status, was a better predictor of gene expression in these pathways. Though no trends were obvious in the VYS (Fig. 5.9B), these antioxidant metabolic pathways appear to be downregulated in EMB due to MEHP-treatment (Fig. 5.9A).

Discussion

In this study, we have examined transcriptomic and epigenomic changes produced by MEHP-treatment during early organogenesis. Comparatively, we also identified changes associated with the incomplete closure of the neural tube. This case-control methodology allowed for novel investigation of the underlying mechanisms surrounding MEHP-induced teratogenesis. Though NTD status was associated with altered signaling and metabolism in numerous pathways, MEHP-treatment had more extensive and broader impacts on expression and promoter methylation. Studies have previously demonstrated altered lipid and steroid metabolism in rat WEC, which was concordant with findings observed in this study [26]. However, additional patterns were observed and further amplified by stratification by NTD status. Following pathway analyses, several conditions were identified as key contributors to NTDs or MEHP-induced toxicity.

Redox environment plays a crucial role in the determination of cell fate in the developing EMB, driving cells towards proliferation, differentiation, or apoptosis fates [27]. In a previous study, it was demonstrated that MEHP-treatment in WEC induced embryonic susceptibility to oxidation at key time points in development (Chapter 3). Here, an overall decrease in the

expression of genes in glutathione metabolism and biosynthesis was observed in EMB that had been treated with MEHP. *Txnrd1* expression was the most significantly altered gene in NTD positive VYS, decreasing by more than 40%. Inhibition of autophagy pathways is associated with altered mitochondrial membrane potential, which may have impacts on oxidative phosphorylation and energy metabolism processes [28]. Because apoptosis and redox potentials are closely related, more work is necessary to elucidate a relationship between autophagy and redox balance during development.

Canonical changes were observed in EMB and VYS due to MEHP-treatment. Numerous lipid metabolism and amino acid metabolism pathways were disrupted by MEHP-treatment, as was steroid hormone biosynthesis. It is also not surprising that MEHP-treatment induced xenobiotic response pathways, nor that treatment induced changes in inflammatory processes. Many of these processes are governed by the activity of peroxisome proliferator-activated receptors (PPARs) [29]. Phthalate exposures have been widely associated with activation of PPAR signaling, especially in reproduction and development [22-25].

The manifestations of MEHP-treatment and of NTDs in pathways involved in cell fate should be underscored. Several studies have associated PPAR activation with repressed interferon (IFN) production and signaling [30,31]. In these tissues, IFNs and *Ins2* were under-expressed and *Pi3K* was overexpressed. Because IFNs shunt towards an apoptotic cell fate and *Pi3K* towards autophagy, it is possible that prolonged exposure to MEHP are instead shunted towards autophagic responses in order to preserve viability and proliferation of these cells.

Autophagy and apoptosis are crucial to development and tissue patterning, including that of the neural tube [32-35]. Autophagy, defined as the lysosomal proteolysis of sequestered cytosolic substrates and organelles, degrades non-essential cellular contents and provides these as

building block for basal cellular functions such as basal energy metabolism [36]. In this study, *Ambra1*, a gene commonly expressed in neuroepithelium at this stage of mouse development, was significantly overexpressed by MEHP-treatment and in NTD-positive EMB [37]. *Ambra1* overexpression has been demonstrated to induce autophagy and decrease proliferation rate [37]. In this study, an increased number of NTDs was observed, mostly those of incomplete neural tube closure. In other studies, decreased *Ambra1* expression was associated with exencephaly and uncontrolled proliferation and outgrowth of early central nervous system cells [37]. Thus, it is possible that the truncation of neural tube growth and closure may be due to improper overexpression of *Ambra1*, or that even the *Ambra1*-indicated induction of autophagy was not enough to maintain cellular homeostasis.

In a previous study, MEHP-treatment in WEC reduced overall conceptal nutrition during early organogenesis (Chapter 4). Here, amino acid metabolism and other energy metabolism pathways were altered by MEHP treatment, and SLC family genes were relatively underexpressed. In cell culture models, increased *Ambra1* expression was observed in serum-starved, or nutrient-deficient cells [38]. Because NTDs are more commonly observed in malnourished EMB, it is possible that *Ambra1* overexpression in deficient EMB are a major contributor to malformations. Future studies should investigate the mechanisms by which nutrient-starvation may induce autophagic teratogenesis.

In recent years, elucidating a mechanism by which endocrine disruptors such as phthalates may increase risk for obesity has been a research priority. Decreased IFN expression and decreased insulin expression have been associated with obesity phenotypes [39]. In this study, pathways involved in the etiology of diabetes were significantly affected in the VYS, the primary metabolic barrier for the early-organogenesis stage of development, and insulin-2 expression was decreased.

Likewise, MEHP-treatment was previously demonstrated to increase conceptal oxidative stress, which has been associated with increased risk for obesity and diabetes through autophagy mechanisms (Chapter 3) [40]. Because MEHP decreases conceptal nutrition and alters conceptal redox potentials, it is possible that *nutrient starvation and redox control of autophagy (NSRCA*) may serve as a mechanism contributing to the development of a "thrifty phenotype" [41].

Epigenetic reprogramming of the genome provides a unique window during which exposures and adverse environmental factors may induce changes to gene expression that could last throughout the lifecourse. In this study, epigenomic changes due to MEHP-treatment or in NTD-positive conceptuses were probed. Numerous metabolic genes and transporters were found to be hyper- or hypomethylated due to treatment or observed in NTDs, such as lactate dehydrogenase or *Cyp11a1*. More work is necessary to identify potential mechanisms by which early exposures and induced autophagy may alter metabolic programming and induce metabolic changes throughout the lifecourse.

In conclusion, this study demonstrated that metabolic pathways may be disrupted in the developing conceptus. It is likely that NSRCA is being induced due to MEHP-treatment, and that these processes may contribute to the development of NTDs. It is possible that amino acid and micronutrient starvation may "shunt" towards autophagy rather than apoptosis, and that these processes may result in metabolic and morphological disruption of development and potentially changes that remain throughout the lifecourse.

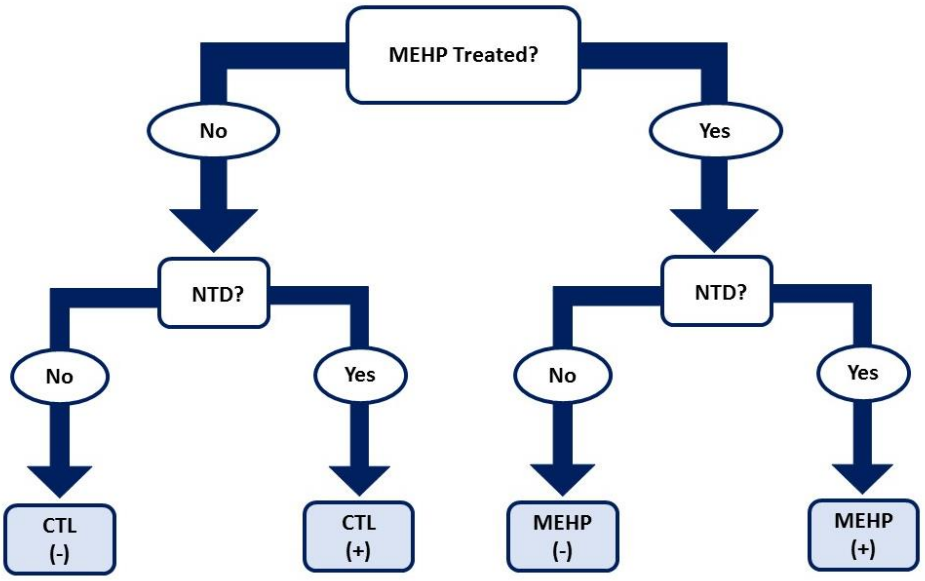

Figure 5.1. Schematic illustrating the sampling techniques employed. At the conclusion of the culture period, conceptuses remained separated into treatment groups but were then stratified by NTD status. Tissues from conceptuses with NTDs were designated as NTD-positive, and those that had no morphological defects were NTD-negative.

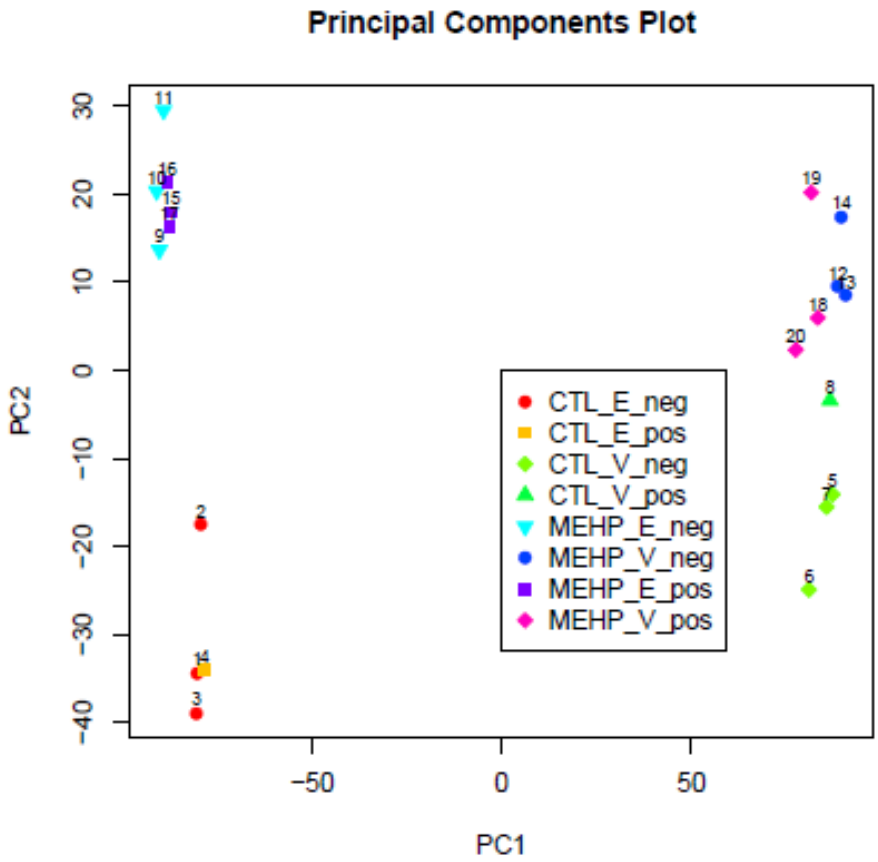

Figure 5.2. Principle component analysis (PCA) plot of RNA from collected tissues. Samples were clustered by overall similarity, revealing expected large differences between the two tissues (EMB and VYS). Variability was greater in EMB samples, and treatment appeared more explanatory than NTD status. In the VYS, there was less overall variability, though distinction between treatment groups was still evident.

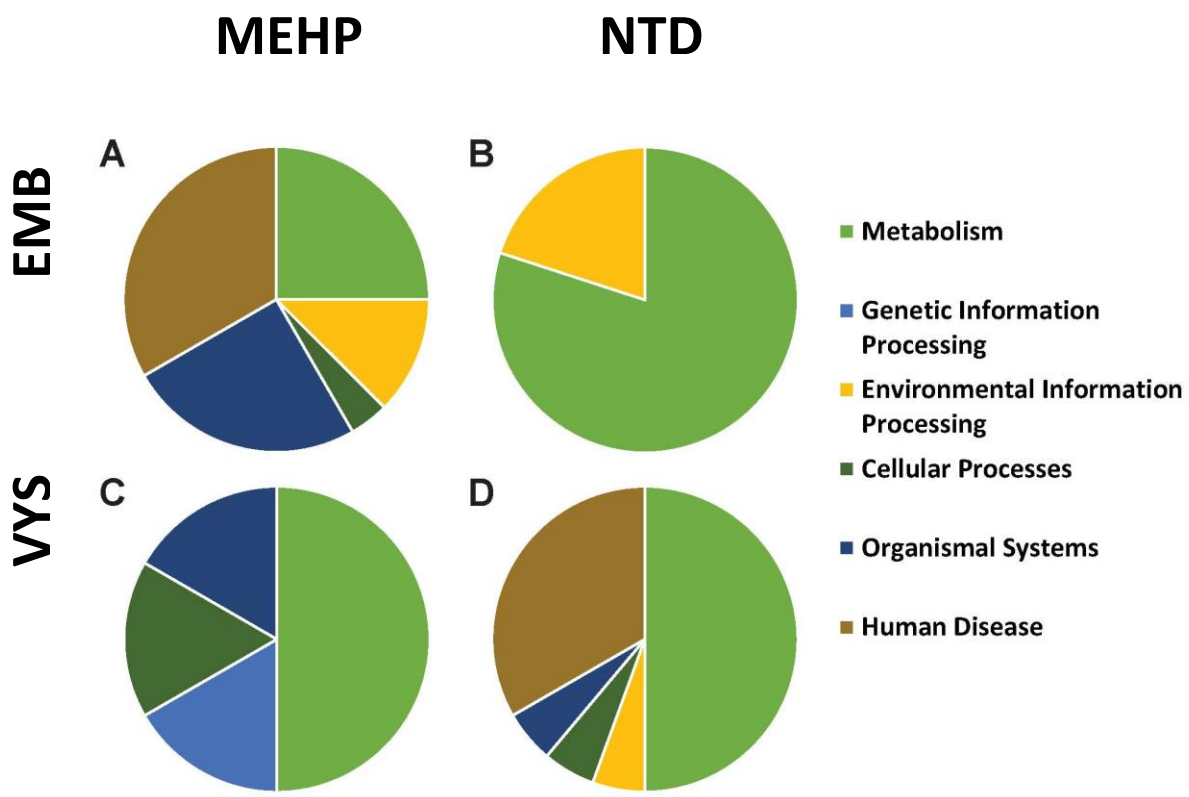

Figure 5.3. Functional pathways of gene expression changes due to MEHP treatment or in NTDs. In the EMB, MEHP treatment (A) primarily affected pathways involved in metabolism, organismal systems, and human disease, as well as some pathways involved in environmental information processes and cellular processes. In EMB with NTDs (B), expression in pathways involved in metabolism were most affected, as well as environmental information processing. In the VYS, MEHP treatment (C) largely affected metabolic pathways, though genetic information processes, cellular processes and organismal systems were also impacted. In VYS from conceptuses with NTDs (D), metabolism was also largely affected, as was human disease.

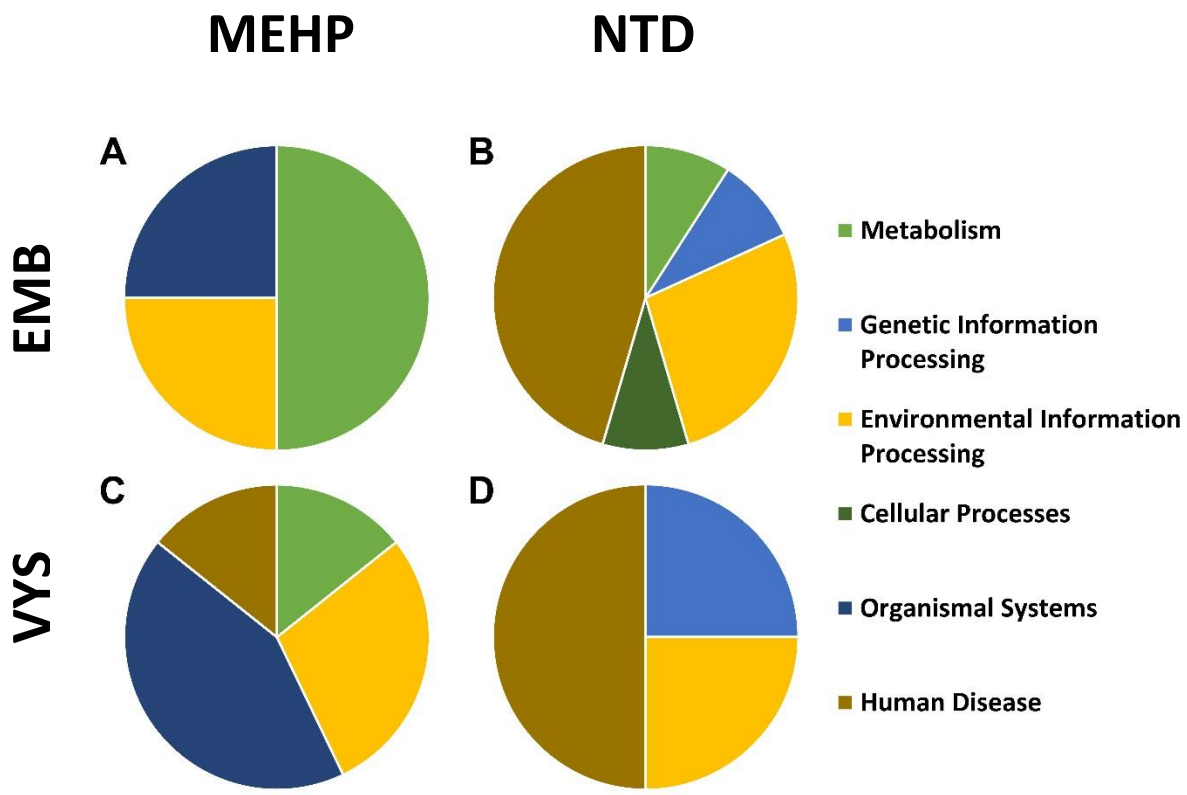

Figure 5.4. Functional pathways of promoter methylation changes due to MEHP treatment or in NTDs. In the EMB, MEHP treatment (A) primarily affected pathways involved in metabolism, organismal systems, and environmental information processing. In EMB with NTDs (B), there was diversity in the functional pathways affected, though human disease accounted for the largest percentage. In the VYS, MEHP treatment (C) also had diversity in affected pathways, though organismal systems encompassed the largest percentage of pathways, though environmental information processing, human disease, and metabolic pathways were also impacted. In VYS from conceptuses with NTDs (D), human disease accounted for half of the affected pathways.

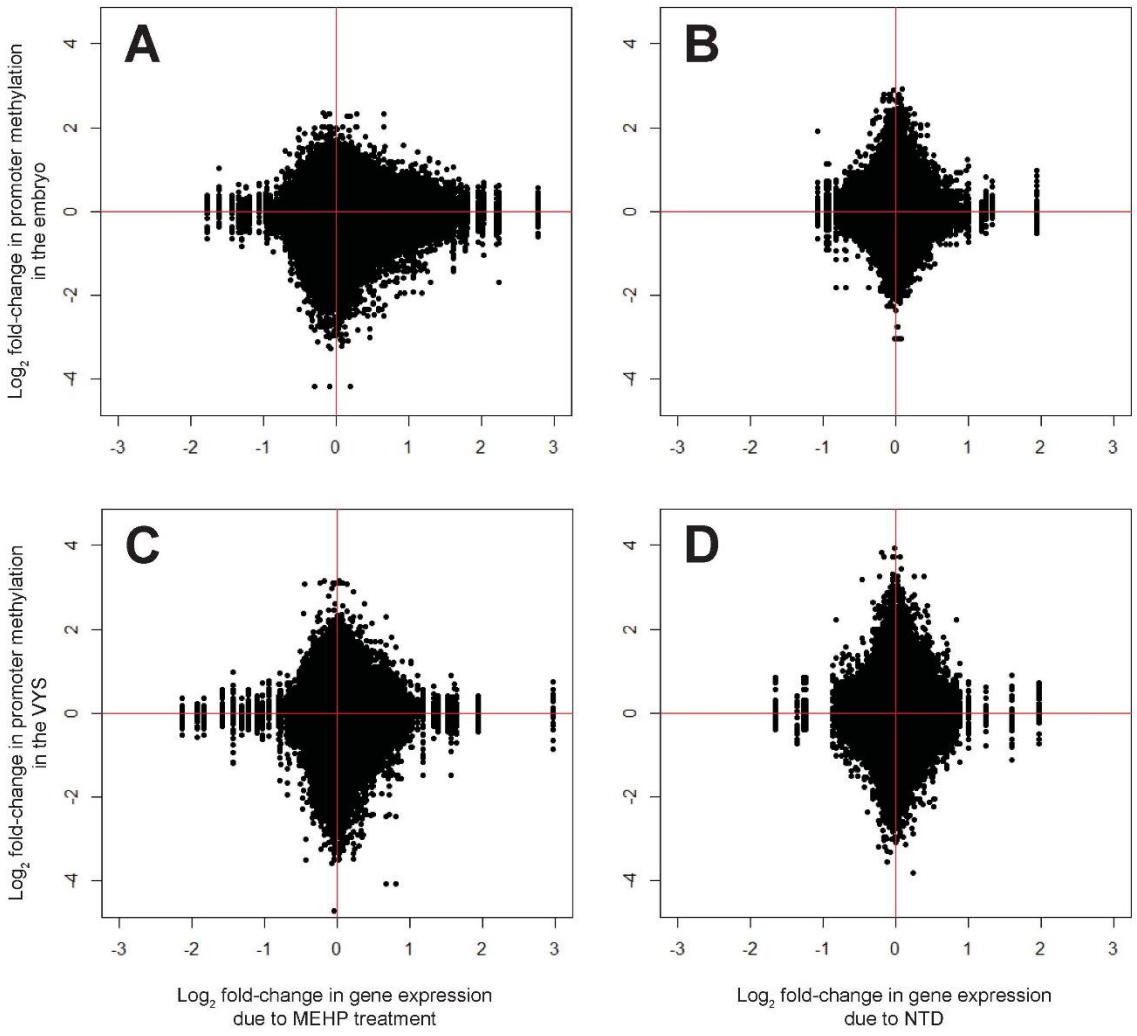

Figure 5.5. Overall fold-change transcriptomic and epigenomic profiles. Data sets were merged and $\log_2$ fold-change ratios were plotted. Profiles were fairly normally-distributed (diamond-shaped) comparing changes in NTD-positive to NTD-negative EMB (B) and VYS (D). Though normally distributed expression and methylation was slightly more variable in MEHP-treated VYS (C). Expression was highly variable, and methylation was skewed toward hypomethylation in MEHP-treated EMB (A). Overall, this suggests that more dysregulation occurs in MEHP-treated EMB than in VYS tissue or by NTD status.

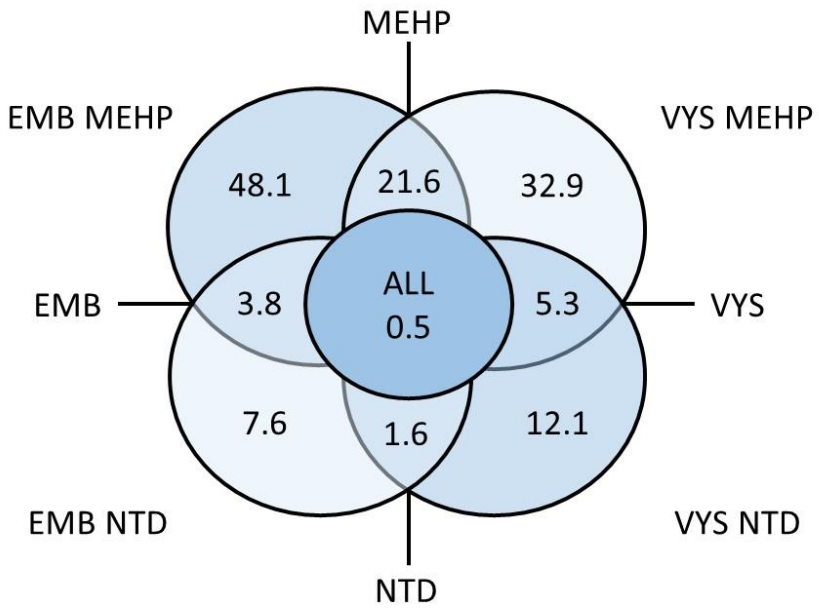

Figure 5.6. Venn diagram of expression changes in EMB and VYS. Numbers shown are the percent of significantly altered genes in each group compared to the total gene count (p=0.05). The four overlapping regions represent the percent of total genes that the overlapping groups have in common. The central circle represents the percentage of genes that were significantly changed and common to all analyses.

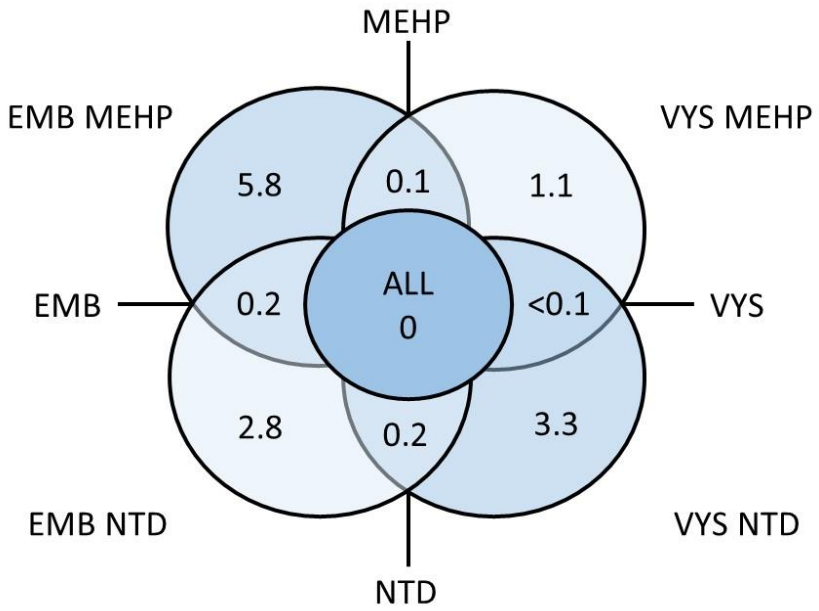

Figure 5.7. Venn diagram of promoter methylation changes in EMB and VYS. Numbers shown are the percent of significantly altered genes in each group compared to the total gene count (p=0.001). The four overlapping regions represent the percent of significantly altered genes that the overlapping groups have in common. The central circle represents the percentage of genes that were significantly changed and common to all analyses.

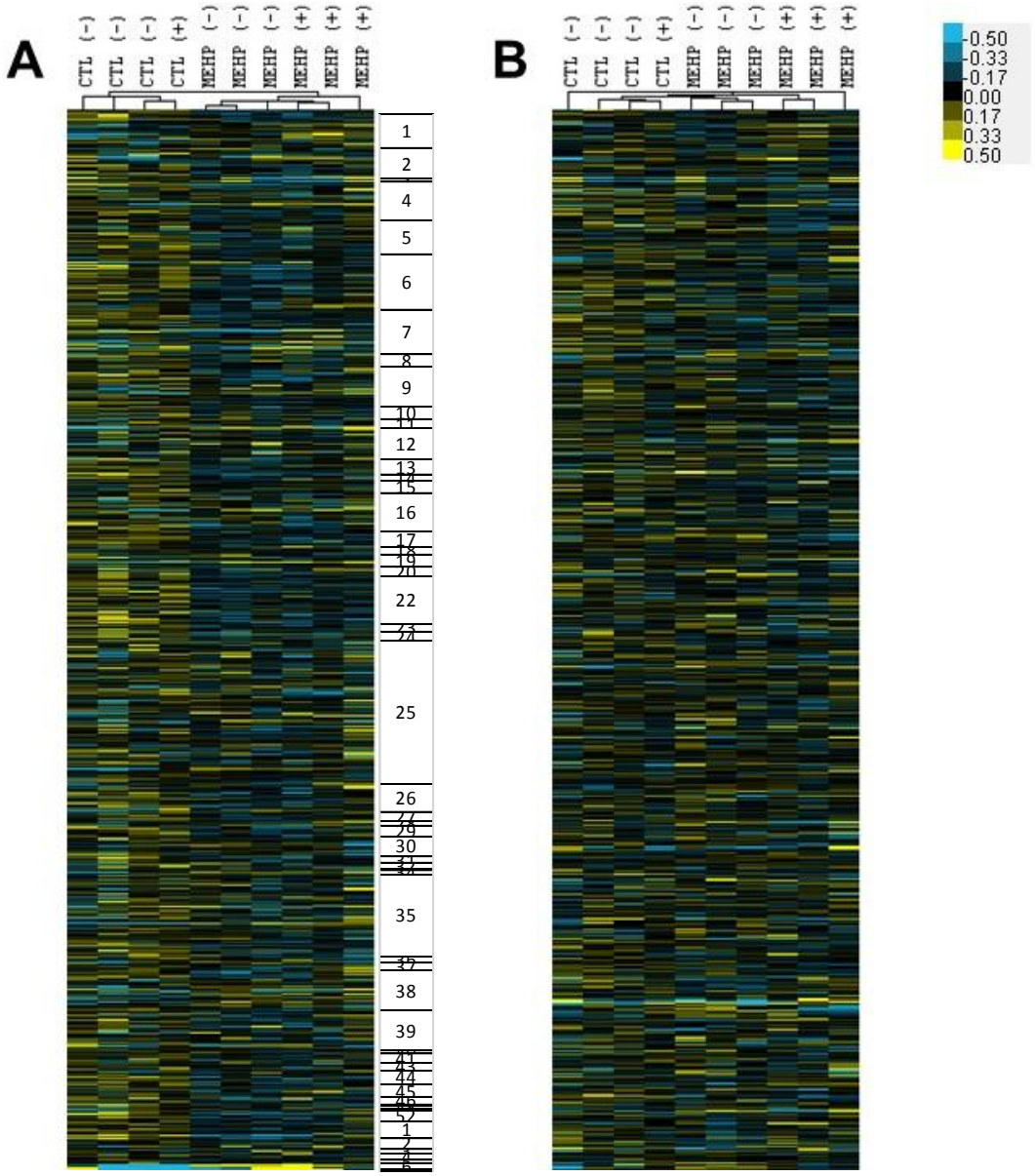

Figure 5.8. Heat map of expression profiles for SLC genes in the EMB and VYS. Expression values were-mean centered and hierarchically clustered by array. Though no obvious trends were detected for VYS (B), MEHP treatment appeared to decrease overall expression of SLC genes in the EMB (A).

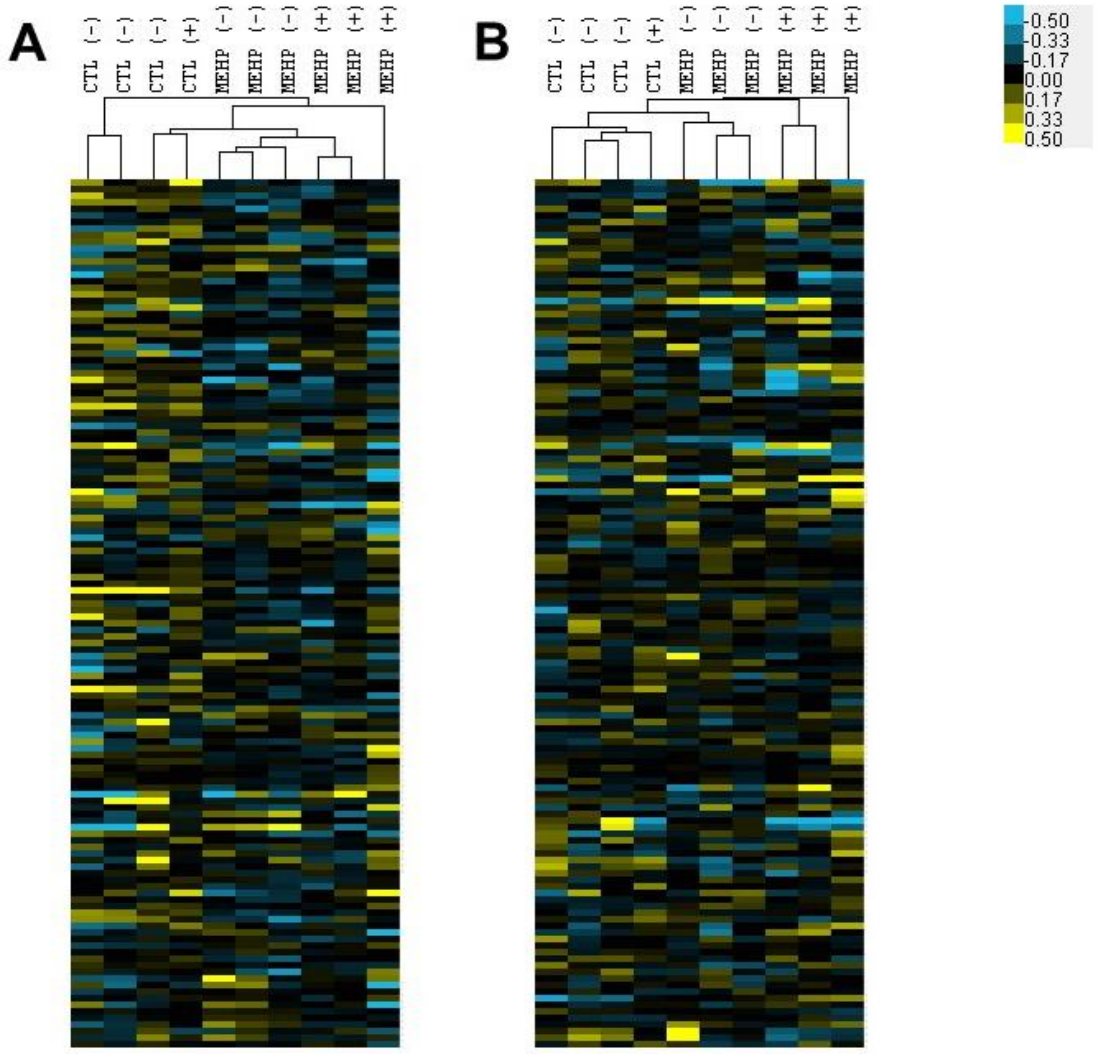

Figure 5.9. Heat map of expression profiles for glutathione and thioredoxin metabolic genes in the EMB and VYS. Expression values were-mean centered and hierarchically clustered by array. Though no obvious trends were detected for VYS (B), MEHP treatment appeared to decrease overall expression of glutathione metabolism genes in the EMB (A).

Table 5.1. Secondary functional pathways included in the functional pathways analyses.

Secondary functional pathways affected by treatment and/or NTD status of EMB and VYS	
EXPRESSION	**METHYLATION**
Metabolism	
Amino acid metabolism Energy metabolism Glycan biosynthesis and metabolism Lipid metabolism Metabolism of cofactors and vitamins Metabolism of other amino acids Xenobiotics biodegradation and metabolism	Amino acid metabolism Carbohydrate metabolism Energy metabolism Glycan biosynthesis and metabolism Metabolism of other amino acids Xenobiotics biodegradation and metabolism
Genetic Information Processing	
Translation	Folding, sorting and degradation Replication and repair Transcription Translation
Environmental Information Processing	
Signal transduction Signaling molecules and interaction	Signal transduction Signaling molecules and interaction
Cellular Processes	
Transport and catabolism	Cellular community Transport and catabolism
Organismal Systems	
Digestive system Endocrine system Immune system Sensory system	Digestive system Endocrine system Immune system
Human Disease	
Endocrine and metabolic diseases Immune diseases Infectious diseases: Bacterial Infectious diseases: Parasitic	Cancers: Overview Cancers: Specific types Immune diseases Infectious diseases: Parasitic Infectious diseases: Viral Neurodegenerative diseases

Table 5.2. A summary of significantly altered expression pathways in GD9 conceptal tissues following 24h exposure to 100μg/ml culture concentrations of MEHP.

Pathways significantly *enriched* in EMB tissue	**P-value**
Neuroactive ligand-receptor interaction	8.21E-12
Cytokine-cytokine receptor interaction	8.60E-07
Arachidonic acid metabolism	1.63E-06
Linoleic acid metabolism	7.59E-05
Complement and coagulation cascades	3.09E-04
Staphylococcus aureus infection	7.19E-04
Metabolism of xenobiotics by cytochrome P450	8.75E-04
Olfactory transduction	1.14E-03
Jak-STAT signaling pathway	1.31E-03
Taste transduction	2.49E-03
Gastric acid secretion	6.50E-03
Steroid hormone biosynthesis	6.60E-03
Asthma	7.32E-03
Rheumatoid arthritis	1.08E-02
Hematopoietic cell lineage	1.12E-02
Drug metabolism - cytochrome P450	1.22E-02
Primary immunodeficiency	1.59E-02
Nicotinate and nicotinamide metabolism	1.66E-02
Regulation of autophagy	2.36E-02
Autoimmune thyroid disease	2.54E-02
Systemic lupus erythematosus	2.77E-02
Malaria	4.08E-02
Renin-angiotensin system	4.43E-02
African trypanosomiasis	4.97E-02
Pathways significantly *enriched* in VYS tissue	**P-value**
Metabolism of xenobiotics by cytochrome P450	1.17E-05
Steroid hormone biosynthesis	3.49E-05
Tryptophan metabolism	2.93E-04
Retinol metabolism	4.28E-03
Cytokine-cytokine receptor interaction	1.74E-02

Table 5.3. A summary of significantly altered expression pathways in GD9 conceptal tissues from conceptuses with open neural tubes.

Pathways significantly enriched in EMB tissue	**P-value**
Aminoacyl-tRNA biosynthesis	7.14E-09
Valine, leucine and isoleucine biosynthesis	6.17E-05
Arginine and proline metabolism	2.26E-03
Complement and coagulation cascades	4.74E-03
Glycine, serine and threonine metabolism	5.63E-03
Pathways significantly enriched in VYS tissue	**P-value**
Allograft rejection	3.11E-05
Lysosome	2.81E-04
Autoimmune thyroid disease	7.08E-04
Primary bile acid biosynthesis	1.08E-03
Asthma	3.81E-03
Other glycan degradation	7.67E-03
Sulfur metabolism	1.08E-02
Type I diabetes mellitus	1.37E-02
Complement and coagulation cascades	1.38E-02
beta-Alanine metabolism	1.50E-02
Tryptophan metabolism	1.70E-02
Glycine, serine and threonine metabolism	2.34E-02
Glycosaminoglycan biosynthesis - keratan sulfate	3.12E-02
N-Glycan biosynthesis	3.16E-02
Graft-versus-host disease	3.31E-02
TGF-beta signaling pathway	3.47E-02
Histidine metabolism	3.89E-02
Maturity onset diabetes of the young	4.32E-02

Table 5.4. A summary of significantly altered promoter methylation pathways in GD9 conceptal tissues following 24h exposure to 100μg/ml culture concentrations of MEHP.

Pathways significantly enriched in EMB tissue	**P-value**
Inositol phosphate metabolism	6.71E-05
Phosphatidylinositol signaling system	1.91E-03
Propanoate metabolism	4.03E-02
Vitamin digestion and absorption	4.59E-02
Pathways significantly enriched in VYS tissue	**P-value**
Jak-STAT signaling pathway	1.59E-03
Other glycan degradation	3.56E-03
B cell receptor signaling pathway	4.22E-03
Natural killer cell mediated cytotoxicity	5.08E-03
RIG-I-like receptor signaling pathway	3.32E-02
Cell adhesion molecules (CAMs)	3.48E-02
Hepatitis C	4.72E-02

Table 5.5. A summary of significantly altered promoter methylation pathways in GD9 conceptal tissues from conceptuses with open neural tubes.

Pathways significantly enriched in EMB tissue	**P-value**
Bladder cancer	2.42E-04
Focal adhesion	5.01E-04
Pathways in cancer	3.43E-03
Selenocompound metabolism	1.07E-02
mTOR signaling pathway	1.27E-02
ECM-receptor interaction	1.72E-02
Pancreatic cancer	1.86E-02
Amoebiasis	2.35E-02
Prostate cancer	3.50E-02
RNA polymerase	3.74E-02
Jak-STAT signaling pathway	3.88E-02
Pathways significantly enriched in VYS tissue	**P-value**
Pancreatic cancer	5.68E-03
Homologous recombination	6.59E-03
Primary immunodeficiency	1.09E-02

References

1. Anderson, O.S., K.E. Sant, and D.C. Dolinoy, *Nutrition and epigenetics: an interplay of dietary methyl donors, one-carbon metabolism and DNA methylation.* The Journal of Nutritional Biochemistry, 2012. **23**(8): p. 853-859.
2. Dunlevy, L.P.E., et al., *Integrity of the methylation cycle is essential for mammalian neural tube closure.* Birth Defects Research Part A: Clinical and Molecular Teratology, 2006. **76**(7): p. 544-552.
3. Wang, L., *Relation between hypomethylation of long interspersed nucleotide elements and risk of neural tube defects.* The American journal of clinical nutrition, 2010. **91**(5): p. 1359-67.
4. Zeisel, S.H., *Importance of methyl donors during reproduction.* Am J Clin Nutr, 2009. **89**(2): p. 673S-7S.
5. Harris, C., *Rodent Whole Embryo Culture*, in *Developmental Toxicology*, C. Harris and J.M. Hansen, Editors. 2012, Humana Press. p. 215-237.
6. Sartor, M.A., G.D. Leikauf, and M. Medvedovic, *LRpath: a logistic regression approach for identifying enriched biological groups in gene expression data.* Bioinformatics, 2009. **25**(2): p. 211-217.
7. *Kyoto Encyclopedia of Genes and Genomes*. [cited 2014]; Available from: http://www.genome.jp/kegg/.
8. Furuya, S., *An essential role for de novo biosynthesis of L-serine in CNS development.* Asia Pac J Clin Nutr, 2008. **17 Suppl 1**: p. 312-5.
9. Shimizu, M., et al., *Functional analysis of mouse 3-phosphoglycerate dehydrogenase (Phgdh) gene promoter in developing brain.* J Neurosci Res, 2004. **76**(5): p. 623-32.
10. Yoshida, K., et al., *Targeted disruption of the mouse 3-phosphoglycerate dehydrogenase gene causes severe neurodevelopmental defects and results in embryonic lethality.* J Biol Chem, 2004. **279**(5): p. 3573-7.
11. Sayano, T., et al., *L-serine deficiency caused by genetic Phgdh deletion leads to robust induction of 4E-BP1 and subsequent repression of translation initiation in the developing central nervous system.* FEBS J, 2013. **280**(6): p. 1502-17.
12. Kawakami, Y., et al., *Impaired neurogenesis in embryonic spinal cord of Phgdh knockout mice, a serine deficiency disorder model.* Neuroscience Research, 2009. **63**(3): p. 184-193.
13. Locasale, J.W., et al., *Phosphoglycerate dehydrogenase diverts glycolytic flux and contributes to oncogenesis.* Nat Genet, 2011. **43**(9): p. 869-74.
14. Kim, S.K., W.H. Jung, and J.S. Koo, *Differential expression of enzymes associated with serine/glycine metabolism in different breast cancer subtypes.* PLoS ONE, 2014. **9**(6): p. e101004.
15. Chen, J., et al., *Phosphoglycerate dehydrogenase is dispensable for breast tumor maintenance and growth.* Oncotarget, 2013. **4**(12): p. 2502-11.
16. Jing, Z., et al., *Expression and clinical significance of phosphoglycerate dehydrogenase and squamous cell carcinoma antigen in cervical cancer.* Int J Gynecol Cancer, 2013. **23**(8): p. 1465-9.
17. Liu, J., et al., *Phosphoglycerate dehydrogenase induces glioma cells proliferation and invasion by stabilizing forkhead box M1.* J Neurooncol, 2013. **111**(3): p. 245-55.
18. Possemato, R., et al., *Functional genomics reveal that the serine synthesis pathway is essential in breast cancer.* Nature, 2011. **476**(7360): p. 346-350.
19. Locasale, J.W. and L.C. Cantley, *Genetic selection for enhanced serine metabolism in cancer development.* Cell Cycle, 2011. **10**(22): p. 3812-3.
20. Shi, X., et al., *Analysis of somatostatin receptors and somatostatin promoter methylation in human gastric cancer.* Oncol Lett, 2013. **6**(6): p. 1794-1798.

21. Ricketts, C.J., et al., *Genome-wide CpG island methylation analysis implicates novel genes in the pathogenesis of renal cell carcinoma.* Epigenetics, 2012. **7**(3): p. 278-90.
22. Jackson, K., et al., *Epigenetic silencing of somatostatin in gastric cancer.* Dig Dis Sci, 2011. **56**(1): p. 125-30.
23. Jin, Z., et al., *Hypermethylation of the somatostatin promoter is a common, early event in human esophageal carcinogenesis.* Cancer, 2008. **112**(1): p. 43-9.
24. de Hoon, M.J., et al., *Open source clustering software.* Bioinformatics, 2004. **20**(9): p. 1453-4.
25. Saldanha, A.J., *Java Treeview—extensible visualization of microarray data.* Bioinformatics, 2004. **20**(17): p. 3246-3248.
26. Robinson, J.F., et al., *Dose–response analysis of phthalate effects on gene expression in rat whole embryo culture.* Toxicology and Applied Pharmacology, 2012. **264**(1): p. 32-41.
27. Hansen, J.M. and C. Harris, *Redox control of teratogenesis.* Reproductive Toxicology, 2013. **35**(0): p. 165-179.
28. Zhu, S., et al., *Inhibiting autophagy potentiates the anticancer activity of IFN1@/IFNalpha in chronic myeloid leukemia cells.* Autophagy, 2013. **9**(3): p. 317-27.
29. Delerive, P., J. Fruchart, and B. Staels, *Peroxisome proliferator-activated receptors in inflammation control.* Journal of Endocrinology, 2001. **169**(3): p. 453-459.
30. Cunard, R., et al., *Repression of IFN-gamma expression by peroxisome proliferator-activated receptor gamma.* J Immunol, 2004. **172**(12): p. 7530-6.
31. Dicitore, A., et al., *Type I interferon-mediated pathway interacts with peroxisome proliferator activated receptor-gamma (PPAR-gamma): at the cross-road of pancreatic cancer cell proliferation.* Biochim Biophys Acta, 2014. **1845**(1): p. 42-52.
32. Cecconi, F., et al., *A novel role for autophagy in neurodevelopment.* Autophagy, 2007. **3**(5): p. 506-8.
33. Cecconi, F., M. Piacentini, and G.M. Fimia, *The involvement of cell death and survival in neural tube defects: a distinct role for apoptosis and autophagy?* Cell Death Differ, 2008. **15**(7): p. 1170-7.
34. Penaloza, C., et al., *Cell death in mammalian development.* Curr Pharm Des, 2008. **14**(2): p. 184-96.
35. Penaloza, C., et al., *Cell death in development: shaping the embryo.* Histochem Cell Biol, 2006. **126**(2): p. 149-58.
36. Mizushima, N., *Autophagy: process and function.* Genes Dev, 2007. **21**(22): p. 2861-73.
37. Fimia, G.M., et al., *Ambra1 regulates autophagy and development of the nervous system.* Nature, 2007. **447**(7148): p. 1121-5.
38. Gu, W., et al., *Ambra1 Is an Essential Regulator of Autophagy and Apoptosis in SW620 Cells: Pro-Survival Role of Ambra1.* PLoS ONE, 2014. **9**(2): p. e90151.
39. Teran-Cabanillas, E., et al., *Decreased interferon-alpha and interferon-beta production in obesity and expression of suppressor of cytokine signaling.* Nutrition, 2013. **29**(1): p. 207-12.
40. Codogno, P. and A.J. Meijer, *Autophagy: A Potential Link between Obesity and Insulin Resistance.* Cell Metabolism. **11**(6): p. 449-451.
41. Barker, D.J.P., *The Developmental Origins of Adult Disease.* Journal of the American College of Nutrition, 2004. **23**(suppl 6): p. 588S-595S.

Chapter VI

Conclusion

I. Summary of Results

The early organogenesis stage of development has not been widely studied. Most developmental toxicology studies focus primarily on the pre-implantation stage with *in vitro* fertilization or later in the fetal stage of development after the placenta is fully functional. The early organogenesis window of development is highly susceptible to external cues, partly because the metabolic demands of the embryo during this phase are so great. Rapid proliferation, programmed and specific differentiation, and spatially-coordinated cell migration and death require precision for normal growth and development. Cellular environmental factors including nutrition, redox potential, and external signaling all play crucial roles in the guidance of these cell fates. In this study, mono-2-ethylhexyl phthalate (MEHP) was used as an environmental toxicant that may potentially disrupt these processes. In a proof-of-principle study, inhibition of histiotrophic nutrition pathways (HNPs) via treatment with the proteolysis inhibitor leupeptin altered one-carbon (C_1) metabolism and epigenetic programming in the embryo (EMB) and visceral yolk sac (VYS) [1]. On this principle, it was hypothesized that oxidation of protein thiols induced by MEHP treatment would disrupt the HNPs, altering C_1 metabolism and epigenetic gene regulation, and this would lead to general dysregulation of gene expression and increase risk for neural tube defects (NTDs).

MEHP significantly decreased overall growth and morphological development. Overall size, as measured by EMB crown-rump length, was decreased by 7-42% depending on the concentration of MEHP treatment; head size was reduced by 7-33% as measured by head length (Chapter 3). From an overall sample of conceptuses from over 60 litters, the background control incidence of NTDs was less than 5%. Incidence of NTDs significantly increased with increasing concentration of MEHP in culture, with over a 33% incidence at the lowest concentration (100 μg/ml). MEHP concentrations of 100 and 250 μg/ml in culture significantly reduced histiotrophic nutrition over 3 h in culture on GD 9 (Chapter 4). Because amino acids and cofactors from the maternal serum (exocoelomic fluids) are the primary building blocks for growth and metabolism, it is no surprise that decreased uptake results in decreased overall growth with increasing dose of MEHP.

After 24 h, the concentrations of methyl donors was relatively unchanged in MEHP-treated conceptuses (Chapter 4). However, components of the C_1 metabolism cycle were increased with increasing concentration of MEHP. This was further confounded by global epigenetic methylation data. Global DNA methylation was decreased in the EMB and increased in the VYS by MEHP treatment. When stratified by NTD status, regardless of treatment, global DNA methylation was decreased in EMB with NTD and increased in VYS with NTD (Chapter 4). Global histone H3K4 and H3K27 methylation was variable. H3K27 methylation was increased in MEHP-treated VYS, and H3K4 methylation was increased in EMB with NTDs. These findings did not fit the original model's expectations, as decreases in HNP function were expected to be coupled with decreased methyl donors and C_1 metabolism component concentrations and decreased epigenetic methylation.

Over the course of 24 h from GD 8 to GD 9, total glutathione concentrations (reduced (GSH) + 2 oxidized (GSSG) glutathione) declined (Chapter 3). Total cysteine concentrations (reduced (cys) + 2 oxidized (cySS) cysteine) were depleted by increasing dose of MEHP in culture over the first 6 h on GD 8. Redox potentials based upon the glutathione (GSH/GSSG) and cysteine (cys/cySS) redox couples were decreased in a dose-dependent manner at 12 and 3 h, respectively. Transcriptomic analysis at 6 h revealed that MEHP treatment induces susceptibility to xenobiotics and oxidative stress, and decreases oxidative phosphorylation and energy and amino acid metabolism. These characteristics are indicative of nutrient starvation, as well as cell survival and apoptosis pathways [2,3]. These changes were further amplified by 24 h, and genes in pathways involved in metabolism and biosynthesis of amino acids as well as autophagy were differentially expressed. Transporters in SLC families were decreased in expression, while the multiligand endocytotic receptor complex (MERC) was increased in expression due to MEHP-treatment in the EMB. Tissue was also an important consideration during this investigation. While all of these changes were amplified in the EMB, almost no significant changes in redox potentials and expression in these pathways were observed. Very few early-organogenesis stage studies investigate mechanisms of toxicity in the VYS, but the conclusions made in this study would not have been evident without the utilization of the VYS. The stratification of the tissues not only by treatment but also by NTD status was also novel and important in these studies. It appeared as though MEHP treatment had a much greater impact on these processes than the presence of an NTD overall, but this approach allowed us to observe some of the potential mechanisms by which penetrance of NTDs is affected.

Over the course of this body of work, it became apparent that the original model was innaccurate (Fig. 6.1). Only upon completion of all experiments could we appreciate the spectrum

of changes observed throughout these chapters, and could not have come to these conclusions using a reductionist approach to study. The utilization of systems biology approaches throughout this work, coupled with reductionist screening methodologies, encouraged a changing of paradigm. The original model proposed that MEHP treatment during embryonic development would induce oxidative stress, and that this would in turn decrease nutrition, decrease epigenetic marks, alter gene expression, and ultimately lead to NTDs (Chapter 1). However, it appears as though MEHP treatment decreases histiotrophic nutrition, and that this major environmental manipulation results in the altered redox states, increased C_1 pool, and altered global epigenetic methylation and dysregulated gene expression measures. It is likely that nutrient starvation may be central to all of these observations. Autophagy, or macroautophagy, is the sequestration and subsequent lysosomal degradation of cytoplasmic proteins and substrates to supply building blocks for basal survival cellular processes such as gluconeogenesis and protein synthesis [4]. Autophagy initially requires formation of a sequestered-substrate-containing vesicle, followed by lysosomal fusion and degradation of the vesicle-bound substrates. This process may also engulf entire organelles, including mitcohondria, that pose additional energy requirements in a time of nutrient starvation. In many ways, autophagy resembles the latter portion of HNPs, with lysosomal fusion of nutrient-containing vesicles. However, HNPs are believed to be an automatic process, governed by the binding of ligands to receptors for receptor-mediated endocytosis (RME), and lysosomally degraded when substrates are available. Autophagy is believed to be a sensory process, occurring due to nutrient starvation or generation of reactive oxygen species (ROS).

Though autophagy was not directly measured in this study, the numerous processes that contribute to the intiation of autophagy were characterized [4]. These processes, herein called nutrient starvation and redox control of autophagy (NSRCA), were probed to quantify redox

potentials and characterize the depleted nutritional status of the conceptal tissues. NSRCA is the synthesis of several existing hypotheses surrounding the induction of autophagy. First, redox state and ROS generation have been repeatedly associated with autophagy activity [5]. These oxidative stress measures have been demonstrated to have direct and indirect impacts on autophagy mechanisms, via oxidation of thiol residues in active sites of crucial signaling molecules, and also indirectly via redox potentials as indicators of deviation from cellular homeostasis [5-8]. Other studies have focused on the role of nutrient starvation as a controlling mechanism for the induction of autophagy, namely amino acid starvation via activation of the general amino acid control (GAAC) pathway [9-14]. Few studies, however, have acknowledged the correlation between these two pathways.

In this chapter, I will address the significance of all results and provide evidence for why NSRCA is proposed to be the overarching mode of action in the etiology of MEHP-induced NTDs. I will additionally enumerate the ways in which future work could build upon this research, and implications of this work in public health.

II. Environmental Modulations of Nutrition and Induction of Nutrient Starvation

The study of nutrition during the embryonic and early organogenesis stages of development has been very limited. During the pre-implantation stage, the increased surface area: volume ratio of the total conceptus does not require more transport than diffusion of nutrients and ligands across a thin layer of cells. The "nutrition" of the pre-implanation conceptus is merely assumed based upon the contents of the culture broth. Once the placenta has become active during the fetal stage of development, active circulation both within the conceptus and supplied by the maternal circulation allows for maximal supply of nutrients and ligands throughout the growing fetus, and

maternal nutrition and serum concentrations of nutrients are often good biomarkers for fetal nutrition. The post-implantation embryo, however, must provide nutrients and ligands to rapidly growing tissues though no systemic transport is yet available.

Many developmental nutrition studies merely use periodically obtained maternal serum nutrient status to estimate the embryonic and fetal nutrition. This may be appropriate for the fetus, since maternal serum is directly transported across the placenta to the fetus. However, as demonstrated in this study, this is not always the case for the embryo. Though the nutrient supply in the maternal serum could be a basic predictor of embryonic nutrition, conditions such as toxicants, oxidation, stress hormones, and other factors may all be able to reduce the actual supply of nutrients crossing the VYS to the EMB. Though other biomarkers, such as nutrient status in amniotic fluid, would be a better choice, these methods are highly invasive and potentially dangerous. Therefore, maternal serum remains the best option. More work to understand the dynamics of pharmacological and toxicological modulation of HNPs is necessary, and should strive to develop mathematical models to predict the nutritional flux following maternal exposures. From a public health perspective, methods to reduce maternal exposures to such toxicants would be the most cost-effective way to circumvent this problem. However, identification of compounds and chemical properties that reduce HNP activity need to be further characterized in order to prioritize the risk of pharmacological, occupational, and environmental exposures.

Decreased HNP function would limit the total supply of nutrients to the growing conceptus. However, it is important to consider the mode of HNP disruption. Inhibition of endocytosis decreases the overall uptake of new and essential nutrients. Inhibition of proteolysis, on the other hand, leaves the variety of nutrients vesicle bound and unavailable for cellular processes. If endocytosis alone is inhibited, cells may still rely on autophagy for a supply of substrates for

crucial cellular processes (Figure 6.2). If proteolysis is inhibited, minimized lysosome function may not be able to maintain even autophagy functions. This might be a contributing factor to the difference in global DNA methylation patterns observed by leupeptin (Chapter 2) and MEHP inhibition of HNPs (Chapter 4). MEHP, likely inhibiting endocytosis only, decreased global DNA methylation in the EMB but increased methylation in the VYS (Chapter 4). In this case, NSRCA in the VYS may be able to preserve some of the amino acid (and potentially methionine) pools, though this might not translate to the EMB. In the case of leupeptin, a proteolysis inhibitor, autophagy would also be inhibited, and DNA methylation decreased in both the EMB and VYS as a result. This hypothesis is further supported by the anti-malarial chloroquine. Chloroquine is widely used in studies as an inhibitor of autophagy, and studies have demonstrated the anti-proteolytic potential of chloroquine and its abilitiy to inhibit HNPs [15-19]. However, no studies have investigated the effects of chloroquine on epigenetic measures or constructed a nutritional ontogeny after treatment.

The reduced supply of several amino acids has been implicated in intrauterine growth restriction (IUGR), though all of these studies have focused on the fetal stages of development [20-23]. In this experiment, methionine and cysteine were measured after 24 h in culture, and were substantially increased in a dose-dependent manner (Chapter 4). However, HNPs were inhibited in this same manner at a 3 h time point. Either HNP activity must be restored between 3-12 hours, or some other mechanism is contributing to the amino acid pool. Future work should measure C_1 at more time points and over shorter intervals of time in order to characterize whether transporter adaptation is occurring or whether proteolysis is the major supplier of these nutrients in the cellular pool. It is possible that both of these processes were occurring, but that we missed the window of development. It is also likely that NSRCA may augment the C_1 pool after the induction of

autophagy. Because autophagy will degrade non-essential cellular proteins and substrates in favor of essential ones, it is likely that replenishment of the C_1 pool would be favored in order to secure future epigenetic marks, post-translational modifications, and enzymatic and metabolic function in the mitochondria for future energy production.

Because total cysteine and total glutathione exhibit an overall decrease over time, increased HNP activity is unlikely to be a major contributor. The degradation of proteins from other processes and structures to resupply the amino acid pool of substrates is a likely candidate, which is likely to act through proteolytic function and autophagy. Throughout the lifecourse, several amino acids are considered "essential", meaning that they must be obtained through the diet because they cannot be synthesized metabolically from other substrates. The expression of genes directly involved in the metabolism of several essential amino acids, likely due to depletion of these essential amino acids, was significantly altered in NTDs at 24 h, including tryptophan, histidine, valine, leucine, threonine, and isoleucine. During pregnancy, several other amino acids are considered "conditionally essential", meaning that they can be synthesized but this cannot meet the increased gestational demand. Three other conditionally essential amino acids were also affected in EMB with NTDs, namely arginine, glycine, and proline [24]. Deficiencies and altered metabolism in these pathways could be largely responsible for the decreased overall size of the EMB due to MEHP treatment. Furthermore, glycine, serine, and threonine metabolism were significantly altered at 24 h only in EMB and VYS from conceptuses with NTDs (Chapter 5). The abundance of these amino acids, especially serine and glycine, has been implicated in autophagy of a myriad of cell and tissue types, including neurological cells in neurodevelopment and neurodegeneration [25,26]. mTOR, a key signaling molecule in numerous processes including cell

fate and autophagy, is a serine/threonine kinase. In the absence of these amino acids, it is possible that mTOR signaling and function is impaired, which leads to the induction of autophagy.

In this work, transcriptomic and epigenomic data were used to characterize changes in amino acid metabolism. However, no measurement of actual activity of enzymes within these pathways was performed. Future work should focus upon the metabolic activities of these, and related, pathways governing NSRCA. Previous studies in whole embryo culture (WEC) investigated proteomic changes following treatment with other HNP disruptors, namely leupeptin and ethanol (unpublished data). In these studies, proteins involved in the uptake, degradation, translation, and metabolism of bulk proteins and nutrients were altered. Additionally, several proteins involved in key metabolic pathways, such as the rate-limiting C_1 metabolism enzyme Mat2a, were found to have oxidative post-translational modifications due to treatment. Thus, NSRCA may be further governed on the translational or post-translational levels.

III. MEHP-Induced Oxidation: Direct or Indirect?

HNPs are evolutionarily adaptive, as they limit the oxygenation and resultant generation of teratogenic ROS during the first, and most sensitive, trimester [27,28]. In this study, the immediate oxidative effects due to increasing MEHP treatment was minimal. Instead, MEHP dose-dependent oxidation occurred at times when other sources of oxidation were ample. For example, a dose-dependent oxidation of cellular redox state was induced in EMB at the 12 h time point (Chapter 3). This is a time in development when metabolic demands are very high: the heart starts beating, conceptal circulation begins, the embryo rotates, and differentiation and patterning of tissues is widely occurring. Additionally, the oxygenation of culture is increased prior to this time

point in order to mimic the increased oxygenation due to activation of conceptal circulation. Thus, the environment itself is likely contributing to some of this oxidation.

But why does it occur in a dose-dependent manner only at this time point? Because MEHP decreases HNP function, it is likely depleting the building blocks for endogenous antioxidant function, such as cysteine, glutamate, and glycine required for GSH biosynthesis. This decreased reducing buffer capacity and decreased endogenous antioxidant response, coupled with increased oxygenation and likely ROS formation in the conceptus, could produce an MEHP-related oxidation response that is not directly a result of MEHP-induced acute toxicity. An ontogeny of ROS production, as well as amino acid bioavailability, would provide more information about whether or not this oxidation is in fact due to delayed MEHP-related ROS generation or whether it is due to decreased antioxidant biosynthetic capacity.

Total glutathione was decreased as time of treatment with MEHP increased, as would be expected due to decreased HNP function (Chapter 3). There were occasional periods over the first 3 hours of temporarily increased total concentrations, which may be indicative of increased GSH biosynthesis. Further inspection was done using LRpath by probing the TRANSFAC® transcription factor binding sites database [29]. Nrf2 transcription factor binding was identified as maintained after 24 h indicating that Nrf2 binding and induction of the endogenous antioxidant response is still occurring. This would be consistent with increased demand for GSH biosynthesis. Over this time period, glutathione redox potentials are stable, indicating that the continued GSH biosynthesis may be able to preserve the cellular redox potentials. However, the total glutathione continues to decrease after this and dose-dependent oxidation of the EMB still occurred with MEHP exposure. This would not be expected with steady Nrf2 induction of glutathione biosynthesis. Thus, another process may be governing these relationships. Previous studies have

demonstrated impairment of Nrf2 translocation to the nucleus in the presence of cellular oxidation [30]. Future work should investigate the relationship between ROS generation following nutrient starvation and the binding and translocation dynamics of the Nrf2-Keap1 complex. Additionally, the protein p62, a protein involved in the formation of aggregates for proteolysis in autophagy, is also involved in the regulation of Nrf2 [31,32]. Though the consequences of p62 accumulation on the progression of autophagy are complex and diverse, p62 stabilizes the continuous activation of Nrf2, because p62 has a much greater binding affinity to the Keap1 active domain [31]. Thus, this could be another mechanism by which Nrf2 induction is being more highly conserved.

Numerous genes involved in the regulation of autophagy are regulated specifically by ROS and oxidative stress. *Atg4* is a cysteine-protease, and is sulfenated, sulfinated, or sulfonated in oxidizing conditions at either the Cys-77 or Cys-81 residue [33,34]. This oxidative modification inactivates *Atg4*, and activates the lipidation of *Atg8*—which in turn activates autophagy [34]. The sulfenation of *Atg4* is reversible via enzymatic reduction, such as by glutathione and thioredoxin [35]. This sensitivity and reversibility of *Atg4* to oxidative modifications could be a redox-sensor and important initiator of oxidative stress-induced autophagy. The MTORC1 complex is another important sensor molecule. The dephosphorylation of MTORC1 results in a pro-autophagy signaling cascade, and is dependent upon cellular environmental conditions, such as redox environment, amino acid starvation, and glucose starvation [35].

Though the link between starvation and autophagy, and the link between ROS and autophagy have been repeatedly demonstrated, it is likely that starvation and ROS generation are highly correlated via NSRCA. In this study, MEHP induced embryonic oxidation in a dose-dependent manner—but only at time points when other sources of oxidation were already present, such as the increased oxygenation of the culture environment (Chapter 3). It has been previously

demonstrated that nutrient starvation increases cellular superoxide concentrations in the mediation of autophagy, and that this is likely to act at a point upstream of the Atg internal portions of the autophagy pathway [36]. In this study, several PI3K subunits were significantly upregulated, and mimicked these findings. Thus, cellular oxidation and ROS are able to act within the autophagy pathways, and also upstream of PI3K.

IV. Autophagy in Neurodevelopment: A Major Factor?

Decreased histiotrophic nutrient uptake in the conceptus, for the aforementioned reasons, may impair normal cell signaling, and instigate survival mechanisms to avoid aberrant cell death and likely defects in the developing conceptus. Autophagy is a likely mechanism for cellular preservation, because the degradation of existing cellular substrates will serve as the metabolic precursors for energy. NSRCA processes were significantly altered in these MEHP-treated conceptuses and those with NTDs.

In autophagy, cellular proteins and even organelles are degraded to provide substrates for the most essential of cellular processes. Often, despite the growing need for energy production, mitochondria are the first to go because of the high energy demands in maintaining the proton gradient and membrane potential. Cells undergoing autophagy rely primarily on glycolysis at the expense of lower ATP generation rather than oxidative phosphorylation due to the intial ATP and biochemical investment. Expression of genes involved in oxidative phosphorylation and other pathways that interact with the TCA cycle were significantly affected by MEHP treatment and in the conceptuses with NTDs. Thus, mitochondrial function may be either compromised or suppressed throughout this study.

Central nervous system (CNS) tissues have high metabolic demands in order to control and coordinate the physiological systems and neural processes of the body. For this reason, the developing brain is particularly susceptible to oxidative damage, and exposures coupled with nutrient starvation may result in autophagy [37]. Initially, autophagy is a preservation mechanism for the developing CNS, providing substrates for basal cellular processes. However, with no new influx of nutrients, autophagy cannot be maintained and ultimately aberrant and potentially excessive cell death may occur [38-41]. The balance between autophagy and apoptosis in embryonic morphology is an emerging topic of research, and it is possible that developmental exposures to chemicals may play a role in the disruption of this balance in teratogenesis. In the CNS, coordinated autophagy and apoptosis help to guide closure of the neural tube, and also the proliferation of neural cells [41]. The gene *Ambra1* has been implicated to be central to the direction of cell fate in the developing neural tube, as it is widely expressed in the neuroepithelium during neural tube closure and expressed widely throughout the CNS during organogenesis [39]. *Ambra1* is an activator of Beclin-1 mediated autophagy in the CNS. Its overexpression results in the initiation of autophagy; its underexpression results in rapid, uncontrolled cellular proliferation, exencephaly of the midbrain and hindbrain regions, and ultimately embryonic death (Table 6.1) [39]. In this study, Ambra1 expression was significantly increased in the EMB both due to MEHP-treatment and in EMB with NTDs. This is a strong indicator that autophagy has been initiated in the EMB, specifically in the neural tube, but that this energetic shunt was still not enough to support normal morphology in development.

V. Epigenetic Consequences & the Developmental Origins of Health and Disease

The overall hypothesis proposed in the introduction was not observed in this study. If absolute nutrient starvation were truly occurring, we would expect to see decreased global histone and DNA methylation due to the decreased availability of methyl group substrates following MEHP treatment. However, this was not the case. Though decreased global DNA methylation was observed in the EMB, DNA methylation was actually increased in the VYS. Almost all histone methylation was maintained or even increased, with the exception of H3K27 methylation in the MEHP-treated EMB. Because histiotrophic nutrition was decreased, some other mechanisms must be contributing to the methyl pool. Given all of the aforementioned supporting data, NSRCA is a likely candidate. Due to the importance of epigenetic gene regulation during development, the maintenance of those processes might be considered a cellular priority. It is possible that the resultant degradation products from autophagy could be shunted towards epigenetic marks, since proper placement of these marks may conditionally govern survival. This is further amplified because the NTD status was more influential on H3K4 and DNA methylation than MEHP-treatment. It is possible that the inability to retain or restore these epigenetic marks in NSRCA may play a role in the etiology of NTDs.

The VYS is a "selfish" tissue. It serves as the metabolic barrier during the first trimester of development, regulating what passes from the maternal interface to the embryonic interface. From an evolutionary standpoint, it is important to note that many genes involved in the uptake of nutrients and investment into increased growth and likely larger birth size are expressed from the paternal-allelic origin [42]. This would increase the overall ecological fitness of the progeny, resulting in successive generations of progeny carrying those paternal genes. During development, the VYS is primarily maternally-imprinted, facilitating the "selfish" conceptal uptake of nutrients from the mother [43]. One cluster of these imprinted genes on chromosome 7 are demonstrative

of this relationship, and to no surprise, it contains several genes central to insulin signaling and nutrient uptake. Insulin II (*Ins2*) is a paternally-expressed gene in the VYS, located directly upstream of the *Igf2* gene, which is also maternally-imprinted in the VYS [44,45]. This cluster of genes on chromosome 7 are particularly enriched for processes involved in growth, especially the insulin signaling pathway and increased uptake of glucose substrates. These genes are suggested to be biallelically expressed during this window development, but are soon-after reduced solely to paternal expression in the VYS. These genes, including *Ins2*, *Igf2*, and *H19* are regulated by imprinting in the same region of chromosome 7 [44]. One such region, known as the *H19* DMR, is located several thousand bp upstream of the *H19* transcription start site. This locus is primarily maternally expressed and paternally imprinted. Methylation of the regions flanking the *H19* DMR were highly hypomethylated in MEHP-treated VYS and in NTD-positive VYS, and was slightly hypomethylated in MEHP-treated and NTD-positive EMB. This suggests that there may be a loss of paternal imprinting of these regions following MEHP treatment and in conceptuses with NTDs, namely in the VYS. Surprisingly, there was no significant change in the expression of *Igf2* or *H19* in the VYS.

Studies have demonstrated that *Ins2* is the only insulin gene expressed in the head and developing central nervous system during this phase of development, but is expressed biallelically [43]. In this study, *Ins2* expression was decreased in the EMB due to MEHP treatment and in EMB with NTDs, and was also decreased in VYS from conceptuses with NTDs. This would be expected, considering the importance of insulin signaling for the uptake of glucose and nutrients via epithelia. However, this decreased expression is contradictory to the hypomethylation of the regulatory *H19* DMR, and suggests that other regulatory factors are influential in Ins2 expression. Alterations to pathways involved in Type I Diabetes and maturity onset diabetes of the young were

observed in VYSs with NTDs. Conceptuses with NTDs on average were much smaller in size and exhibited numerous signs of gene dysregulation. It is possible that a "tipping point" was reached in these conceptuses, which makes them no longer able to regulate insulin signaling. Phthalate exposure, namely DEHP and thus MEHP exposure), during development has been widely associated with increased risk for obesity and potentially diabetes [46-49]. Unlike in the VYS, *Ins2* is expressed biallelically in the developing pancreas [44]. Studies have demonstrated the importance of autophagy in the function of the β-cells of the pancreatic islets, and that impaired autophagy may result in pancreatic cell death and contribute to increased risk for obesity and diabetes [50-52]. The importance of Nrf2 mediation of oxidative stress and autophagy in the pancreatic islets has also been proposed [53]. Therefore, it is possible that NSRCA is responsible for the reprogramming or decay of pancreatic cells, which alters these signaling pathways and may predispose these progeny to diabetes and obesity later in life. Future work should investigate the long term expression and epigenetic regulation of expression profiles of insulin and insulin II in the pancreas to characterize whether embryonic alterations in these pathways may predispose progeny to metabolic diseases later in the life course.

Other aging and degenerative diseases have identified autophagy as a potential mechanism. Numerous studies have implicated NSRCA processes and autophagy in neurodegenerative disorders [54-59]. Though only morphological defects of the CNS were measured in this study, it is possible that the altered nutrition, cellular signaling profiles, and epigenetic modifications accrued during this study may contribute to other functional or cognitive defects postnatally and throughout the lifecourse, including neurodegenerative disease. Because neurogenesis is initiated during this developmental period, it is possible that delayed or halted neural tube closure may alter the chemical and spatial patterning of the brain. From the growing body of evidence implicating

the role of autophagy in aberrant neurodevelopment, one may hypothesize that adaptation to nutrient starvation early in development may result in altered signaling and capacity throughout the life course, and may predispose individuals to neurodegenerative diseases such as Parkinson's and Alzheimer's diseases. Autophagy has been associated with histone deacetylase (HDAC) inhibition has been implicated in neurodegeneration and cancer [60,61]. However, HDAC6 activity is often impaired in cells with protein aggregation and dysfunctional autophagy [61,62]. Therefore, more work is necessary to understand the role of HDACs and histone epigenetics in the progression of developmental autophagy and potential for altered programming that may result in adult-onset disease.

VI. Now What?: Public Health Recommendations

Several studies have demonstrated that pharmacological remediation of impaired autophagy can in fact prevent NSRCA-induced neural tube defects [63]. Development of more pregnancy-safe pharmacological agents to target NSRCA via restoring HNPs and reducing oxidative stress is a potential option for intervention. However, the use of preventative pharmaceuticals during pregnancy is controversial. Minimization of chemical exposures during pregnancy and consumption of a balanced diet would be the best preventative plan. However, the chemicals that may inhibit HNPs and induce NSRCA pathways are relatively uncharacterized. More studies should focus on classes of toxicants that may impose the effects seen in this study, with specific regard to whether or not they are inhibitors of HNPs. HNP function appears to be the primary mechanism for induction of NSRCA during early organogenesis, so understanding which chemicals modify HNPs and whether or not they inhibit the endocytosis or proteolysis stages of HNPs would provide guidance for risk assessment.

Controversy surrounds the timeline of the embryo-fetal transition in humans. In humans, the time at which the placenta becomes an active and functional metabolic barrier and delivery system for nutrients is somewhat controversial. Though it was previously believed that the placenta was formed and functional before the 8th week of pregnancy, more studies have suggested that it is more likely to occur during weeks 10-13 of gestation [27,64-66]. Regardless of whether or not this occurs as early as week 8 or as late as week 13, this is still a very susceptible window of development. Histiotrophic function still serves as the primary delivery system for nutrition, and altered function may induce NSRCA. The work performed in this dissertation was performed in mouse and rat conceptuses, which have an inverted VYS relative to the human anatomy. While the rodent VYS completely surrounds the EMB, the human yolk sac is an umbilical vesicle in the amniotic cavity [67]. The human amnion surrounds the entire embryo, and also serves as a barrier for post-implanation and pre-placental development. However, similar to in rodents, the human yolk sac collects the nutrients required for growth and then they are distributed to the EMB. Thus, the yolk sac would control the progression of NSRCA processes in humans as well as in rodents.

These studies were all performed in whole embryo culture, which is an excellent model for embryonic development. However, it is unknown whether or not these compounds would have the same effects *in vivo* as they do *in vitro*. Preliminary unpublished data has suggested that DEHP treatment *in vivo* in mice, regardless of antioxidant supplementation with the pharmacological Nrf2 inducer dithiole-3-thione (D3T), may impact conceptal redox status at temporary windows of embryonic development. However, no characterization of HNP function has been performed to assess embryonic nutritional status to date. Currently, maternal nutritional statuses are utilized for these purposes, but this study suggests that this may not be an accurate biomarker. Methods should be developed in order to help characterize *in vivo* nutritional relationships.

VII. Study Strengths & Limitations

This study has several limitations that give rise to opportunities for future studies. One limitation of this study was the selection of MEHP and DEHP concentrations for culture. Quantitative measures of environmental MEHP concentrations reaching the VYS and EMB tissues have yet to be obtained. At the time this study was initiated, only one mouse WEC study investigating MEHP treatment had been performed, and correlated *in vivo* morphological effects with WEC benchmark concentrations (BMC) [68]. MEHP was found to be the most potent DEHP metabolite in this study, with a BMC of approximately 0.3 mM in WEC [68]. Our lowest concentration investigated in this study was 100 μg/ml, or approximately 0.359 mM. Soon after the initiation of the work in this thesis, another study was conducted using the same range of culture concentrations as used in this study (Chapter 3) [69]. However, the effects observed in this study, namely NTDs, were found in about one third of conceptuses at this lowest concentration. Future studies should investigate these effects at lower, more environmentally relevant concentrations. However, *in vivo* studies measuring the concentrations of MEHP and other toxicants measured in these tissues would be crucial to construct these environmentally-relevant dose ranges.

DEHP has been implicated in numerous cancers and adverse reproductive outcomes. It is believed that this toxicity is largely due to the endocrine-disruptor activities of phthalates, mediated by the peroxisome proliferator–activated receptors (PPARs) and steroidogenic acute regulatory protein (StAR) [70-74]. These effects have often been found to be sex-specific, acting through different mechanisms. Because of the endocrine-disrupting potential of DEHP treatment, bimodal responses due to sex differences often contribute to variability in the physiological effects of phthalate exposures. Because the primordial germ cells have not yet begun migration or tissue

patterning of the reproductive systems during the investigated window of development, these sex-specific physiological differences were not expected to contribute to early organogenesis teratogenicity in this study [75]. However, it is possible that sex of the offspring may contribute to differences in the penetrance of NTDs in conceptuses, or play a role in the metabolic consequences of exposures. Future work should address sex-specific differences in morphological, metabolic, and mechanistic responses.

Additional studies would also provide more opportunity to study control (untreated) conceptuses with NTDs. Because this study also investigated the mechanisms that may contribute to NTDs, having untreated conceptuses with NTDs would provide insight into the mechanisms that may contribute to penetrance. In this study, NSRCA was identified as a potential mechanism that contributes to the etiology of NTDs. However, the relationship between autophagy and NTDs in untreated, non-mutant EMB has yet to be characterized. Likewise, several endpoints in this study utilized tissues that were not qualified as NTD negative or positive, including the measurement of redox profiles. Future work should stratify all tissues, including those used in the histiotrophic nutrition studies.

This study also has many strengths and novel facets. First, we have identified a model pathway by which MEHP may induce NTDs and other morphological deficits. However, this model is not limited to MEHP, nor to phthalates. The model proposed in this study could be investigated following a myriad of developmental exposures to various chemicals. Numerous antiviral, antimalarial, and antiepileptic drugs have chemical components that are known or suggested inhibitors of HNPs, and thus this model could be used to investigate whether these pharmacological agents are detrimental during pregnancies. Likewise, numerous dietary and environmental exposures may also fit the proposed model, yet very few studies have been

conducted to date. This study suggests future investigation of common exposures to determine whether or not they may increase risk for NTDs or other adverse outcomes that may result from these mechanisms.

The stratification of the samples by NTD status as well as treatment status was novel for teratology studies. This design allowed for us to not only investigate the teratogenic potential of MEHP, but also to determine what mechanisms may play a role in the etiology of NTDs following exposures. Without the use of this study design, it is likely that the conclusion about the proposed NSRCA response would not have been reached. Recent studies suggest that autophagy may play an important role in the normal closure of the neural tube, and disruption of autophagy following complete depletion of resources may lead to apoptosis and ultimately NTDs [40,41].

VIII. Conclusion

In conclusion, I suggest that the best model for the role of MEHP in the etiology of NTDs is via NSRCA pathways leading to autophagy (Figure 6.3). It is proposed that MEHP treatment reduces histiotrophic nutrition, and this nutrient deficiency then results in decreased antioxidant capacity and altered redox signaling, as well as altered epigenetic programming. These changes, in turn, lead to altered gene expression and potentially post-translational modifications that may result in autophagy and ultimately NTDs. These findings and this model have implications across species during the first trimester of development, and may alter gestational outcomes including atypical organogenesis or even spontaneous abortion. Though additional work is needed to elucidate the specific mechanisms by which NSRCA occurs, this serves as a sequence of

physiological and genetic endpoints that may coordinate embryonic exposures and teratogenesis, such as the induction of MEHP in NTDs.

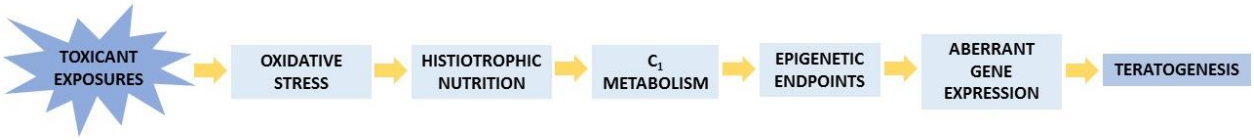

Figure 6.1. Original schematic representing the hypothesized pathway by which MEHP treatment may increase risk for NTDs.

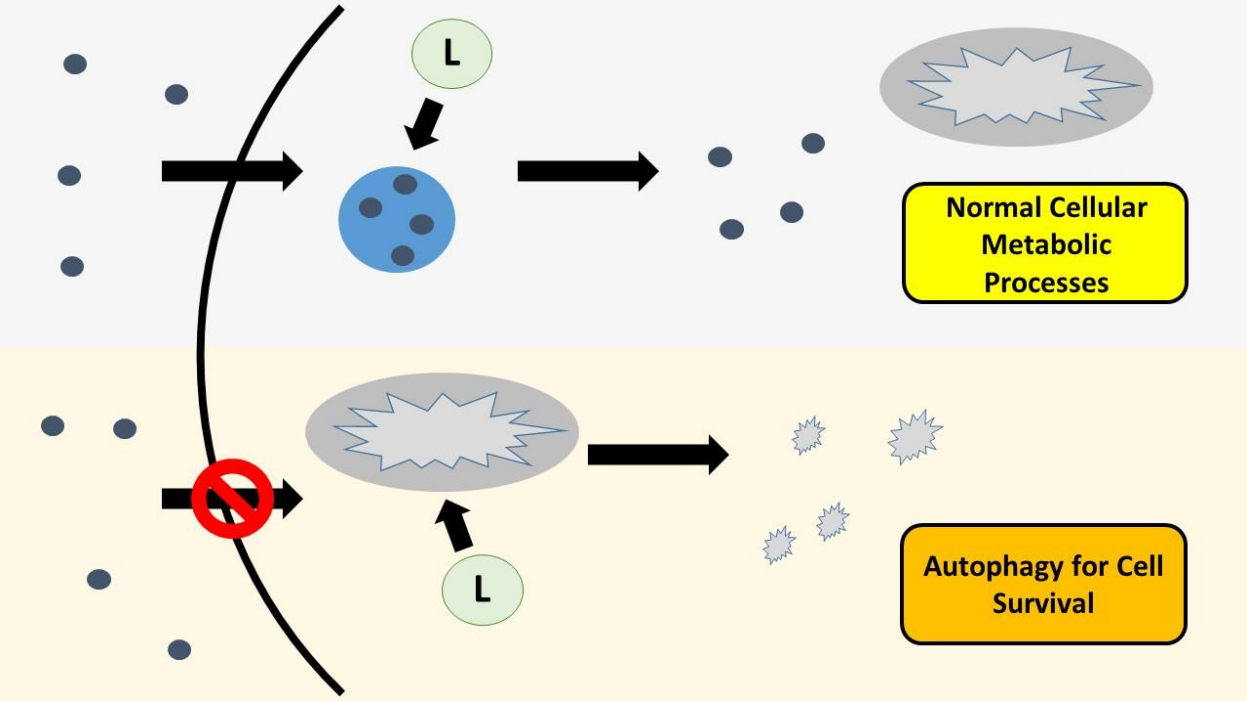

Figure 6.2. Decreased HNP activity shifts proteolytic activity from nutrient-containing vesicles to cellular proteins and organelles. Under normal conditions, nutrients are taken up via endocytosis and bound in vesicles. Lysosomes then degrade the vesicles to release nutrients and substrates for cellular processes. When HNPs are reduced, the cell must rely on degradation of current cellular proteins and structures, often mitochondria, to provide substrates for the most crucial cellular survival processes.

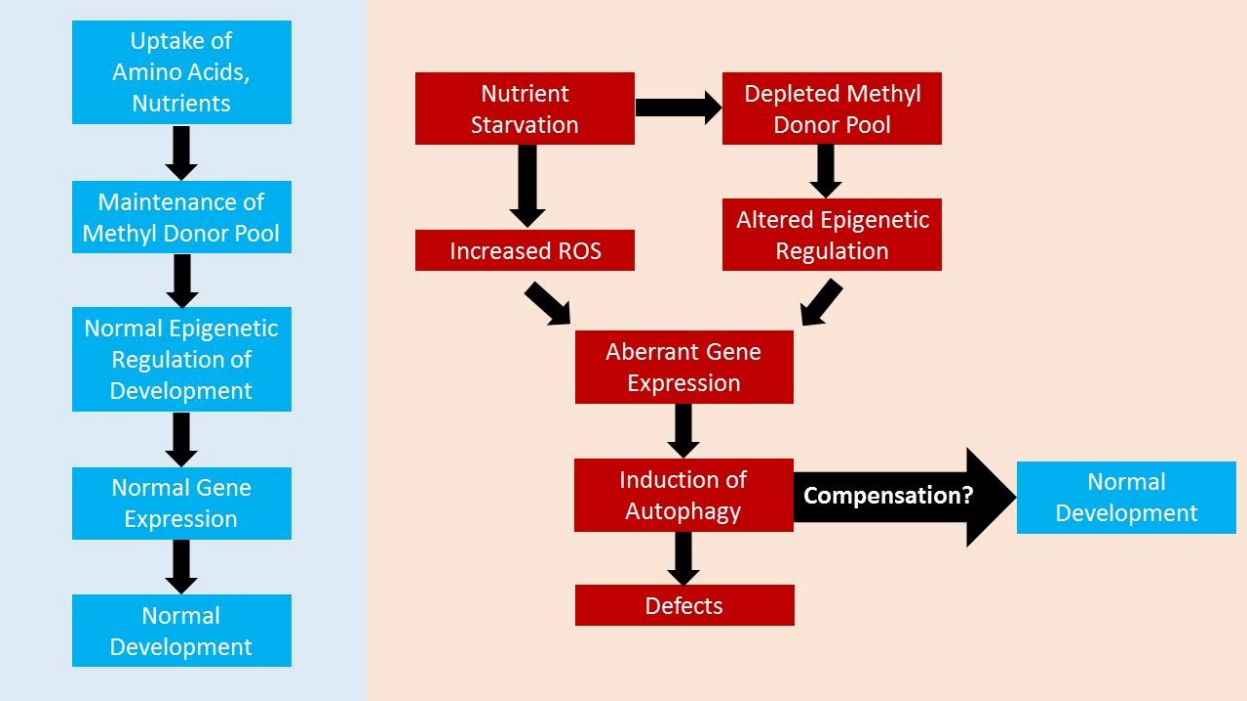

Figure 6.3. Schematic representing the proposed pathway by which MEHP treatment may increase risk for NTDs. Under normal conditions, nutrient uptake is unimpeded, and substrates are readily available for cellular processes (left). When HNPs are inhibited, NSRCA causes dysregulation and may increase risk for defects (right). However, the initiation of autophagy may recycle substrates for essential cellular processes, enabling survival and normal development if full compensation occurs.

Table 6.1. Ambra1 expression is a control of cell fate and morphological outcomes in the developing CNS.

Ambra1 expression?	Response	Morphological Outcome
Normal	Homeostasis	Normal growth & development
Overexpressed	Autophagy	Normal development (nutrient recovery)
Overexpressed	Autophagy	NTDs, Embryonic lethal (nutrient starvation)
Underexpressed	Rapid proliferation	Exencephaly, Embryonic lethal

References

1. Sant, K.E., et al., *Inhibition of proteolysis in histiotrophic nutrition pathways alters DNA methylation and one-carbon metabolism in the organogenesis-stage rat conceptus.* The Journal of Nutritional Biochemistry, 2013. **24**(8): p. 1479-1487.
2. Wu, J., et al., *Global analysis of nutrient control of gene expression in Saccharomyces cerevisiae during growth and starvation.* Proc Natl Acad Sci U S A, 2004. **101**(9): p. 3148-53.
3. Prentice, A.M., P. Rayco-Solon, and S.E. Moore, *Insights from the developing world: thrifty genotypes and thrifty phenotypes.* Proc Nutr Soc, 2005. **64**(2): p. 153-61.
4. Mizushima, N., *Autophagy: process and function.* Genes Dev, 2007. **21**(22): p. 2861-73.
5. Filomeni, G., D. De Zio, and F. Cecconi, *Oxidative stress and autophagy: the clash between damage and metabolic needs.* Cell Death Differ, 2014.
6. Zhang, C.F., et al., *Suppression of Autophagy Dysregulates the Antioxidant Response and Causes Premature Senescence of Melanocytes.* J Invest Dermatol, 2014.
7. Perez-Perez, M.E., et al., *The yeast autophagy protease Atg4 is regulated by thioredoxin.* Autophagy, 2014. **10**(11).
8. Perez-Martin, M., et al., *Oxidative Stress Contributes to Autophagy Induction in Response to Endoplasmic Reticulum Stress in Chlamydomonas reinhardtii.* Plant Physiol, 2014. **166**(2): p. 997-1008.
9. Mizushima, N., *Autophagy: process and function.* Genes & Development, 2007. **21**(22): p. 2861-2873.
10. Mizushima, N., et al., *In vivo analysis of autophagy in response to nutrient starvation using transgenic mice expressing a fluorescent autophagosome marker.* Mol Biol Cell, 2004. **15**(3): p. 1101-11.
11. Jin, H. and J. Lei, *A mathematical model of cell population dynamics with autophagy response to starvation.* Math Biosci, 2014. **258C**: p. 1-10.
12. Karim, M.R., H. Kawanago, and M. Kadowaki, *A quick signal of starvation induced autophagy: Transcription versus post-translational modification of LC3.* Anal Biochem, 2014. **465C**: p. 28-34.
13. Chen, R., et al., *The general amino acid control pathway regulates mTOR and autophagy during serum/glutamine starvation.* J Cell Biol, 2014. **206**(2): p. 173-82.
14. Vlahakis, A., et al., *TOR complex 2-Ypk1 signaling is an essential positive regulator of the general amino acid control response and autophagy.* Proc Natl Acad Sci U S A, 2014. **111**(29): p. 10586-91.
15. Ambroso, J.L. and C. Harris, *Chloroquine accumulation and alterations of proteolysis and pinocytosis in the rat conceptus in vitro.* Biochemical Pharmacology, 1994. **47**(4): p. 679-688.
16. Morgan, M.J., et al., *Regulation of autophagy and chloroquine sensitivity by oncogenic RAS in vitro is context-dependent.* Autophagy, 2014. **10**(10): p. 1814-26.
17. Liang, X., et al., *Suppression of autophagy by chloroquine sensitizes 5-fluorouracil-mediated cell death in gallbladder carcinoma cells.* Cell Biosci, 2014. **4**(1): p. 10.
18. Pellegrini, P., et al., *Acidic extracellular pH neutralizes the autophagy-inhibiting activity of chloroquine: implications for cancer therapies.* Autophagy, 2014. **10**(4): p. 562-71.
19. Zhu, S., et al., *Inhibiting autophagy potentiates the anticancer activity of IFN1@/IFNalpha in chronic myeloid leukemia cells.* Autophagy, 2013. **9**(3): p. 317-27.
20. Regnault, T.R., et al., *Fetoplacental transport and utilization of amino acids in IUGR--a review.* Placenta, 2005. **26 Suppl A**: p. S52-62.
21. Cetin, I., *Placental transport of amino acids in normal and growth-restricted pregnancies.* Eur J Obstet Gynecol Reprod Biol, 2003. **110 Suppl 1**: p. S50-4.

22. Kalhan, S.C., *Metabolism of methionine in vivo: impact of pregnancy, protein restriction, and fatty liver disease.* Nestle Nutr Workshop Ser Pediatr Program, 2009. **63**: p. 121-31; discussion 131-3, 259-68.
23. Bhasin, K.K., et al., *Maternal low-protein diet or hypercholesterolemia reduces circulating essential amino acids and leads to intrauterine growth restriction.* Diabetes, 2009. **58**(3): p. 559-66.
24. Otten, J.J., et al., *DRI, dietary reference intakes: the essential guide to nutrient requirements*. Dietary reference intakes2006, Washington, D.C.: National Academies Press. xiii, 543 p.
25. Paul, P. and J. de Belleroche, *The role of D-serine and glycine as co-agonists of NMDA receptors in motor neuron degeneration and amyotrophic lateral sclerosis (ALS).* Front Synaptic Neurosci, 2014. **6**: p. 10.
26. Ogura, K., et al., *Protein phosphatase 2A cooperates with the autophagy-related kinase UNC-51 to regulate axon guidance in Caenorhabditis elegans.* Development, 2010. **137**(10): p. 1657-67.
27. Burton, G.J., J. Hempstock, and E. Jauniaux, *Nutrition of the human fetus during the first trimester--a review.* Placenta, 2001. **22 Suppl A**: p. S70-7.
28. Jauniaux, E., B. Gulbis, and G.J. Burton, *The human first trimester gestational sac limits rather than facilitates oxygen transfer to the foetus--a review.* Placenta, 2003. **24 Suppl A**: p. S86-93.
29. Wingender, E., et al., *TRANSFAC: an integrated system for gene expression regulation.* Nucleic Acids Res, 2000. **28**(1): p. 316-9.
30. Paupe, V., et al., *Impaired nuclear Nrf2 translocation undermines the oxidative stress response in Friedreich ataxia.* PLoS ONE, 2009. **4**(1): p. e4253.
31. Komatsu, M., et al., *The selective autophagy substrate p62 activates the stress responsive transcription factor Nrf2 through inactivation of Keap1.* Nat Cell Biol, 2010. **12**(3): p. 213-223.
32. Lippai, M. and P. Low, *The role of the selective adaptor p62 and ubiquitin-like proteins in autophagy.* Biomed Res Int, 2014. **2014**: p. 832704.
33. Scherz-Shouval, R., E. Shvets, and Z. Elazar, *Oxidation as a post-translational modification that regulates autophagy.* Autophagy, 2007. **3**(4): p. 371-3.
34. Scherz-Shouval, R., et al., *Reactive oxygen species are essential for autophagy and specifically regulate the activity of Atg4.* EMBO J, 2007. **26**(7): p. 1749-60.
35. Filomeni, G., et al., *Under the ROS...thiol network is the principal suspect for autophagy commitment.* Autophagy, 2010. **6**(7): p. 999-1005.
36. Chen, Y., M.B. Azad, and S.B. Gibson, *Superoxide is the major reactive oxygen species regulating autophagy.* Cell Death Differ, 2009. **16**(7): p. 1040-52.
37. Ikonomidou, C. and A.M. Kaindl, *Neuronal death and oxidative stress in the developing brain.* Antioxid Redox Signal, 2011. **14**(8): p. 1535-50.
38. Boya, P., et al., *Inhibition of macroautophagy triggers apoptosis.* Mol Cell Biol, 2005. **25**(3): p. 1025-40.
39. Fimia, G.M., et al., *Ambra1 regulates autophagy and development of the nervous system.* Nature, 2007. **447**(7148): p. 1121-5.
40. Cecconi, F., et al., *A novel role for autophagy in neurodevelopment.* Autophagy, 2007. **3**(5): p. 506-8.
41. Cecconi, F., M. Piacentini, and G.M. Fimia, *The involvement of cell death and survival in neural tube defects: a distinct role for apoptosis and autophagy?* Cell Death Differ, 2008. **15**(7): p. 1170-7.
42. Wilkins, J.F. and D. Haig, *What good is genomic imprinting: the function of parent-specific gene expression.* Nat Rev Genet, 2003. **4**(5): p. 359-368.
43. Deltour, L., et al., *Tissue- and developmental stage-specific imprinting of the mouse proinsulin gene, Ins2.* Dev Biol, 1995. **168**(2): p. 686-8.
44. Giddings, S.J., et al., *Allele specific inactivation of insulin 1 and 2, in the mouse yolk sac, indicates imprinting.* Nat Genet, 1994. **6**(3): p. 310-3.

45. Moore, G.E., et al., *Evidence that insulin is imprinted in the human yolk sac.* Diabetes, 2001. **50**(1): p. 199-203.
46. Kim, S.H. and M.J. Park, *Phthalate exposure and childhood obesity.* Ann Pediatr Endocrinol Metab, 2014. **19**(2): p. 69-75.
47. Buser, M.C., H.E. Murray, and F. Scinicariello, *Age and sex differences in childhood and adulthood obesity association with phthalates: analyses of NHANES 2007-2010.* Int J Hyg Environ Health, 2014. **217**(6): p. 687-94.
48. Hao, C., et al., *Perinatal exposure to diethyl-hexyl-phthalate induces obesity in mice.* Front Biosci (Elite Ed), 2013. **5**: p. 725-33.
49. Hao, C., et al., *The endocrine disruptor mono-(2-ethylhexyl) phthalate promotes adipocyte differentiation and induces obesity in mice.* Biosci Rep, 2012. **32**(6): p. 619-29.
50. Marselli, L., et al., *β-Cell inflammation in human type 2 diabetes and the role of autophagy.* Diabetes, Obesity and Metabolism, 2013. **15**(s3): p. 130-136.
51. Bugliani, M., et al., *Microarray analysis of isolated human islet transcriptome in type 2 diabetes and the role of the ubiquitin-proteasome system in pancreatic beta cell dysfunction.* Mol Cell Endocrinol, 2013. **367**(1-2): p. 1-10.
52. Quan, W., E.K. Jo, and M.S. Lee, *Role of pancreatic beta-cell death and inflammation in diabetes.* Diabetes Obes Metab, 2013. **15 Suppl 3**: p. 141-51.
53. Li, W., et al., *Targeting Nrf2 by dihydro-CDDO-trifluoroethyl amide enhances autophagic clearance and viability of beta-cells in a setting of oxidative stress.* FEBS Lett, 2014. **588**(12): p. 2115-24.
54. Giordano, S., V. Darley-Usmar, and J. Zhang, *Autophagy as an essential cellular antioxidant pathway in neurodegenerative disease.* Redox Biol, 2014. **2**: p. 82-90.
55. Heras-Sandoval, D., et al., *The role of PI3K/AKT/mTOR pathway in the modulation of autophagy and the clearance of protein aggregates in neurodegeneration.* Cell Signal, 2014. **26**(12): p. 2694-2701.
56. Kesidou, E., et al., *Autophagy and neurodegenerative disorders.* Neural Regen Res, 2013. **8**(24): p. 2275-83.
57. Wang, G. and Z. Mao, *Chaperone-mediated autophagy: roles in neurodegeneration.* Transl Neurodegener, 2014. **3**: p. 20.
58. Fleming, A., et al., *Chemical modulators of autophagy as biological probes and potential therapeutics.* Nat Chem Biol, 2011. **7**(1): p. 9-17.
59. Eskelinen, E.L. and P. Saftig, *Autophagy: a lysosomal degradation pathway with a central role in health and disease.* Biochim Biophys Acta, 2009. **1793**(4): p. 664-73.
60. Shao, Y., et al., *Apoptotic and autophagic cell death induced by histone deacetylase inhibitors.* Proc Natl Acad Sci U S A, 2004. **101**(52): p. 18030-5.
61. True, O. and P. Matthias, *Interplay between histone deacetylases and autophagy--from cancer therapy to neurodegeneration.* Immunol Cell Biol, 2012. **90**(1): p. 78-84.
62. Lee, J.Y., et al., *HDAC6 controls autophagosome maturation essential for ubiquitin-selective quality-control autophagy.* EMBO J, 2010. **29**(5): p. 969-80.
63. Xu, C., et al., *Trehalose prevents neural tube defects by correcting maternal diabetes-suppressed autophagy and neurogenesis.* Am J Physiol Endocrinol Metab, 2013. **305**(5): p. E667-78.
64. Burton, G.J., et al., *Uterine glands provide histiotrophic nutrition for the human fetus during the first trimester of pregnancy.* J Clin Endocrinol Metab, 2002. **87**(6): p. 2954-9.
65. Weissgerber, T.L. and L.A. Wolfe, *Physiological adaptation in early human pregnancy: adaptation to balance maternal-fetal demands.* Appl Physiol Nutr Metab, 2006. **31**(1): p. 1-11.
66. Huppertz, B., G. Weiss, and G. Moser, *Trophoblast invasion and oxygenation of the placenta: measurements versus presumptions.* Journal of Reproductive Immunology, 2014. **101–102**(0): p. 74-79.
67. Larsen, W.J., *Human embryology*2001, New York: Churchill Livingstone. xix, 548 p.

68. Janer, G., et al., *Use of the rat postimplantation embryo culture to assess the embryotoxic potency within a chemical category and to identify toxic metabolites.* Toxicology in Vitro, 2008. **22**(7): p. 1797-1805.
69. Robinson, J.F., et al., *Dose–response analysis of phthalate effects on gene expression in rat whole embryo culture.* Toxicology and Applied Pharmacology, 2012. **264**(1): p. 32-41.
70. Lehmann, K.P., et al., *Dose-Dependent Alterations in Gene Expression and Testosterone Synthesis in the Fetal Testes of Male Rats Exposed to Di (n-butyl) phthalate.* Toxicological Sciences, 2004. **81**(1): p. 60-68.
71. Thompson, C.J., S.M. Ross, and K.W. Gaido, *Di(n-Butyl) Phthalate Impairs Cholesterol Transport and Steroidogenesis in the Fetal Rat Testis through a Rapid and Reversible Mechanism.* Endocrinology, 2004. **145**(3): p. 1227-1237.
72. Hurst, C.H. and D.J. Waxman, *Activation of PPARalpha and PPARgamma by environmental phthalate monoesters.* Toxicol Sci, 2003. **74**(2): p. 297-308.
73. Bility, M.T., et al., *Activation of mouse and human peroxisome proliferator-activated receptors (PPARs) by phthalate monoesters.* Toxicol Sci, 2004. **82**(1): p. 170-82.
74. Feige, J.N., et al., *The endocrine disruptor monoethyl-hexyl-phthalate is a selective peroxisome proliferator-activated receptor gamma modulator that promotes adipogenesis.* J Biol Chem, 2007. **282**(26): p. 19152-66.
75. National Institutes of Health, *Appendix A: Early Development*, in *Stem Cell Information*2009, U.S. Department of Health and Human Services: Bethesda, MD.